STEREOSPECIFIC LONG-RANGE NUCLEAR SPIN-SPIN COUPLING CONSTANTS IN FLUOROANILINE DERIVATIVES. BARRIERS TO INTERNAL ROTATION IN SOME ORTHO DISUBSTITUTED N-METHYLANILINE DERIVATIVES.

by

GLENN H. PENNER

A thesis Submitted to
the Faculty of Graduate Studies and Research
of the University of Manitoba
in partial fulfillment
of the requirements of the degree

Master of Science

Winnipeg, Manitoba,
August, 1984

STEREOSPECIFIC LONG-RANGE NUCLEAR SPIN-SPIN COUPLING CONSTANTS IN FLUOROANILINE DERIVATIVES. BARRIERS TO INTERNAL ROTATION IN SOME ORTHO DISUBSTITUTED N-METHYLANILINE DERIVATIVES

BY

GLENN H. PENNER

A thesis submitted to the Faculty of Graduate Studies of the University of Manitoba in partial fulfillment of the requirements of the degree of

MASTER OF SCIENCE

ACKNOWLEDGEMENTS

I wish to thank Dr. Ted Schaefer for his encouragement, guidance and thoughtful critisism during the course of this work. His patience with me during my many tangents into other projects is greatly appreciated.

I thank Mr. Rudy Sebastian for instructing me in the art of running and analyzing an nmr spectrum. His help with the computer work in this project was invaluable.

I thank Dr. Frank Hruska for access to the Bruker WH-90 spectrometer, without which this work could not have been done. The guidance of Mr. Kirk Marat while using the Bruker WH-90 is very much appreciated.

I am grateful to Dr. D. M. McKinnon and Dr. N. R. Hunter for their advice regarding the syntheses in this project.

I thank my friends and colleagues Mike Sowa, Gil Prive, Jim Baleja, Rudy Sebastian and Dr. Jim Peeling for interesting conversation regarding this work and other matters.

I would also like to thank my parents, whose support throughout my undergraduate years enabled me to pursue a career in chemistry.

I am grateful to Donna Harris for enduring my bad handwriting during the typing of these pages.

TABLE OF CONTENTS

Page

LIST OF FIGURES

PART I

Figure | Page

Part II

Figure | Page

LIST OF TABLES

Part I

Part II

PART I

Stereospecific Long-Range Nuclear Spin-Spin Coupling Between Amino Protons and Ring Fluorine Nuclei in Fluoroaniline Derivatives.

A. INTRODUCTION

1. Calculation of Coupling Constants

Nuclear magnetic resonance spin-spin coupling was first observed, independently, by Gutowsky and McCall[1] and by Hahn and Maxwell[2] in 1951. Both groups suggested that the observed spin-spin splitting was due to the coupling of nuclear angular momenta and that the magnitude of this coupling energy was proportional to the dot product of the nuclear spin angular momentum operators.

Experimentally the relationship has the form

$$E_{AB} = h\, J_{AB}\, \hat{\underline{I}}_A \bullet \hat{\underline{I}}_B \qquad (1)$$

where E_{AB} is the interaction energy, h is Plank's constant, J_{AB} is the coupling constant in s^{-1} and $\hat{\underline{I}}_A$ and $\hat{\underline{I}}_B$ represent the nuclear spin angular momentum vector operators for nuclei A and B, respectively.

In 1952 Ramsey and Purcell[3] proposed a mechanism for nuclear spin-spin coupling. They proposed that the transmission of spin information went via the molecular electrons. The nuclear spin A polarizes the electrons which in turn polarize the nuclear spin B. The proportionality constant in equation (1) can then be thought of as a measure of the ability of the electrons to transmit nuclear spin state information between nucleus A and nucleus B.

Within a year Ramsey[4], using second-order perturbation theory, had developed the mathematical theory for this electron-mediated coupling mechanism. The second-order interaction energy was written as

$$E_{AB} = \sum_n \frac{\langle 0|\hat{H}|n\rangle\langle n|\hat{H}|0\rangle}{E_o - E_n} \qquad (2)$$

where $|0\rangle$ and $|n\rangle$ are the ground state and excited state molecular wave functions and E_o and E_n are the ground and excited state energies. The summation in (2) is over all excited states including the continuum states.

Ramsey's Hamiltonian was a sum of Hamiltonians for three different electronic coupling mechanisms

$$H = H_{1a} + H_{1b} + H_2 + H_3 \tag{3}$$

The first two terms H_{1a} and H_{1b} are for the energy of interation between the orbital angular momentum of the electrons and the nuclear angular momentum. They take the form

$$H_{1a} = \frac{eh\beta}{c} \sum_{A,B,k} \gamma_A \gamma_B r_{kA}^{-3} r_{kB}^{-3} [(\hat{\underline{I}}_A \cdot \hat{\underline{I}}_B)(\underline{r}_{kA} \cdot \underline{r}_{kB}) - (\hat{\underline{I}}_A \cdot \underline{r}_{kB})(\hat{\underline{I}}_B \cdot r_{kA})] \tag{4}$$

and

$$H_{1b} = \frac{2\beta h}{i} \sum_{A,k} \gamma_A r_{kA}^{-3} \hat{\underline{I}}_A \cdot (\underline{r}_{kA} \times \hat{\underline{\nabla}}_k) \tag{5}$$

where β is the Bohr magneton, γ_A and γ_B are the magnetogyric ratios of nuclei A and B, r_{kA} and r_{kB} are the radius vectors from electron k to nuclei A and B, and $\hat{\underline{\nabla}}$ is the electron velocity vector operator.

The term that describes the dipole-dipole interaction between the nuclear magnetic moments and the electron magnetic moments takes the form

$$H_2 = 2\beta h \sum_{A,k} \gamma_A [3(\hat{\underline{S}}_k \cdot \underline{r}_{kA})(\hat{\underline{I}}_A \cdot \underline{r}_{kA}) r_{kA}^{-5} - (\hat{\underline{S}}_k \cdot \hat{\underline{I}}) r_{kA}^{-3}] \tag{6}$$

where $\hat{\underline{S}}_k$ is the spin angular momentum operator of electron k.

The last term is the Fermi contact Hamiltonian and describes the interaction between the nuclear spin and the electron spin at the nucleus. It is given by

$$H_3 = \frac{16\pi\beta h}{3} \sum_{A,k} \gamma_A \delta(\underline{r}_{kA}) \, \hat{\underline{S}}_k \cdot \hat{\underline{I}}_A \tag{7}$$

where $\delta(\underline{r}_{kA})$ is the Dirac delta function and causes H_3 to operate on the wave function at the site of the nucleus.

Calculations show that for most couplings between protons and other light nuclei the Fermi contact term dominates the other contributions.

Since spin-spin coupling between nuclei is a second-order property, the coupling constants must be calculated either by variation theory or by perturbation theory. Although the variation method has been used for small molecules[5], application of the perturbation method to larger molecules is much easier.

Assuming dominance of the Fermi contact interaction, a second-order perturbation treatment yields the equation for the spin-spin coupling between nucleus A and nucleus B as

$$J_{AB} = \frac{-2}{3h} \left(\frac{16\pi\beta h}{3}\right)^3 \gamma_A \gamma_B \sum_{n=1}^{\infty} \sum_{k}^{N} \sum_{j}^{N} \frac{\langle 0 | \delta(\underline{r}_{kA}) \hat{\underline{S}}_k | n \rangle \langle n | \delta(\underline{r}_{jB}) \hat{\underline{S}}_j | 0 \rangle}{E_n - E_o} \tag{8}$$

The summations over j and k are over all electrons and the other symbols have been previously defined. Application of the closure approximation to equation (8) yields

$$J_{AB} = \frac{-2}{3h} \left(\frac{16\pi\beta h}{3}\right)^2 \frac{\gamma_A \gamma_B}{\Delta E} \sum_{j}^{N} \langle 0 | \delta(\underline{r}_{kA}) \delta(\underline{r}_{jB}) \hat{\underline{S}}_k \cdot \hat{\underline{S}}_j | 0 \rangle \tag{9}$$

The expression now involves only ground state wavefunctions, making the integrals easier to evaluate.

Pople, McIver and Ostlund[6] have developed a method for describing second-order properties that result from distorsion or polarization of the molecular electronic system. This method involves the calculation of self-consistent single determinant molecular orbital wavefunctions in the presence of a samll finite perturbation.

The perturbed Hamiltonian has the form

$$\hat{H}(\lambda) = \hat{H}_o + \sum_r \lambda_r H_r \tag{10}$$

where the $\hat{H}_r$ are independent of the λ paramters. They showed that the Hellman-Feynman theorem holds for L.C.A.O. self-consistent molecular orbital functions as long as the perturbation, λ_r, does not depend on the nuclear configuration. They could then show, using the Hellman-Feynman theorem, that for second-order properties

$$\frac{\partial^2 E}{\partial\lambda_s \partial\lambda_r}\Big|_{\lambda=0} = \frac{\partial}{\partial\lambda}\langle\Psi(\lambda_s)|\hat{H}_r|\Psi(\lambda_s)\rangle\Big|_{\lambda_s=0} \tag{11}$$

where E is the second-order interaction energy, and $\Psi(\lambda_s)$ is the wavefunction such that $\Psi(\lambda_s) = \Psi(0,0,0\ldots\lambda_s\ldots0,0,0)$, ie. all λ's except λ_s are set to zero.

Pople, McIver and Ostlund[7] then applied this technique to the calculation of isotropic nuclear spin coupling. If only the Fermi contact term is considered the total Hamiltonian (10) becomes

$$\hat{H} = H_o + \frac{16\beta}{3}\sum_k^N \sum_l^M \delta(\underline{r}_{kN})\,\hat{\underline{S}}_k \cdot \hat{\underline{I}} \tag{12}$$

where the sum is over N electrons and M nuclei. When calculating the coupling between two nuclei A and B, it is convenient to consider a molecule with the two nuclear moments μ_A and μ_B both directed along the z axis. Then (12) becomes

$$\hat{H} = \hat{H}_o + \mu_A \hat{H}_A' + \mu_B \hat{H}_B' \tag{13}$$

where

$$\hat{H}_A' = \frac{16\beta}{2\pi} \sum_k^N \delta(\underline{r}_{kA}) \hat{S}_{zk} \tag{14}$$

and similarly for $\hat{H}'_B$.

Now using equation (11), the reduced coupling constant can be written as

$$k_{AB} = \frac{\partial}{\partial \mu_B} \langle \Psi(\mu_B) | \hat{H}_A' | \Psi(\mu_B) \rangle |_{\mu_B=0} \tag{15}$$

where the reduced coupling constant K_{AB} and J_{AB} are related by

$$J_{AB} = \frac{h}{2\pi} \gamma_A \gamma_B K_{AB} \tag{15b}$$

and where $\Psi(\mu_B)$ is the wavefunction when only the nuclear moment μ_B is present. The Hamiltonian used to calculate $\Psi(\mu_B)$ is then

$$\hat{H}(\mu_B) = \hat{H}_o + \mu_B \hat{H}_B' \tag{16}$$

The wavefunction $\Psi(\mu_B)$ is calculated as an unrestricted self-consistent molecular orbital function. This is necessary in order to account for the uneven distribution of α and β electrons induced by the perturbation $\mu_B \hat{H}_B$.

Ψ then takes the form

$$\Psi = |\psi_1^{\alpha}(1)\alpha(1)\ldots\psi_n{}^{\alpha}(n)\alpha(n),\psi_1^{\beta}(n+1)\beta(n+1)\ldots\ \psi_n^{\beta}(2n)\beta(2n)| \qquad (17)$$

where the total number of electrons is 2n. Ψ is unrestricted in the sense that ψ_i^{α} and ψ_i^{β} are not required to be identical spatial functions.

The molecular orbitals are linear combinations of atomic orbitals

$$\psi_i^{\alpha} = \sum_{\mu} C_{\mu i}^{\alpha}\ \phi_{\mu} \qquad (18a)$$

$$\psi_i^{\beta} = \sum_{\mu} C_{\mu i}^{\beta}\ \phi_{\mu} \qquad (18b)$$

The coefficients in equation (18) satisfy the matrix form of the Roothan equation

$$\underline{\underline{F}}^{\alpha}\ \underline{\underline{C}}^{\alpha} = \underline{\underline{S}}\ \underline{\underline{C}}^{\alpha}\ \underline{\underline{\varepsilon}}^{\alpha} \qquad (19a)$$

$$\underline{\underline{F}}^{\beta}\ \underline{\underline{C}}^{\beta} = \underline{\underline{S}}\ \underline{\underline{C}}^{\beta}\ \underline{\underline{\varepsilon}}^{\beta} \qquad (19b)$$

where $\underline{S}$ is the overlap matrix, $\underline{\varepsilon}$ is the orbital energy matrix and $\underline{F}$ is the Hartree-Fock energy matrix.

In the presence of a perturbation the S.C.F. equations are modified by a change in the one-electron core part of the Fock matrices

$$F^{\alpha}_{\mu\nu} = H^{core}_{\mu\nu} + \frac{8\pi}{3}\beta\mu_B \int \phi_\mu \delta(\underline{r}_B)\phi_\nu \, d\tau \qquad (20a)$$

$$F^{\beta}_{\mu\nu} = H^{core}_{\mu\nu} - \frac{8\pi}{3}\beta\mu_B \int \phi_\mu \delta(\underline{r}_B)\phi_\nu \, d\tau \qquad (20b)$$

Equation (15) can then be written as

$$K_{AB} = \frac{8\pi\beta}{3} \sum_{\mu} \sum_{\nu} \int \phi_\mu \delta(\underline{r}_A)\phi_\nu d\tau \left[\frac{\partial}{\partial\mu_B} \rho_{\mu\nu}(\mu_B)\right]_{\mu_B=0} \qquad (21)$$

where the summations are over all atomic orbitals and $\rho_{\mu\nu}(\mu_B)$ is an element of the spin density matrix defined as the difference

$$\underline{\rho} = \underline{\rho}^{\alpha} = \underline{\rho}^{\beta}$$

where ρ^{α} and ρ^{β} are the density matrices for α and β spins.

Equation (22) can be used with unrestricted LCAO-SCF wavefunctions for any basis set $\{\phi_\mu\}$ and at any level of approximation.

Although the use of the LCAO-SCF approach without further approximation has yielded accurate calculations for small molecules, its usefulness for larger molecules, unfortunately, is limited by computational difficulties. Two approximations introduced by Pople and co-workers have enjoyed considerable popularity. In the CNDO[8,9] (Complete Neglect of Differential Overlap) approximation the essential features are the use of semi-empirical calculations of parameters, the use of a valence basis set and the neglect of the overlap distributions, $\phi_\mu \phi_\nu$, everywhere except where μ and ν are equal.

The INDO[10] (Intermediate Neglect of Differential Overlap) method is similar to CNDO except that one-center exchange integrals are not neglected. In the INDO approximation the integral in equation (20) is set equal to the valence s orbital of atom B if $\mu = \nu$

$$\int \phi_\mu \, \delta(\underline{r}_B) \phi_\nu \, d\tau = S_B^2(0) \tag{23}$$

The perturbation term in equation (20) simply becomes a constant

$$h_B = \frac{8\pi}{3} \beta\mu_B \, S^2{}_B \, (0) \tag{24}$$

From equation (22) the reduced coupling constant is now

$$K_{AB} = (\frac{8\pi\beta}{3})^2 \, S_A^2 \, (0) S_B^2(0) \, [\frac{\partial}{\partial h_B} \rho_{S_A S_B}(h_B)]_{h_B=0} \tag{25}$$

According to (25) the nuclear spin-spin coupling is then proportional to the derivative of the diagonal element of the spin-density matrix, ρ, corresponding to the valence s orbital of atom A.

Pople et al.[7] used the method of finite differences to approximate the derivative in (25)

$$K_{AB} = (\frac{8\pi\beta}{3})^3 S_A^2(0) S_B^2(0) \; [\frac{\rho(h_B)}{h_B}] \qquad (26)$$

The error in approximation was shown to be a minimum when h_B is approximately 10^{-3} hartrees.

With the vast improvements in computer capabilities and the increased availability of computer facilities, CNDO FPT and INDO FPT calculations have become commonplace. The calculation of nmr coupling constants has been reviewed by Kowalewski[11,12].

2. Stereospecific couplings between sidechain protons and protons on the benzene ring

The long-range coupling between sidechain nuclei and benzene ring nuclei can be discussed in terms of three mechanisms; the σ mechanism, the π mechanism and the through-space mechanism.

In the σ mechanism, coupling is transmitted by the σ bond framework. This does not necessarily mean that spin information is passed on through each intervening σ bond. In the vicinal fragment, for example, coupling might contain σ contributions from the direct interaction of the electrons in the carbon-hydrogen bonds. (see Figure 1).

Karplus[13] predicted the dependence of the vicinal proton-proton coupling in ethane on the dihedral angle ϕ between the two proton-carbon bonds. The coupling constant is approximately

$$^{3}J/Hz = 4.42 - 0.5\cos\theta + 4.5\cos^{2}\theta \qquad (27)$$

Wasylishen and Schaefer[14a], in an attempt to decompose the angular dependance of $^{5}J_{CH_3,H}$ in toluene, suggest that the σ electron dependence of $^{5}J_{CH_3,H}$ takes the form

$$^{5}J_{H_5,CH_3} = B\sin^{2}(\theta/2) \qquad (28)$$

where B is $^{5}J^{\sigma}_{180}$, the maximum value of the coupling when θ is 180°. θ is the angle by which the C-H bond of the methyl group twists out of the benzene plane (see Figure 2). This relationship has recently been

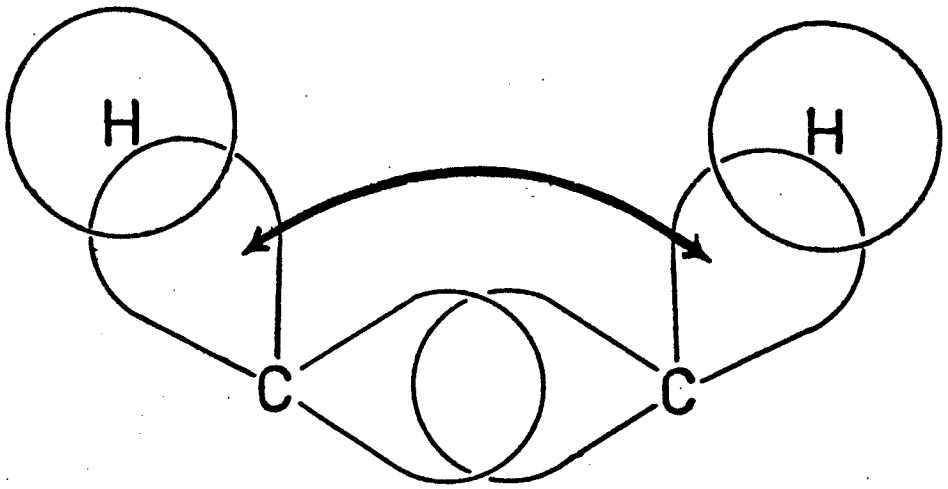
H
H
C
C

Figure 1.

A valence bond picture of the fragment involved in the vicinal proton-proton coupling.

The double-headed arrow connects orbitals for which the exchange interaction dominates the coupling.

substantiated by experimental data on toluene derivatives[14b]. $^5J_{SH,H4}$ in thiophenols[15] appears to have a similar σ component.

The π mechanism[16] involves transmission of spin state information via the π electrons. The p orbitals of the π system have their nodes at the nuclei, hence π electron density at the nuclei vanishes and there can be no Fermi contact interaction. McConnel stated in 1957 that a polarization of the σ electrons by the π electrons, known as the σ-π interaction, could result in transmission of spin density from the π electron system to the nuclear site.

An angular dependence has been proposed[14a] for the σ-π contribution to the coupling between α-protons and the benzene ring protons. The relationship can be written as

$$J = J_{90}^{\pi} \sin^2\theta \qquad (29)$$

where J_{90}^{π} is the value of the coupling when θ is 90°. This is analogous to the McConnel-Heller equation[17] in electron spin resonance spectroscopy. Equation (30) can be rationalized by a π mechanism transmitted via hyperconjugation between the σ orbital of the side chain group and the π orbitals of the aromatic ring, followed by a σ-π interaction of the aromatic π orbitals with the σ orbitals of the C-H or C-X bonds of the ring.

The third mechanism, known as the through-space or proximate coupling, involves transmission of spin information between two spatially proximate nuclei via overlap of their electron orbitals. This mechanism does not involve spin coupling through the formal bonds.

The INDO FPT and CNDO FPT methods are capable of calculating some

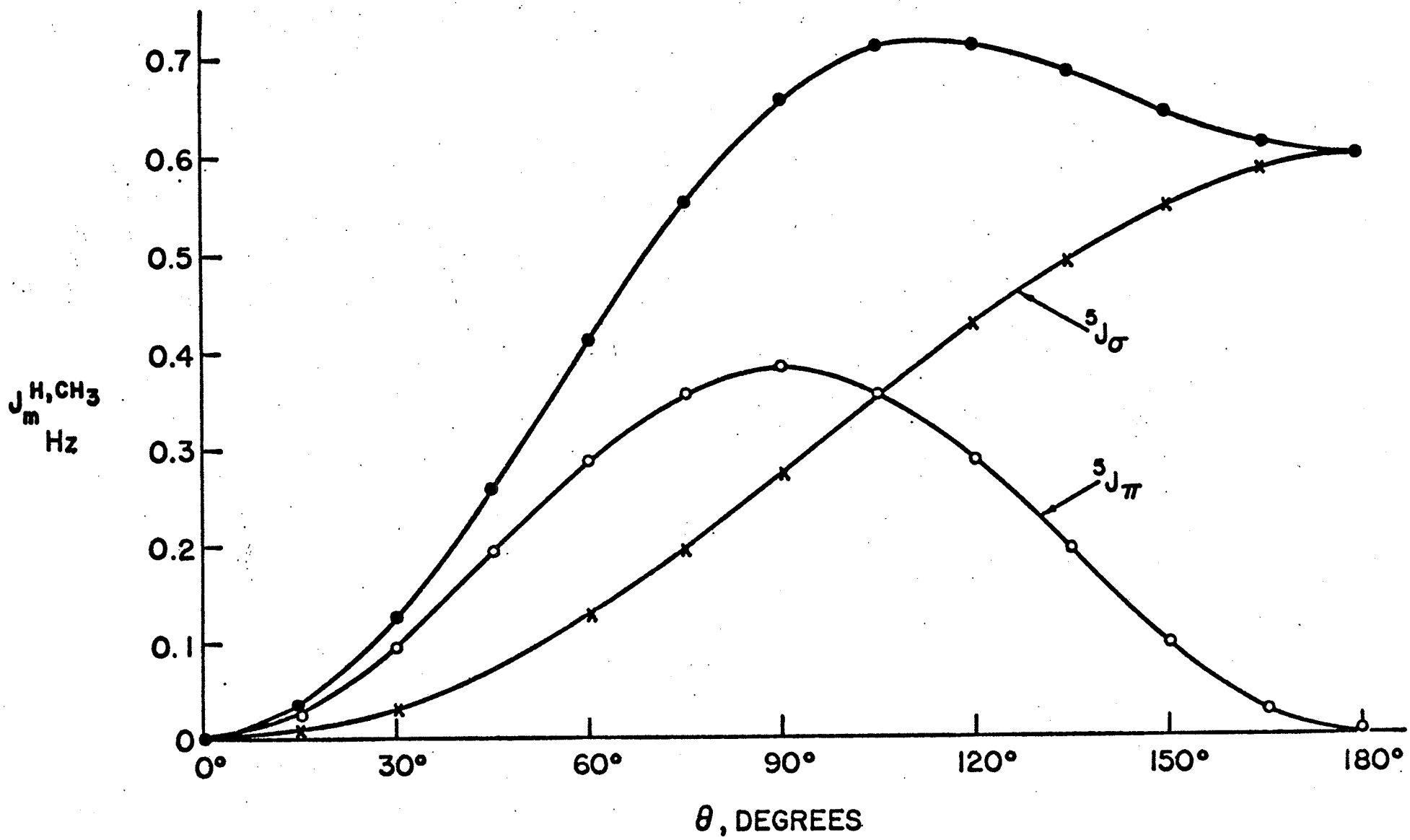
0.7
0.6
0.5
0.4
0.3
0.2
0.1
0
J_m^{H,CH_3} Hz
$^5J_\sigma$
$^5J_\pi$
0°
30°
60°
90°
120°
150°
180°
θ, DEGREES

Figure 2

The coupling over five bonds between ring and methyl protons in toluene, $^{5}J_{H,CH_3}$, as calculated by Wasylishen and Schaefer (reference 14a). Closed circles represent the INDO calculated coupling, open circles and crosses are the π and σ contributions respectively.

through-space couplings. Such calculations were first done by Wasylishen and Schaefer[14a] for o-xylene and gave a negative coupling when the protons were spatially proximate. Unpublished calculations by Wasylishen and Schaefer suggest that through-space coupling between protons separated by more than 2.2 Å is unlikely. The rather strong dependence of the through-space coupling on spatial proximity renders it a valuable tool for conformational analysis[18]. The subject of through-space coupling was reviewed by Hilton and Sutcliffe[19] in 1975.

3. Streospecific coupling between sidechain protons and fluorine nuclei on the benzene ring

Couplings from α protons to ring fluorine nuclei have not been investigated to as great an extent as proton-proton couplings. The benzene derivatives most studied are toluenes[20,21], phenols[22,23] and benzaldehydes[24]. Of the three, fluorotoluenes have received the most attention.

In a recent investigation of 22 derivatives of 2-fluorotoluene[21], $^4J_{CH_3,F_2}$ is attributed to a dominant σ-π mechanism together with contributions from the σ electron and/or proximate mechanisms. Evidence for mechanisms other than the σ-π interaction comes from the substituent dependence of $^4J_{CH_3,F}$. Since the σ-π mechanism is approximately substituent independent, other substituent dependent mechanisms must be present. Figure 3 shows the INDO MO FPT values for $^4J_{CH_3,F}$ as a function of the angle θ. The empirical couplings are also plotted in figure 3. The INDO curve shows the dominance of a positive σ-π component and the importance of a through-space component. Although the empirical curve also contains the large σ-π component, there exists a positive interaction as θ approaches 0°. This is thought to be due to positive σ and/or through-space interactions.

Unpublished INDO FPT calculations for 2-fluorophenol delineate a curve similar to that in figure 3. The $^4J_{OH,F}$ values at 0° and 180° have been determined for 2-fluorophenol derivatives as $^4J^{OH,F}_{cis} = -4.42$ Hz and $^4J^{OH,F}_{trans} = -0.45$ Hz and for 2-fluorobenzaldehyde derivatives as $^4J^{OCH,F}_{cis} = -0.20$ Hz and $^4J^{OCH,F}_{trans} = -1.60$ Hz.

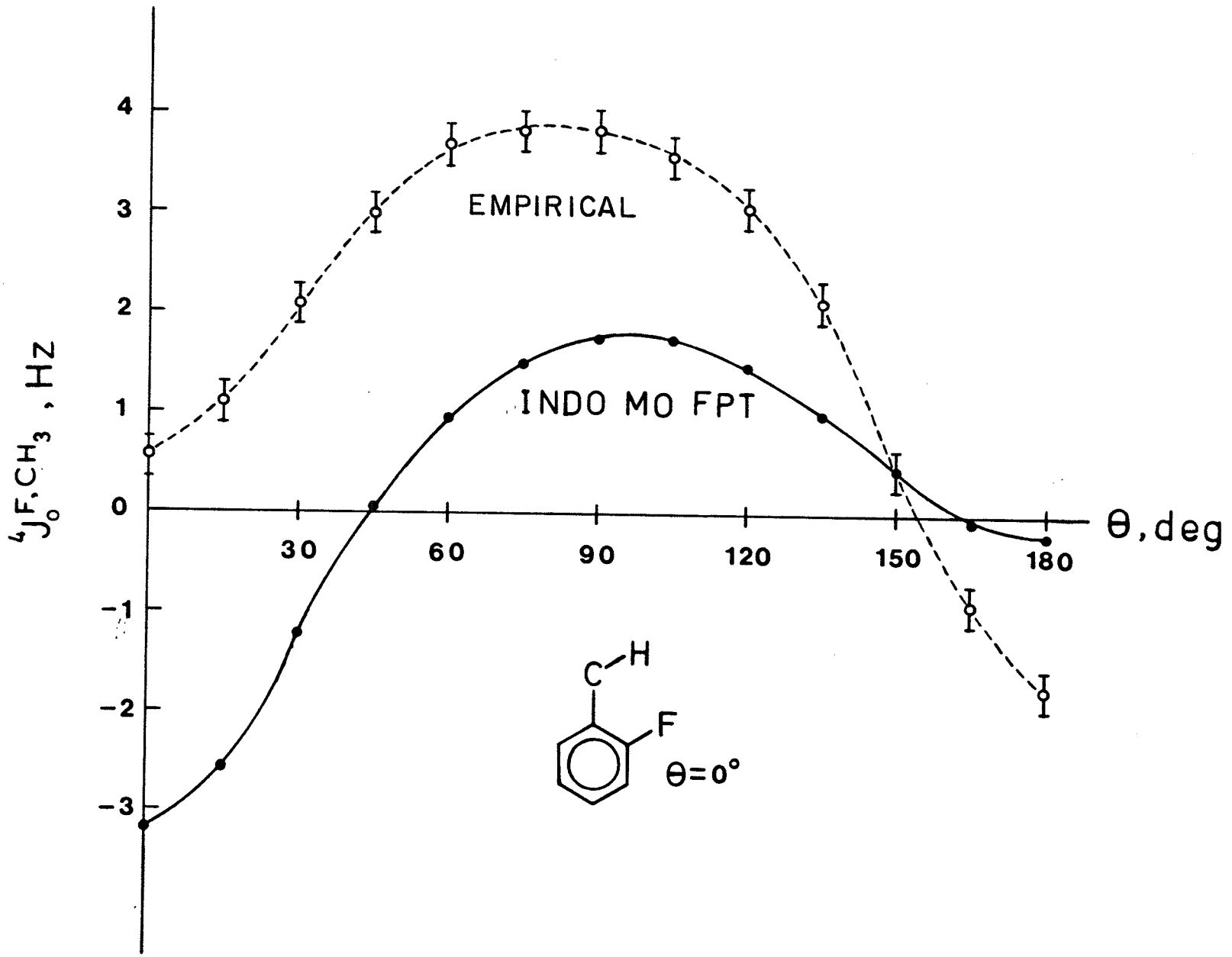
4
3
2
1
0
−1
−2
−3
$^4J_{o}^{F,CH_3}$, Hz
EMPIRICAL
INDO MO FPT
30
60
90
120
150
180
θ, deg
C
H
F
θ=0°

Figure 3

A plot of the INDO MO FPT values of $^{4}J^{F,CH_3}$ for 2-fluorotoluene versus the angle θ. The empirical couplings as determined by Schaefer *et al.* are shown in the upper curve. Taken from reference 21.

The coupling mechanism of $^5J_m{}^{CH_3,F}$ in 3-fluorotoluene derivatives has been investigated by Schaefer, Danchura and Niemczura[20]. INDO FPT calculations for $^5J_m{}^{CH_3,F}$ give an angular dependence that can be reproduced by

$$^5J^{CH_3,F}_{meta} = 0.57 - 2.60 \sin^2\theta + 1.68 \sin^2(\theta/2) \qquad (30)$$

in which the $\sin^2\theta$ term arises from the σ-π mechanism and the $\sin^2(\theta/2)$ term arises from the σ mechanism. Since the barrier in 3-fluorotoluene is only 42 cal/mol (175 J/mol)[25], an average of 13 calculated values can be reasonably taken and is +0.11 Hz. This is fairly close to the experimental value of -0.23 Hz. It may well be that the constant term, 0.57 Hz, is an artifact of the calculations. In that event, $^5J^{CH_3,F}$ becomes -0.46 Hz, because both $\langle\sin^2\theta\rangle$ and $\langle\sin^2(\theta/2)\rangle$, the expectation values of $\sin^2\theta$ and $\sin^2(\theta/2)$, are very near 0.5. An experimental check of equation (30) could be done by "locking" benzal compounds into the cis and trans conformers with the appropriate ortho substituents.

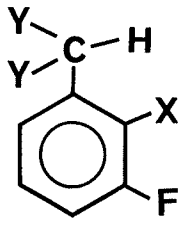

CIS

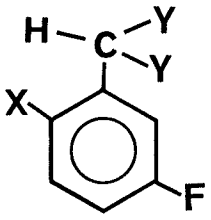

TRANS

This would be reasonable only if substitution at the α and ortho positions did not significantly perturb the coupling mechanism of $^5J_{meta}^{CH,F}$.

Unpublished INDO MO FPT data for 3-fluorophenol show the same angular relationship

$$^5J_{meta}^{OH,F} = 0.31 - 2.76 \sin^2\theta + 2.62 \sin^2\theta/2 \qquad (31)$$

Experiment gives $^5J_{trans}^{OH,F} = 1.56$ and $^5J_{cis}^{OH,F} = -0.35$. Apparently INDO overestimates the all-trans coupling. This is not surprising since the INDO method usually overestimates $^5J_{trans}$ in benzene derivatives. Phenols have a planar ground state conformation and rather high barriers to internal rotation, hence can be discussed in terms of a cis-trans equilibrium[22,26,27]. With this is mind, the $^5J^{OH,F}$ in pentafluorophenol should then be the average of cis and trans couplings, (1.56-0.35)/2 = 0.61 Hz. The experimental value is 0.59 Hz[22].

INDO MO FPT calculations for 4-fluorotoluene suggest that $^6J_p^{CH_3,F}$ is transmitted via a σ-π mechanism and do indeed obey a $\sin^2\theta$ relationship. The angular dependence of $^6J^{CH_3,F}$ can be written

$$^6J_p^{CH,F} = -0.008 + 1.872 \sin^2\theta \qquad (32)$$

$$\simeq 1.87 \sin^2\theta$$

Since the rotational barrier in 4-fluorotoluene is only 13.8 cal/mol (57.7 J/mol)[28], $\langle\sin^2\theta\rangle$ is 0.5, yielding a predicted $^6J_p^{CH_3,F}$ of 1.87 x 0.5 = 0.94 Hz. The experimental value is 1.12 Hz[29].

The $\sin^2\theta$ dependence of $^6J_p^{CH,F}$ lends itself to an application of the J method[30] to the determination of small (<20 kJ/mol) twofold barriers to internal rotation about the ring carbon to methylene carbon bond for 4-fluorobenzyl compounds. A number of 4-fluorobenzyl compounds were analyzed by Schaefer, Danchura, Niemczura and Peeling[29]. The barriers they calculated were in fair agreement with the more reliable barriers derived from the $^6J^{CH_2X,H}$ values in 3,5-dihalobenzyl compounds.

The six-bond α-proton to ring fluorine couplings have been investigated to a lesser extent in other <u>para</u>-fluorobenzene derivatives. In 4-fluorothiophenol, where the barrier is small (0.5 ± 0.2 kcal/mol, 2.1 ± 0.8 kJ/mol), the value of $^6J^{SH,F}$ is 1.00 Hz. In 2,6-dibromo-4-fluorophenol, where the hydroxyl group is held in the plane of the benzene ring by intramolecular hydrogen bonding to bromine, $^6J^{OH,F}$ is -0.27 Hz[22]. In 4-fluorobenzaldehyde, in which planar conformations presumably predominate, $^6J_p^{OCH,F}$ is -0.44 Hz[24].

4. Introduction to the Problem

Stereospecific long-range nmr spin-spin couplings between side chain protons and ring fluorine nuclei have been investigated in fluorotoluenes, fluorophenols and fluorobenzaldehydes. Comparisons have been made with coupling constants calculated by the INDO MO FPT method.

It is the intent of this work to investigate the stereospecific long-range nmr spin-spin couplings between the amino protons and the ring fluorine nuclei in some fluoroaniline derivatives both experimentally and by application of the INDO method.

B. EXPERIMENTAL METHOD

1. Preparation of Compounds

Most of the N-methylaniline derivatives were made by monomethylation of the corresponding anilines. 2,5-difluoro-N-methylaniline (the aniline from Aldrich), 2-cyano-3-fluoro-N-methylaniline (the aniline from Maybridge), 2-fluoro-N-methylaniline (the aniline from Aldrich) and 2,6-difluoro-N-methylaniline (the aniline from Aldrich) were made by the method of Johnstone, Payling and Thomas[31] (see figure 4). 2,6-dibromoaniline (Aldrich) could not be methylated in this way due to the steric bulk of the ortho bromine substituents and was made from 2,6-dibromoaniline via the formamide[32] (see figure 5). 4-fluoro-N-methylaniline was purchased from Aldrich. 2,4-Dibromo-6-fluoro-N-methylaniline was made by the standard method of brominaton in acetic acid of 2-fluoro-N-methylaniline, as were 4-bromo-2,6-difluoroaniline, 2,4,6-tribromo-3-fluoroaniline. All products were characterized by mass spectroscopy and by nmr spectrosocpy. Yields were not optimized. Products were usually better than 90% pure.

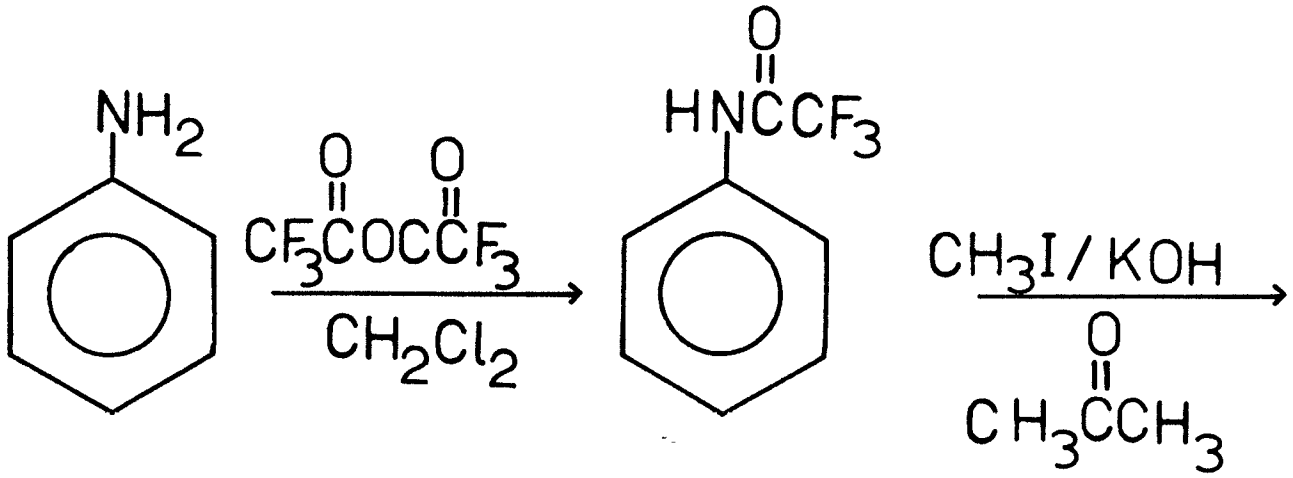
NH2
O O
CF3COCCF3
CH2Cl2
O
HNCCF3
CH3I / KOH
O
CH3CCH3

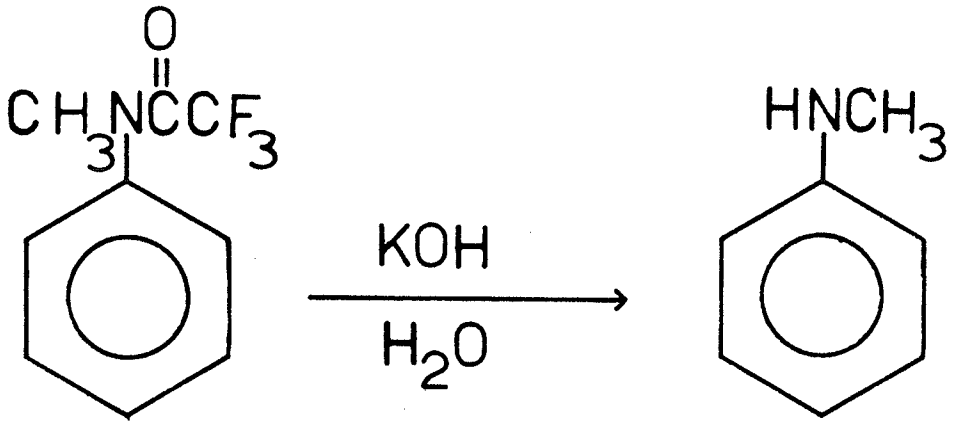
O
CH3NCCF3
KOH
H2O
HNCH3

Figure 4

Preparation of N-methylaniline by the method of Johnstone, Payling and Thomas.

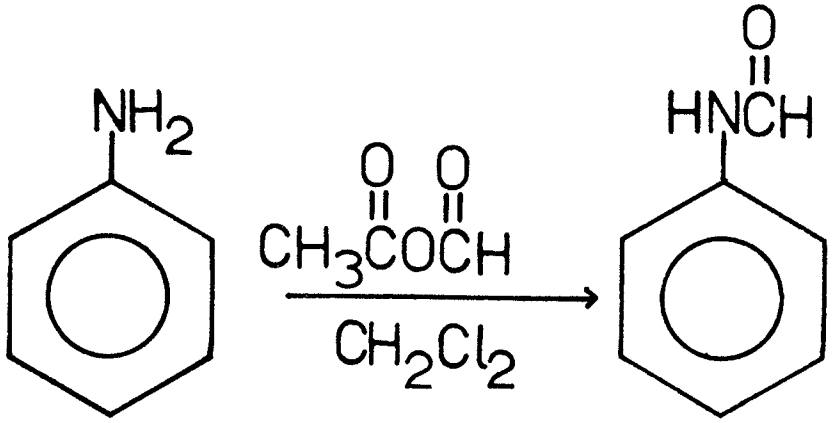
NH2
O O
CH3COCH
CH2Cl2
O
HNCH

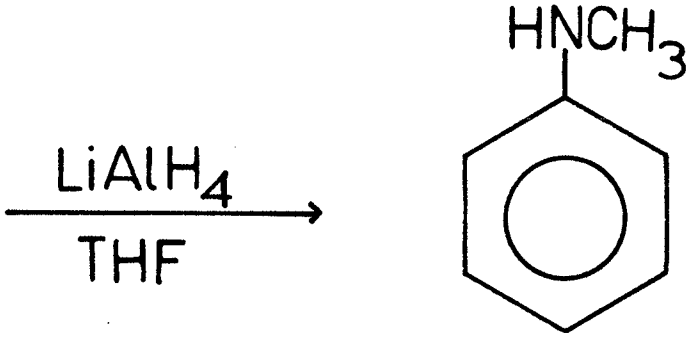
LiAlH4
THF
HNCH3

Figure 5

Preparation of N-methylaniline from aniline via the formamide.

2. Sample preparation

The procedure for retarding intermolecular exchange of the amino protons follows.

Alfa-Ventron sieve (1/16 inch pellets with 3Å pore size), Davison molecular sieve from Lisher (4-8 mesh beads with 3Å pore size), basic alumina, precission bore 5 mm od nmr sample tubes fitted with ground glass joints, stopcocks fitted with ground glass joints and Pasteur pipettes were dried in an oven at 200°C. Some of the pipettes contained wads of cotton wool to serve as filters. The dried materials were transferred to a hot-plate held at 150°C inside a dry-box. All solvents used in the sample preparation had been previously dried by storing over the dry sieve.

5 mole % solutions of the compounds in benzene were prepared with a small amount of tetramethylsilane added as an internal lock for the Varian HA-100 (several drops) or as an internal shift reference for the Bruker WH-90 (1 drop). A drop of hexafluorobenzene was added as an internal shift reference for the ^{19}F nmr samples. Degassing the 2,5-difluoro-N-methylaniline in benzene solution always resulted in cracking of the sample tubes. A sample of this compound in toluene-d_8 was successfully prepared. The solutions were dried over sieve in a sealed vial, inside the dry box, for approximately five days. The vials were shaken occasionally during this period. In the dry box, the sample solutions were filtered through cotton wads in pipettes into nmr tubes, each containing two pellets of dried sieve and a small amount (about equal to two pellets in volume) of basic alumina. Before the tubes were removed from the drybox, stopcocks were attached

to close off the samples. The samples were then degassed using the freeze-pump-thaw technique. Five degassing cycles were performed before the nmr tubes were flame-sealed. Note that due to solvent evaporation during the drying period, the transfer of solutions in the dry box, and degassing cycles, the actual concentration of the samples will have increased slightly; hence only approximate sample concentration will be given.

In several samples the intermolecular exchange could not be sufficiently retarded. In 4-fluoro-N-methylaniline, 2,6-difluoro-4-bromo-N-methylaniline and 2,6-dibromo-N-methylaniline intermolecular exchange of the amino protons yielded spectra displaying no coupling between amino and ring protons.

3. Spectroscopic Method

Proton and fluorine nuclear magnetic resonance experiments were done on a Bruker WH-90 Fourier transform spectrometer and proton experiments were performed on a Varian HA-100-D continuous wave spectrometer in the frequency sweep mode.

The calibration of spectra on the HA-100 has been described recently[33]. Peak frequencies were calculated by interpolation of peak positions between calibration lines. The frequencies of these lines were the differences between the manual and sweep oscillator frequencies, which were read from a Hewlett-Packard HP5323A frequency counter. These calibrations were repeated several times and the standard deviations were usually ≤ 0.020 Hz.

Strong (decoupling) and weak (tickling) irradiation experiments on the HA-100 were performed with a second HP-4204A oscillator, which was adjusted to perturb the desired transition while avoiding proximate transitions. Since the methyl proton part of the spectra consisted of two peaks separated by about 5 Hz due to coupling to the amino proton, irradiation by a single external oscillator could not decouple the methyl protons. Hence a triple resonance experiment, using both HP4204A oscillators to irradiate the two methyl peaks, was performed. The manual oscillator was then used as an internal oscillator to supply the lock frequency during these triple resonance experiments.

The experiments on the Bruker WH-90-DS made use of a dedicated Nicolet 1180 computer system. The deuterated solvent was used as the internal locking material. The probe temperature was maintained at 305 ± 1 K by a Bruker B-ST100/700 temperature controller. Quadrature

phase detection and automatic baseline correction were used. In some cases it was necessary to decouple the methyl protons. Proton sweep widths were 800 Hz or 200 Hz. Due to the wide range of fluorine chemical shifts, survey spectra with sweep width of 10,000 Hz were acquired before the spectral regions of interest were more closely examined with sweep widths of 200 Hz. Digital resolution was typically 0.05 Hz/real point. Exponential multiplication of the free induction decay with line broadenings of -0.01 or -0.02 was performed in order to decrease linewidth and to improve resolution.

4. Computations

Spectral analyses and simulations were performed with the programs LAME[34,35] or NUMARIT[36] in the iterative and non-iterative modes; both programs were coupled to a plotting routine.

Ab initio molecular orbital calculations were performed at the STO-3G level[37] with the program GAUSSIAN 70[38].

Coupling constants were calculated using the INDO FPT technique[10] and employed the optimum geometries from the ab initio calculations (the actual optimum geometries are given in Part II of this thesis).

All curves were statistically fitted to $\sin^2\theta$ and $\sin^2(\theta/2)$ functions using the SAS nonlinear regression program NLIN[39]. Both the Gauss-Newton method, where derivatives of the functions must be supplied in the input data and the multivariant secant method, where derivatives are estimated from the history of the iterations, were used. SAS/GRAPH[40] programs were written in order to plot the curves on a VERSATEC plotter. Smooth curves through data points were obtained by using a spline interpolation which is part of the SAS/GRAPH library.

Computations were performed on an Amdahl 470/V8 or Amdahl 580/5850 system.

C. EXPERIMENTAL RESULTS

1. 2,4-dibromo-6-fluoro-N-methylaniline

Results of the analyses of proton and fluorine spectra of a 5.0 mol % solution of 2,4-dibromo-6-fluoro-N-methylaniline in C_6D_6 appear in table 1. No difficulties were encountered in the analysis. The spectral lines are rather broad as are the lines for most of the N-methylanilines in this work. Small couplings from the methyl and ring nuclei to the "incompletely relaxing" quadrupolar ^{14}N nucleus is a likely reason.

A first-order representation of the line spectrum of the methyl protons, of the ortho fluorine nucleus and of the meta proton H5, is depicted in figure 6.

Table 1.

Spectral parameters[a] for a 5.0 mol% solution of 2,4-dibromo-6-fluoro-N-methylaniline in C_6D_6.

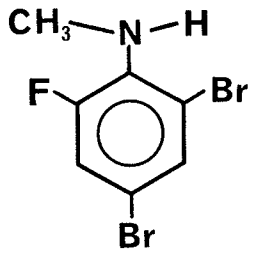

	^{19}F analysis[b]	^{1}H analysis[c]
ν_{CH_3}		258.216(1)
ν_{H3}		714.917(1)
ν_{H5}		682.103(1)
ν_{NH}		360.0[d]
ν_{F}	999.519(2)	
$^{3}J_{NH,CH_3}$		5.557(3)
$^{3}J_{F6,H5}$	12.345(4)	12.309(2)
$^{4}J_{H3,H5}$		2.221(1)
$^{4}J_{NH,F6}$	-2.549(4)[e]	
$^{5}J_{H3,F6}$	-1.695(4)	-1.676(2)
$^{5}J_{F6,CH_3}$	4.779(2)[e]	4.757(3)[e]
$^{5}J_{NH,H5}$		0.570(2)
$^{5}J_{NH,H3}$		<0.05[f]
$^{6}J_{CH_3,H5}$		0.035(10)[f]

Table 1...cont'd...

transitions calculated		256
transitions assigned	42	128
observed peaks	27	16
largest difference	0.029	0.020
r.m.s. error	0.013	0.007

[a] At 305 ± 1 K, signs of couping constants are taken from related compounds, except where noted; numbers in parentheses are standard deviations in the last digit of parameters; all parameters determined by a LAME analysis.

[b] ^{19}F spectrum recorded at 84.700 MHz; coupling constants in Hz; F6 was treated in the X approximation and given an arbitrary value. Blanks indicate parameters not iterated on in the ^{19}F analysis.

[c] Chemical shifts are in Hz at 100.001 MHz, to low-field of internal TMS. Blanks indicate parameters not iterated on in the ^{1}H analysis.

[d] Estimated, no transitions were assigned.

[e] Signs determined by double resonance experiments.

[f] Estimated from decoupling experiments and linewidth simulations (deconvolution of Lorentzian peaks).

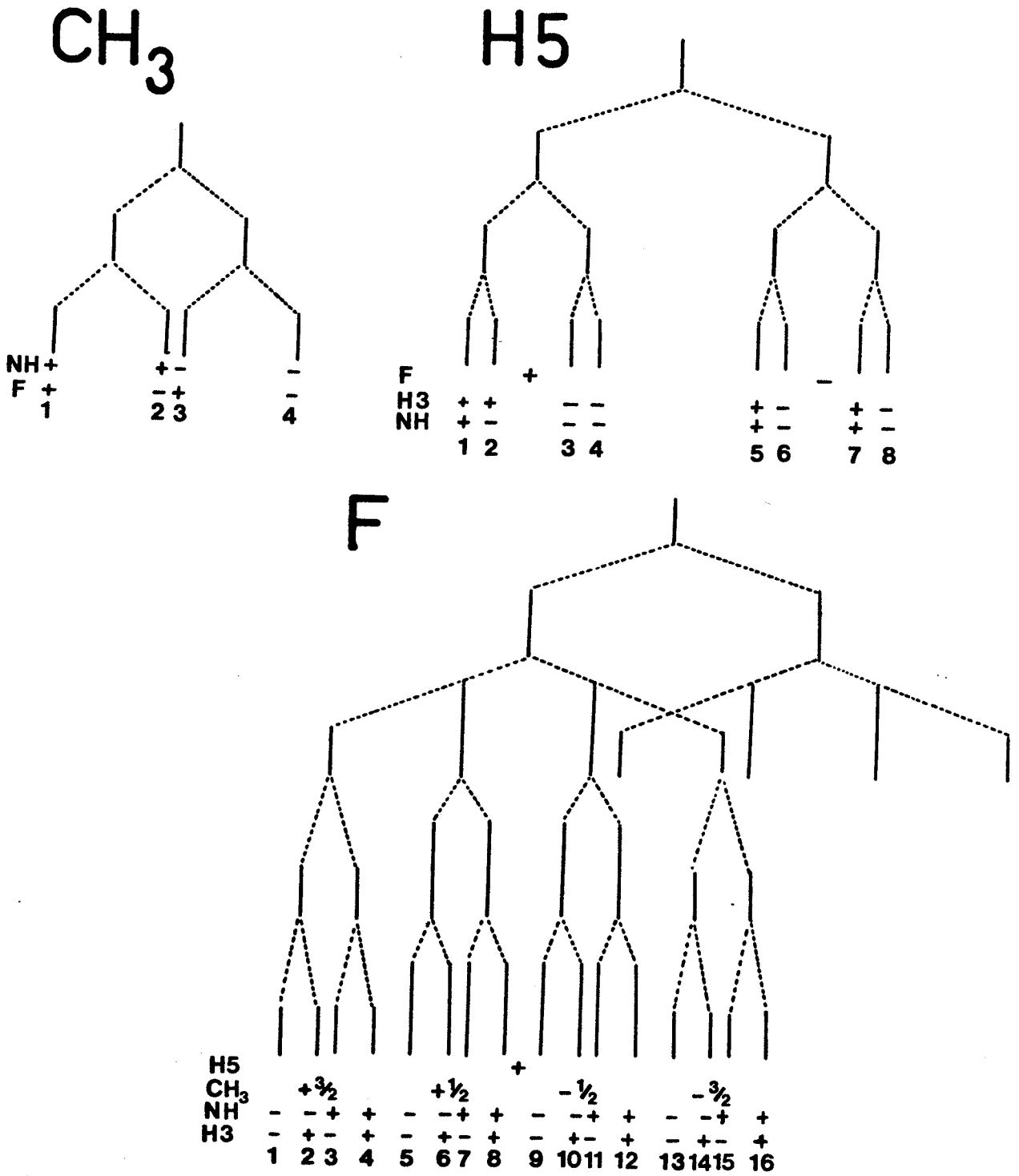
CH3
NH + F + 1
+ − − + 2 3
− − 4
H5
F + − H3 + + − − NH + − − − 1 2 3 4 + − + − 5 6 7 8
F
H5 CH3 +3/2 +1/2 −1/2 −3/2
NH − − + + − − + + − − + + − − + +
H3 − + − + − + + − + − + − − + − +
1 2 3 4 5 6 7 8 9 10 11 12 13 14 15 16

Figure 6

A first-order representation of the line spectrum of the methyl protons, of the meta proton H5, and of part of the multiplets due to F6 of 2,4-dibromo-6-fluoro-N-methylaniline.

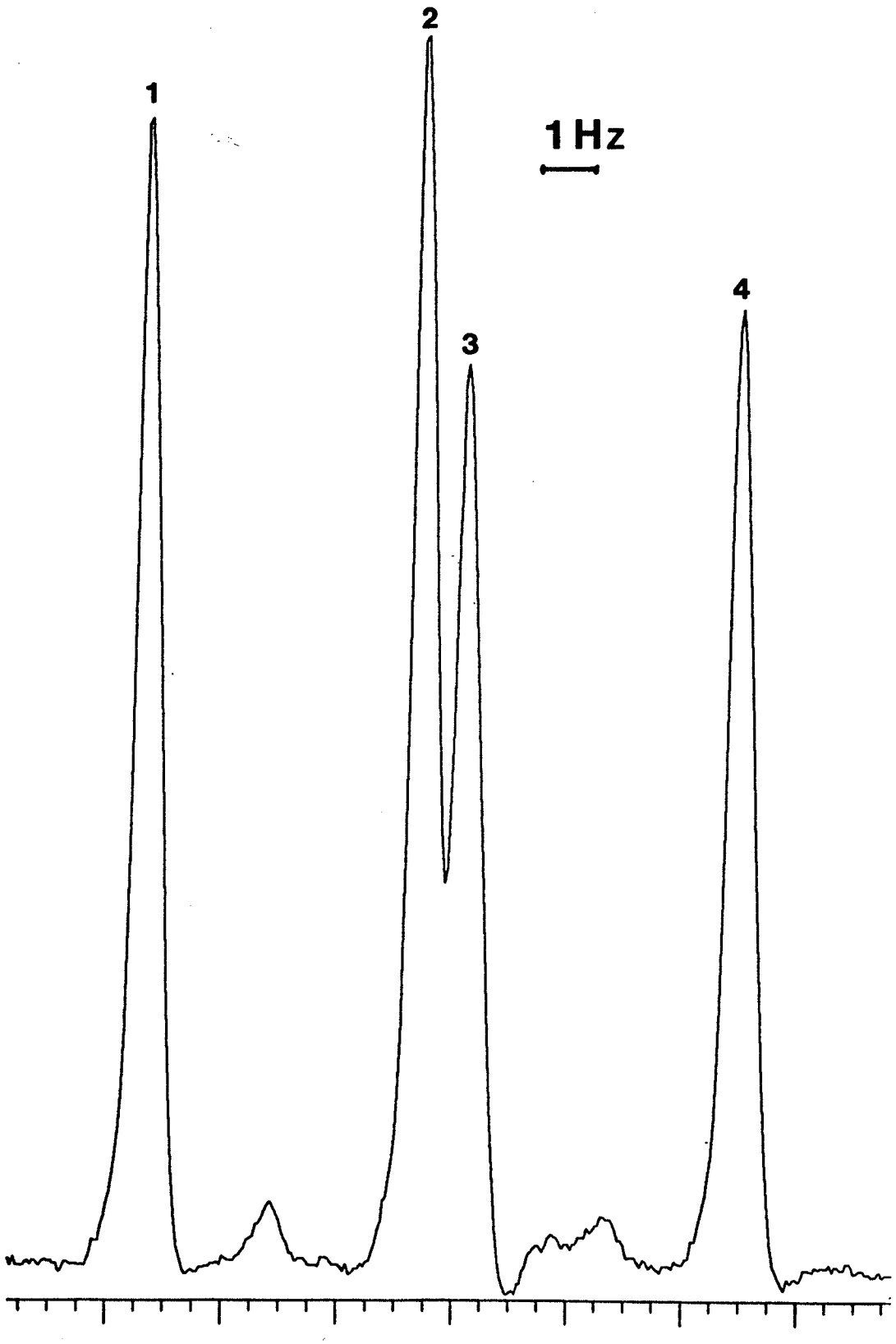
1
2
3
4
1 Hz

Figure 7

The methyl proton peaks for 2,4-dibromo-6-fluoro-N-methylaniline.

a) determination of the relative sign of $^{5}J_{CH_3,F}$ by double resonance experiments

The position of a transition within a multiplet depends on the magnetic environment of the nucleus undergoing that transition. Hence each transition for a nucleus corresponds to a specific orientation of the other coupled nuclei in the molecule. If the spin states of a nucleus are designated by + and -, and the low-field (high frequency) transition is taken as + when the coupling constant is positive, the relative signs of the nuclear spin-spin coupling may be determined by double resonance experiments. Irradiation of a transition in the multiplet of a nucleus will perturb only transitions, in the multiplets of other nuclei, that share a common energy level. Since the high resolution nmr Hamiltonian is symmetric with respect to reversal of all signs, only the relative sign of coupling constants can be determined. Signs of coupling constants are taken relative to the one bond carbon-proton coupling which is known to be positive.

With reference to figure 6; irradiation of line 1 of the methyl protons perturbs lines 1 and 3 of the H5 proton resonance (see figure 8b). The irradiation causes the intensity of these two lines to increase. These lines are associated with the + spin state of fluorine, since the sign of $^{3}J_{H5,F6}$ is positive. Therefore line 1 of the methyl group is designated as +, i.e. $^{5}J_{CH_3,F}$ is also positive.

Irradiation of line 4 of the methyl protons perturbs lines 6 and 8 of H5 (figure 8c). These two lines are associated with the - spin state of fluorine, thus confirming the positive sign of $^{5}J_{CH_3,F}$. The decoupling of the methyl protons causes the connected H5 to sharpen.

They sharpen because the coupling to the methyl protons is present but is too small to be observed.

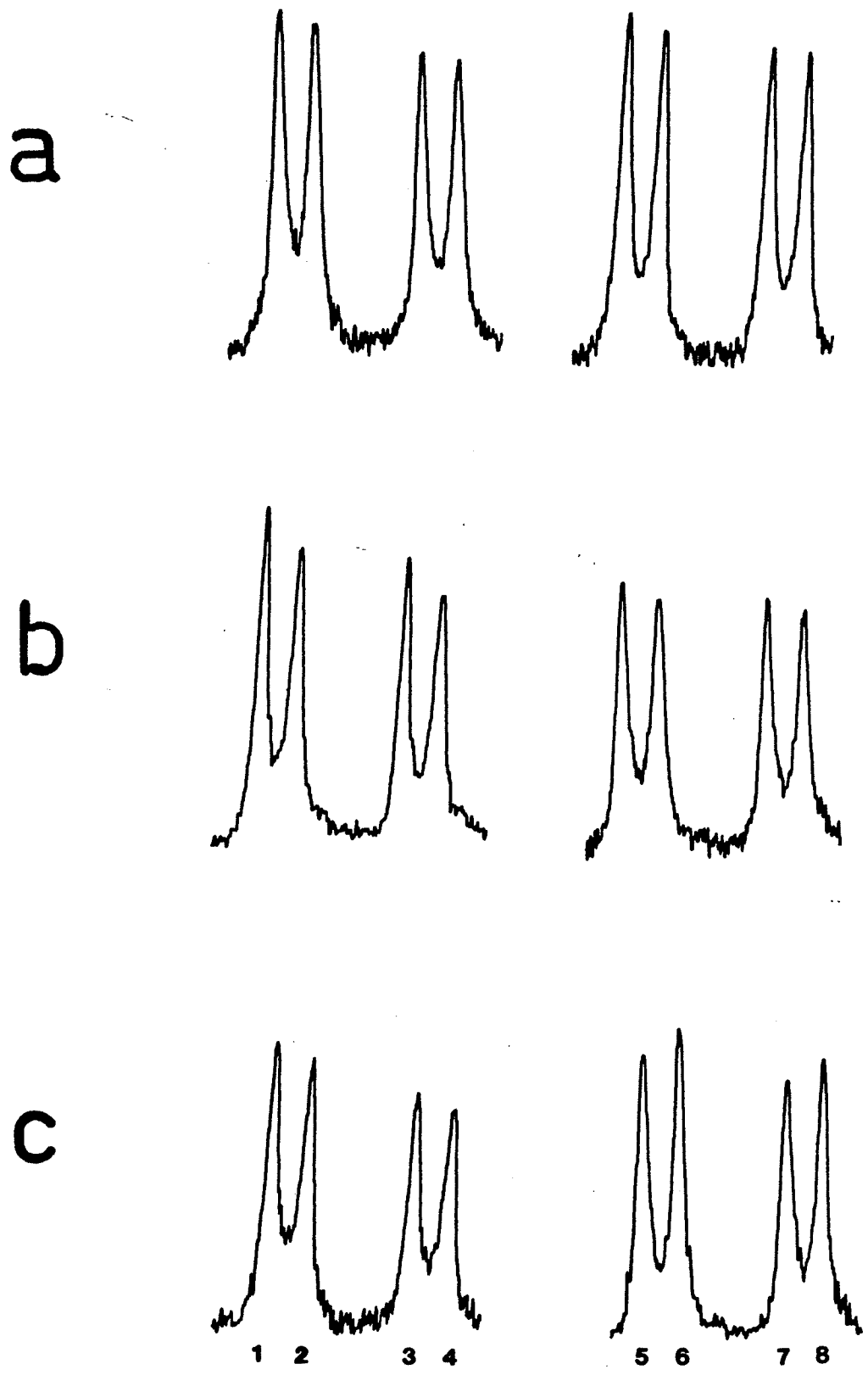
a
b
c
1 2 3 4
5 6 7 8

Figure 8

a) The proton magnetic resonance spectrum of H5 of 2,4-dibromo-6-fluoro-N-methylaniline.

b) With irradiation of line 1 of the methyl group.

c) With irradiation of line 4 of the methyl group.

b) determination of the relative sign of $^4J^{NH,F6}$ by double resonance experiments

The fluorine spectrum of F6 is shown in figure 9. The line spectrum of F6 is shown in figure 6. Only half the lines in this spectrum are numbered, so as not to complicate the diagram. There are a total of 32 lines in the F6 spectrum. Weak irradiation of line 1 of the methyl protons causes a dramatic reduction in the intensity of lines 3,4,7,8,11,12,19,20,23,24,27 and 28 of the F6 spectrum. These are indicated by arrows in figure 10a. These are the high-field peaks associated with splitting due to the amino proton. Since line 1 is the low-field methyl peak associated with the splitting due to the amino proton, $^4J^{NH,F}$ and $^3J^{NH,CH_3}$ are of opposite signs. $^3J^{NH,CH_3}$ is known to be positive[41]. Therefore $^4J^{NH,F}$ is negative. This assignment is confirmed by irradiation of line 4 of the methyl group, designated as - for the amino proton spin state. The alternative lines 5,6,9,10,13,14,17,18,21,22,25,26,29 and 30 decrease in intensity as indicated by the arrows in figure 10b.

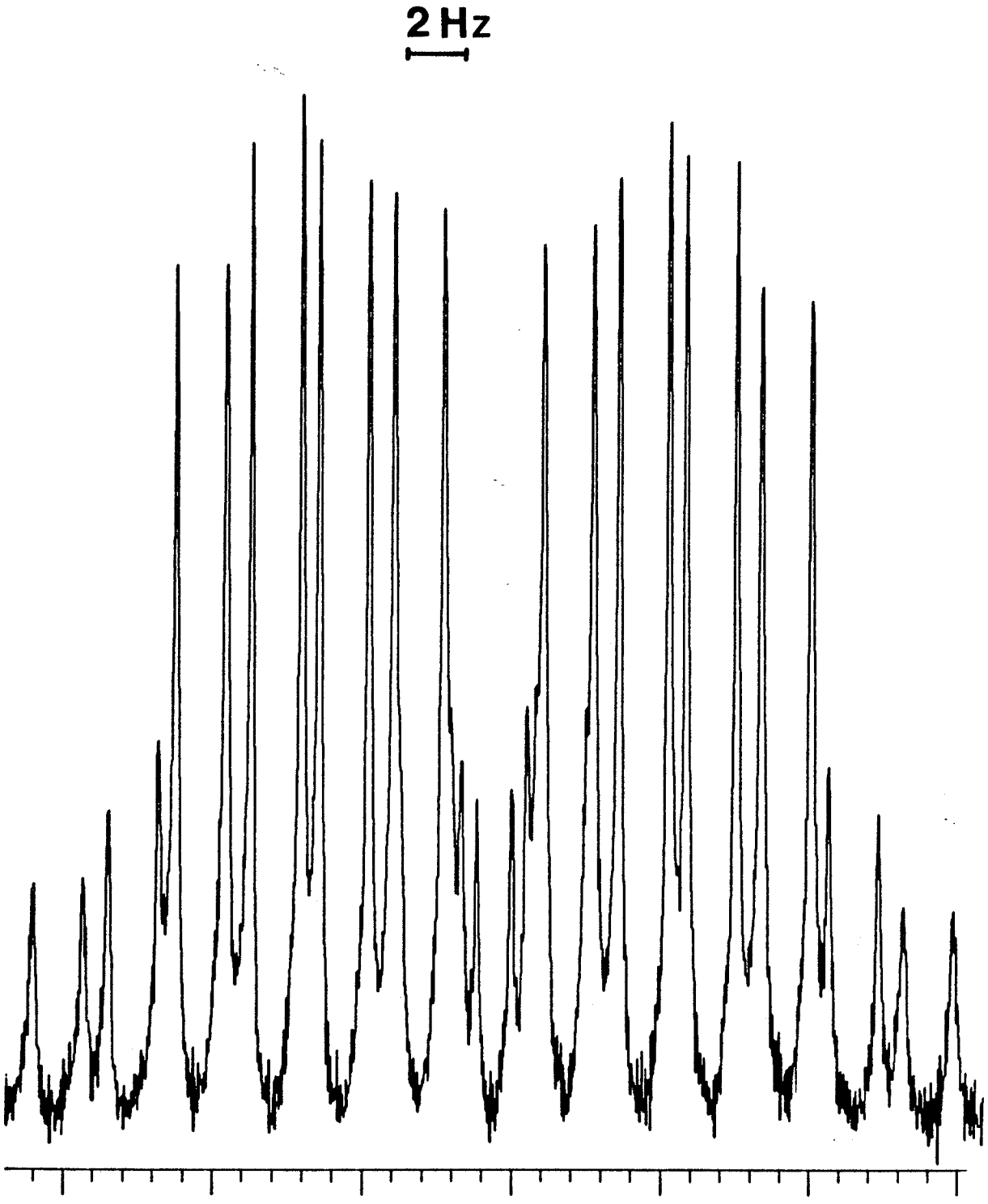
2 Hz

Figure 9

The ^{19}F spectrum of 2,4-dibromo-6-fluoro-N-methylaniline.

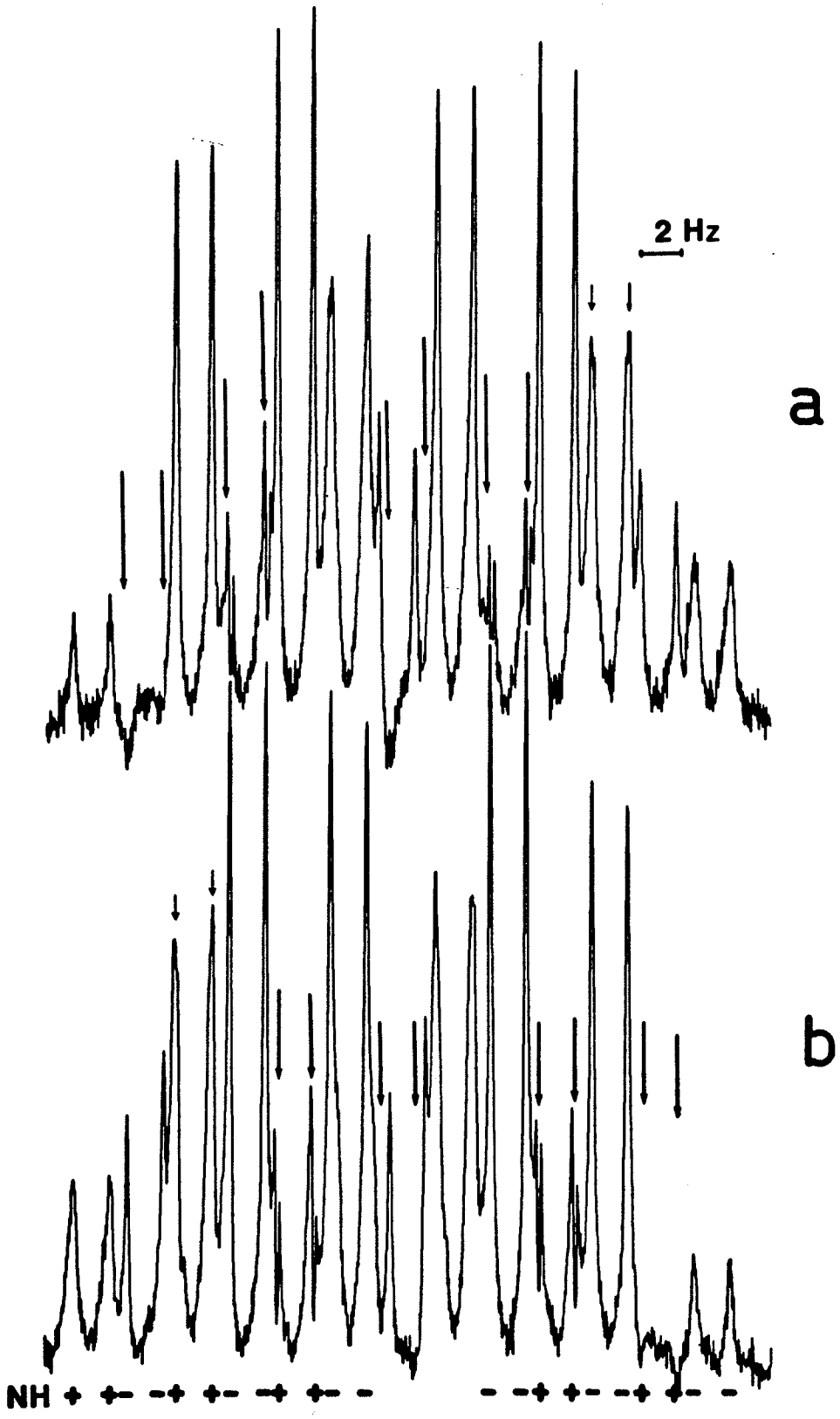
2 Hz
a
b
NH + +- -+ +- -+ +- - - -+ +- -+ +- -

Figure 10

a) The ^{19}F spectrum of 2,4-dibromo-6-fluoro-N-methylaniline while irradiating peak 1 of the methyl multiplet.

b) While irradiating peak 4 of the methyl multiplet.

2. 2-bromo-4,6-difluoroaniline

Results of the analyses of proton and fluorine spectra of a 5.0 mol % solution of 2-bromo-4,6-difluoroaniline in C_6D_6 appear in table 2.

Difficulties were encountered in the determination of the sign of $^4J_{NH_2,F}$ on the Bruker WH-90. Therefore the double resonance experiments were performed on the Bruker AM-300.

A first-order representation of the line spectrum of the ortho fluorine, F6, and of the meta proton, H5, is depicted in figure 11.

Table 2. Spectral parameters[a] for a 5.0 mol % solution of 2-bromo-4,6-difluoroaniline in C_6D_6.

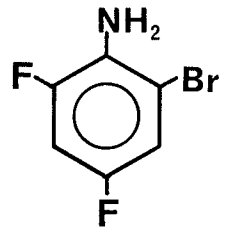

ν_{NH_2}	250.000		
ν_{H3}	530.968(3)	ν_{F4}	1141.690(3)
ν_{H5}	501.840(3)	ν_{F6}	879.664(3)
$^3J_{H3,F4}$	7.966(4)	$^4J_{NH_2,F6}$	-0.348(4)
$^3J_{H5,F4}$	8.332(4)	$^5J_{H3,F6}$	-2.057(4)
$^4J_{H5,F6}$	10.830(4)	$^5J_{NH_2,H3}$	0.294(4)
$^4J_{H3,H5}$	2.797(4)	$^5J_{NH_2,H5}$	0.408(4)
$^4J_{F4,F6}$	0.331(4)	$^6J_{NH_2,F4}$	0.001(4)[c]

rms deviation	0.014
largest difference	0.043
peaks observed	66
transitions calculated	128 plus 32 for NH_2
transitions assigned	120

[a] In Hertz at 90.023 MHz for proton and 84.700 MHz for fluorine. Shifts are not referenced. Analysis done by LAME[70].

[b] Amino proton shift held constant during iterations, no transitions assigned.

[c] This coupling was not observed but was allowed to vary in the LAME analysis.

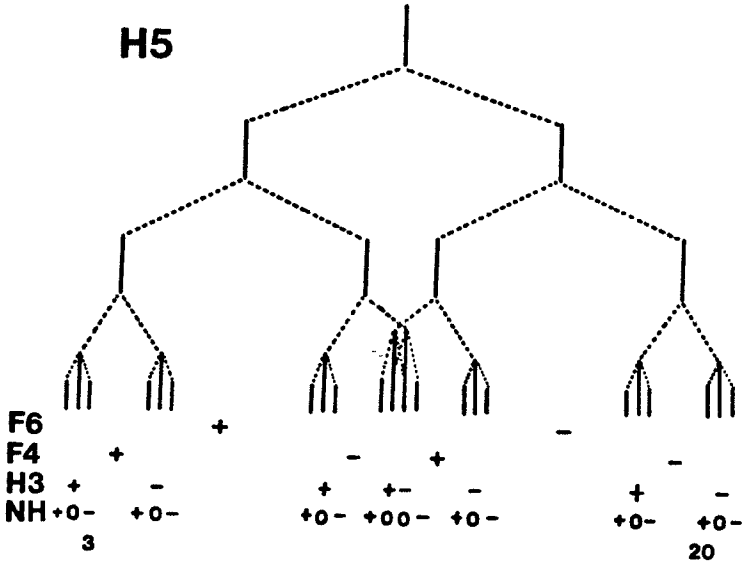
H5
F6
F4
H3
NH
3
20

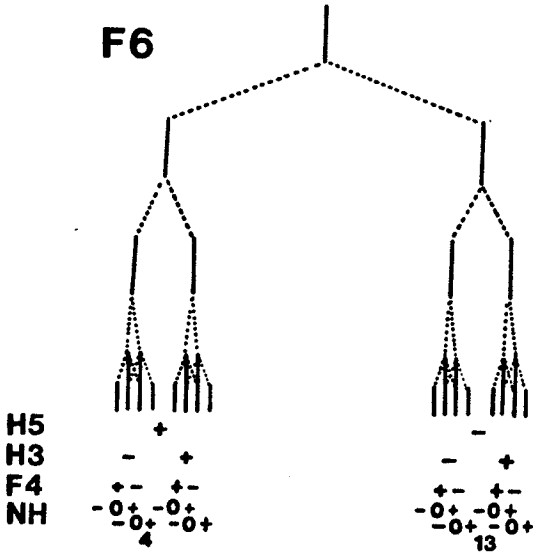
F6
H5
H3
F4
NH
4
13

Figure 11.

A first-order representation of the spectrum of the meta proton, H5, and the ortho fluorine, F6, in 2-bromo-4,6-difluoroaniline. Lines involved in the double resonance experiment are numbered.

a) determination of the relative sign of $^{4}J_{NH_2,F6}$ by weak irradiation experiments

A proton spectrum of H5 and a fluorine spectrum of F6 appear in figure 12. Weak irradiation of line 3 of the H5 proton resonance caused splitting of line 13 in the fluorine spectrum of F6 (see figure 13a). Line 3 of H5 is the high-field transition associated with a - spin state of NH_2, since $^{5}J_{NH_2,H5}$ is positive[42]. Line 13 of F6 is the low-field transition of the triplet due to the amino protons. Therefore $^{5}J_{NH_2,H5}$ and $^{4}J_{NH_2,F6}$ are of opposite sign, i.e. $^{4}J_{NH_2,F6}$ is a negative coupling constant. Confirmation of this sign came from results of tickling line 20 of H5 for the low field + spin state of NH_2, causing a perturbation of the high field line 4 of F6, (see figure 13b).

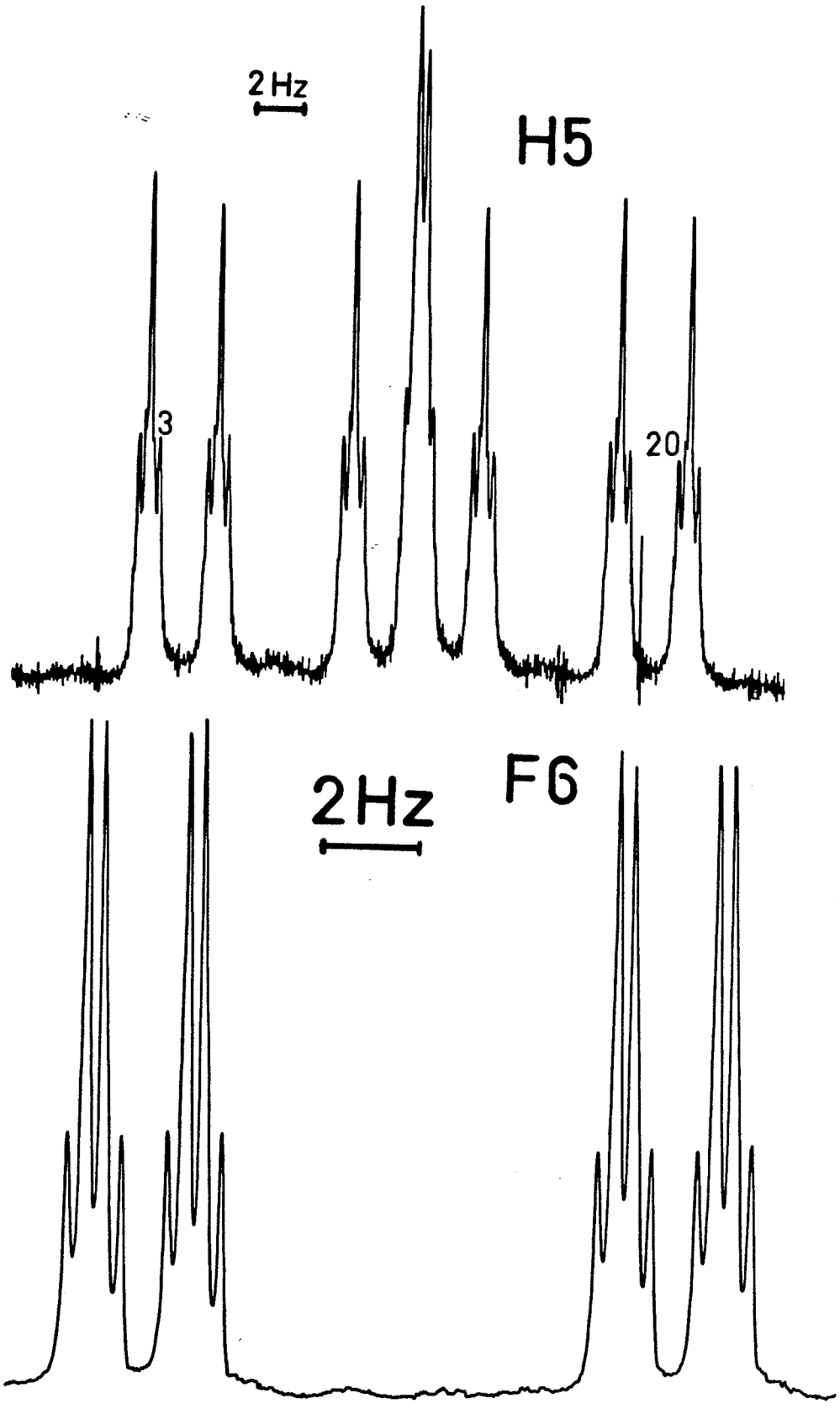
2 Hz
H5
3
20
2Hz
F6

Figure 12

The proton magnetic resonance spectrum of H5 and the fluorine magnetic resonance spectrum of F6 in 2-bromo-4,6-difluoroaniline at 300.135 MHz and 282.358 MHz, respectively.

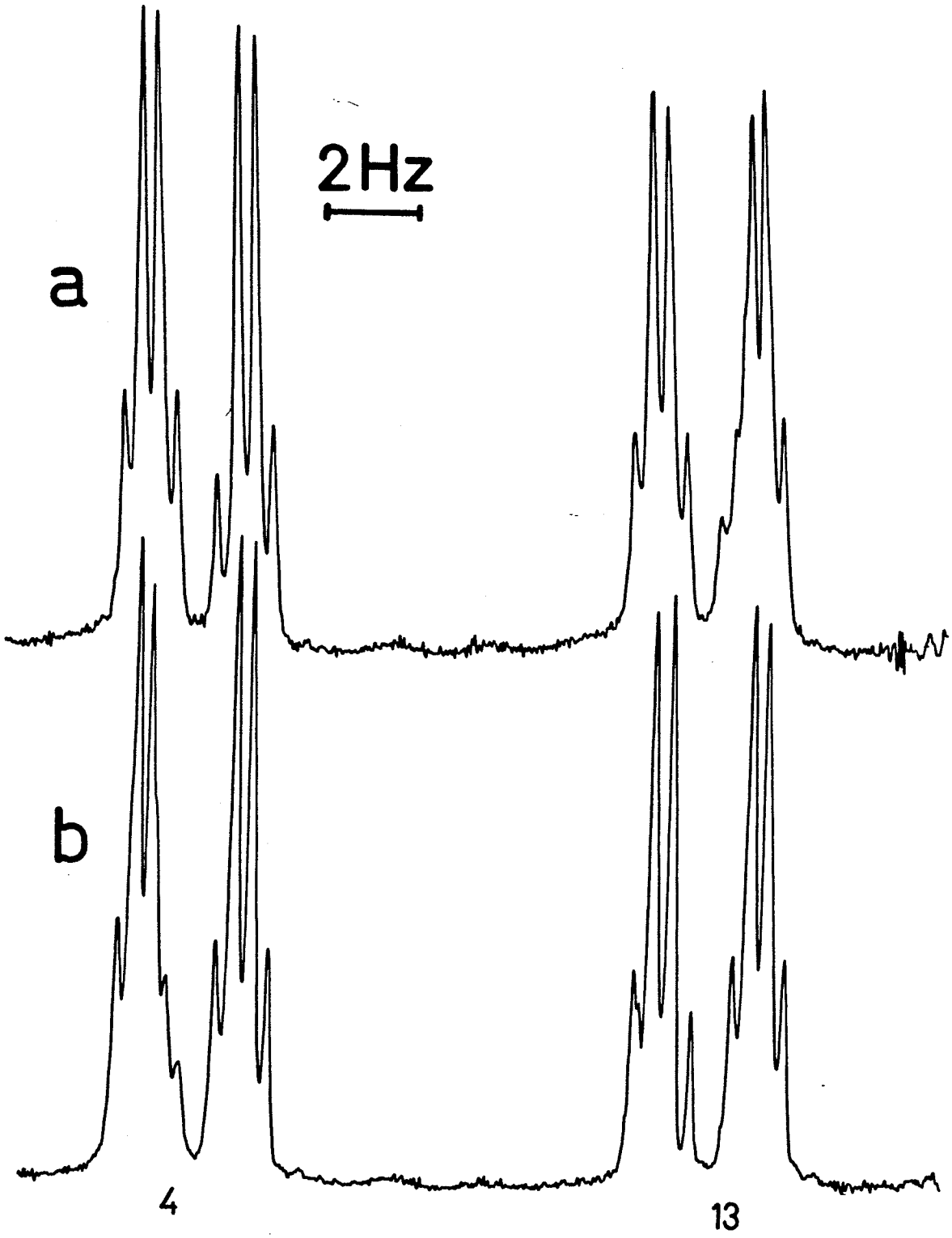
2Hz
a
b
4
13

Figure 13

a) The ^{19}F spectrum of F6 in 2-bromo-4,6-difluoroaniline with weak irradiation of line 3 of the H5 spectrum.

b) With weak irradiation of line 20 of the H5 spectrum.

3. 4-bromo-2,6-difluoroaniline

The analysis of this $A_2BB'XX'$ spin system was relatively straightforward. The signs of the coupling between ring nuclei were taken from an early analysis of 2,6-difluoroaniline[44]. The sign of $^4J_{NH_2,F}$ was taken to be the same as that in 2-bromo-4,6-difluoroaniline. Results of the analysis are given in table 3.

Table 3. Spectral Parameters[a] for a 5.0 mol % solution of 4-bromo-2,6-difluoroaniline in C_6D_6.

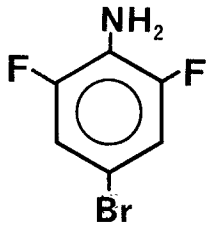

ν_{H3}	600.675(1)		
ν_{F2}	1499.722(3)		
ν_{NH_2}	261.000[b]		
$^3J_{F2,H3}$	9.904(3)	$^5J_{F2,H5}$	-1.951(4)
$^4J_{F2,F6}$	12.691(3)	$^4J_{F2,NH_2}$	-0.552(4)
$^4J_{H5,H5}$	2.105(3)	$^5J_{H3,NH_2}$	0.388(2)
transitions calculated	128		
transitions assigned	61		
observed peaks	36		
largest difference	0.046		
rms deviation	0.009		

[a] In Hertz. ^1H nmr at 90.023 MHz relative to TMS. ^{19F}nmr at 84.700 MHz; shift is not referenced. Analysis done by LAME.

[b] Amino proton shift not included in the iterative mode of LAME. No amino proton transitions were assigned.

4. 2,4,6-trifluoroaniline

The analysis of this $A_2BB'MXX'$ spin system yielded the parameters in table 4. Signs of the coupling between ring nuclei were taken from related molecules[43]. The sign of $^4J_{NH_2,F}$ was assumed to be that in 2-bromo-4,6-difluoroaniline. The coupling between the amino protons and the para fluorine could not be resolved. However, the linewidths of the F4 peaks are reduced from 0.25 Hz to 0.15 Hz when the amino protons are decoupled. The computer program NUMARIT was used to simulate the overlap of a triplet of Lorentzian peaks, each with linewidth of 0.15 Hz, with separations changing from 0.02 Hz to 0.10 Hz. Comparison of the observed para fluorine lineshapes with those from the computer simulation suggests a value of ±0.08 ± 0.01 Hz for the unresolved coupling.

Table 4. Spectral[a] parameters for a 5.0 mol % solution of 2,4,6-trifluoroaniline in C_6D_6.

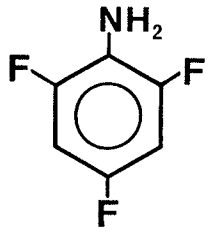

ν_{NH_2}	250.000[b]		
ν_{H3}	564.387(1)		
ν_{F2}	2487.251(1)	ν_{F4}	1966.731(1)
$^3J_{F2,H3}$	10.725(1)	$^5J_{F2,H5}$	-2.161(2)
$^3J_{H3,F4}$	8.646(2)	$^4J_{F2,NH_2}$	-0.495(2)
$^4J_{F2,F4}$	0.503(1)	$^5J_{H3,NH_2}$	0.378(2)
$^4J_{H3,H5}$	2.804(2)	$^6J_{F4,NH_2}$	±0.080(10)[c]
$^4J_{F2,F6}$	12.009(2)		

transitions calculated	256 (plus 64 amino)
transitions assigned	185
largest difference	0.032
rms deviation	0.010

[a] In Hertz. ^1H nmr at 90.023 MHz referenced to TMS. ^{19}F nmr at 84.700 MHz referenced to C_6F_6, calculated by NUMARIT.

[b] Held constant during iterations. No amino proton transitions were assigned.

[c] Determined by linewidth simulations.

5. 2,5-difluoro-N-methylaniline

At 90 MHz the ^{1}H nmr spectrum of 2,5-difluoro-N-methylaniline could not be analyzed. Fortunately, splittings attributable to the couplings $^{4}J^{NH,F2}$ and $^{5}J^{NH,F5}$ were easily recognized. An average of 10 splittings yielded a value of -2.847(19) for $^{4}J^{NH,F2}$ and 11 values were averaged to give a $^{5}J^{NH,F5}$ value of 1.803(17). The numbers in parentheses are the standard deviations in the last two significant figures.

Ortho and meta fluorine resonances were assigned by comparison with the ^{19}F spectrum of 2-fluoro-N-methylaniline. Splittings in the ^{19}F spectrum due to coupling to the amino proton were recognized by comparing spectra under conditions of fast and slow amino proton exchange.

a) determination of the relative sign of $^4J_{NH,F_2}$ by double resonance experiments.

There is a small coupling between the methyl protons and the ortho fluorine nucleus. Since $^3J_{CH_3,NH}$ is +5.25 Hz, it is possible to observe the ortho fluorine spectrum and to decouple the methyl protons for different spin states of the amino proton. When the low-field peak of the methyl doublet, associated with a + spin state of the amino proton, is irradiated, the high-field peaks of the doublets in the ortho fluorine spectrum collapse from quartets to singlets (see figure 14a). When the high-field peak of the methyl doublet is irradiated, the low-field peaks of the fluorine doublets collapse (see figure 14b). These results are consistent with a negative $^4J_{NH,F2}$. In figure 14 some of the peaks are labelled with the associated amino proton spin states.

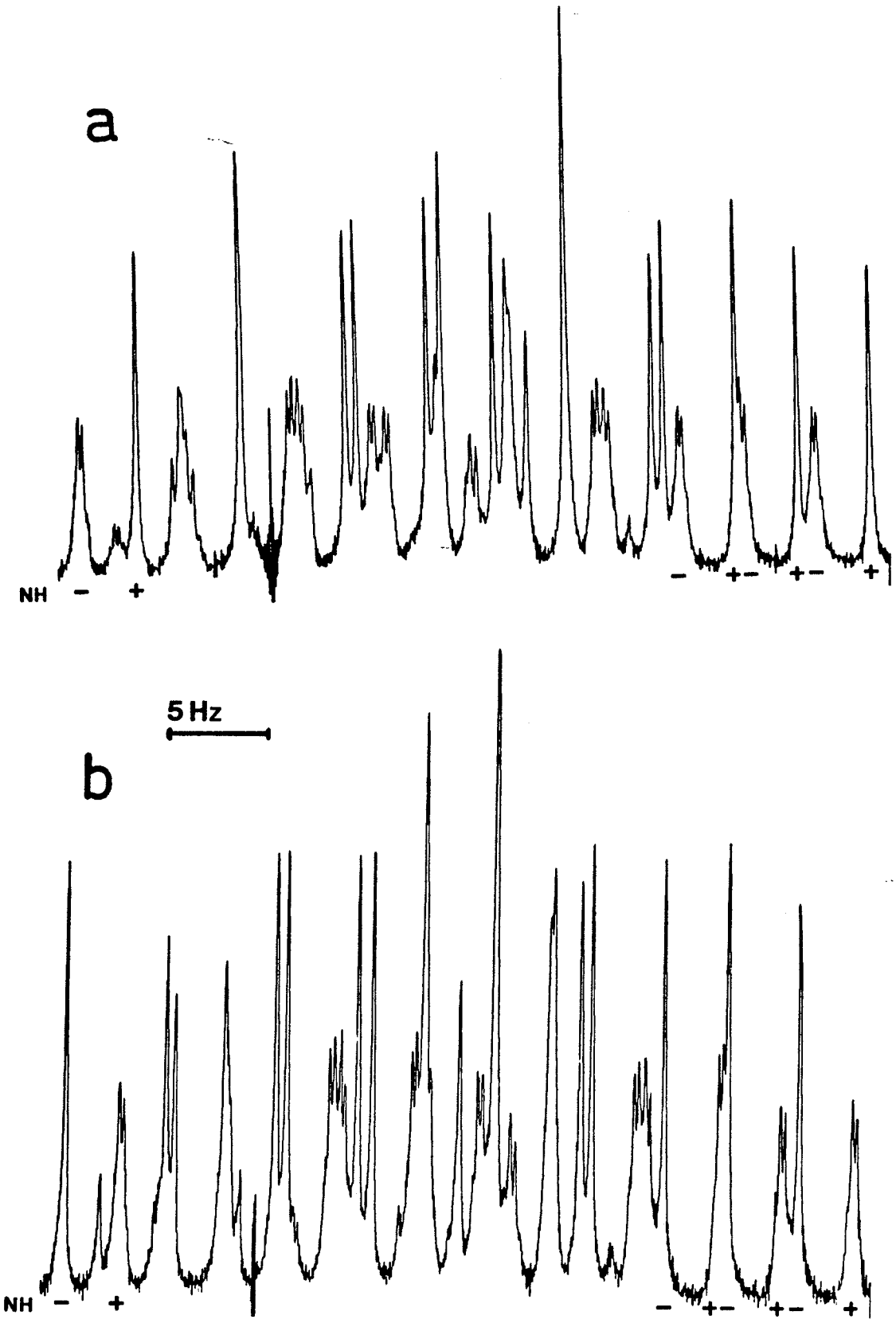
a
NH
5 Hz
b
NH

Figure 14

a) The ^{19}F spectrum of the ortho fluorine in 2,5-difluoro-N-methylaniline with irradiation of the low-field peak of the methyl proton doublet.

b) With irradiation of the high-field peak of the methyl proton doublet.

b) determination of the relative sign of $^{5}J^{NH,F}$ by double resonance experiments.

A very small coupling exists between the methyl protons and the meta fluorine nucleus. Irradiation of the low-field peak of the methyl doublet results in a decrease in linewidth and an increase in intensity of the low-field peaks of the doublets associated with coupling to the amino proton (see figure 15b). Irradiation of the high-field methyl peak effected the high field peaks of the meta fluorine doublets (see figure 15c). These experiments imply a positive value of $^{5}J^{NH,F5}$.

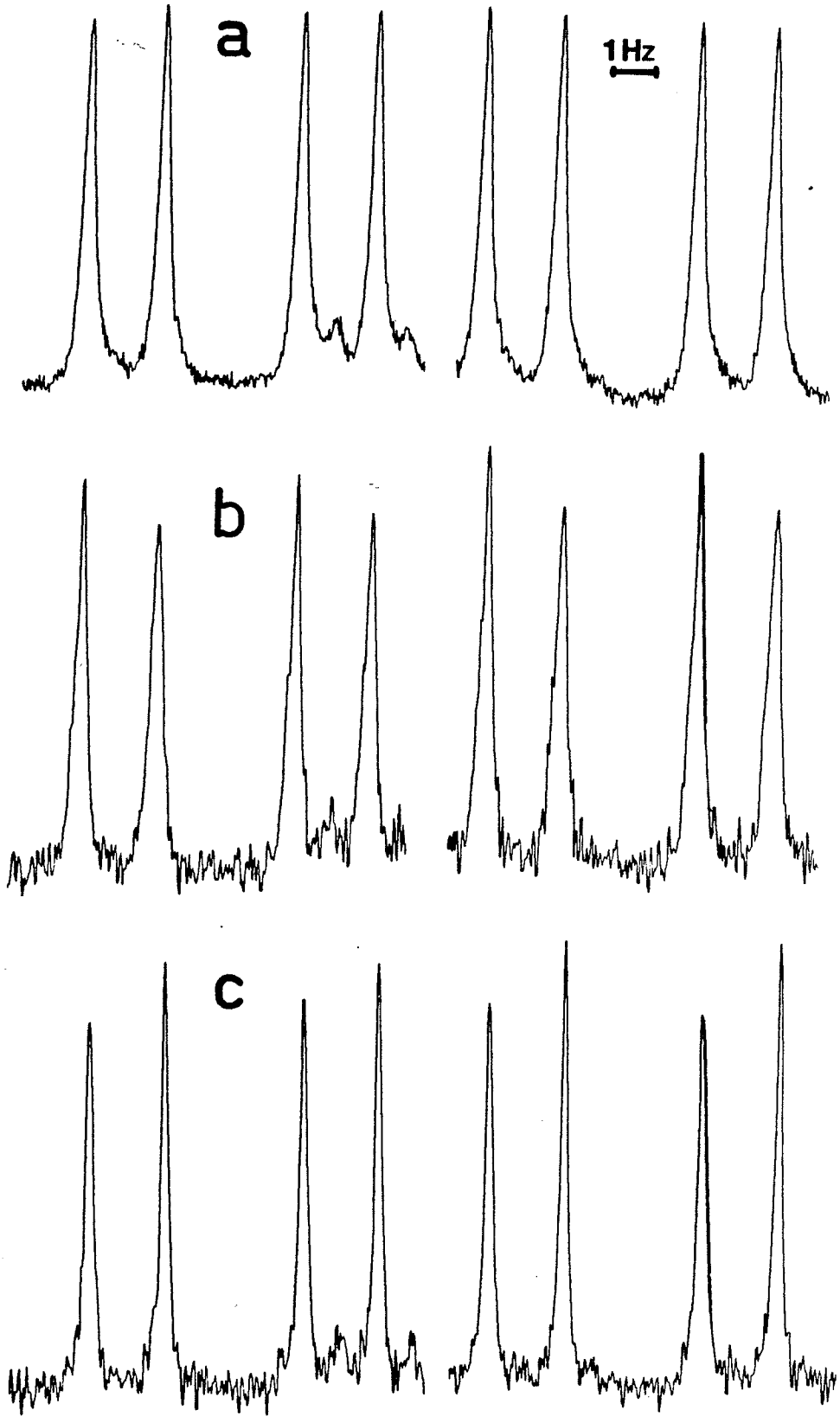
a
1Hz
b
c

Figure 15

a) The low-field and high-field ends of the ^{19}F spectrum of the <u>meta</u> fluorine in 2,5-difluoro-N-methylaniline.

b) With irradiation of the low-field peak of the methyl proton doublet.

c) With irradiaton of the high-field peak of the methyl proton doublet.

6. 2-cyano-3-fluoro-N-methylaniline

This was the only 2-X-3-fluoro-N-methylaniline compound available. Unfortunately, the presence of the cyano group reduced the solubility of the molecule in benzene and provided a slowly relaxing ^{14}N nucleus to which the ring nuclei could couple. These two problems resulted in poor signal to noise and broad linewidths in the proton and fluorine nmr spectra; hence standard deviations and the rms error in the spectral analysis are rather large. An important coupling, $^{5}J_{NH,F}$, could only be estimated by linewidth simulations and for this reason the sign could not be determined. The results of a spectral analysis of 2-cyano-3-fluoro-N-methylaniline are presented in table 5.

Table 5. Spectral parameters[a] for a 1.0 mol % solution of 2-cyano-3-fluoro-N-methylaniline in C_6D_6.

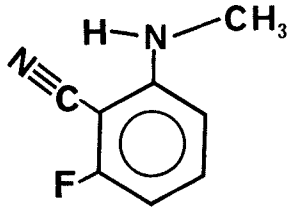

ν_{NH}	~369.5[b]		
ν_{F3}	4694.903(4)		
ν_{H4}	538.958(4)		
ν_{H5}	600.684(4)		
ν_{H6}	512.061(4)		
$^3J_{H5,H6}$	8.564(6)	$^4J_{H5,F3}$	6.603(6)
$^3J_{H4,F3}$	8.908(6)	$^5J_{NH,H5}$	0.625(8)
$^3J_{H3,H4}$	8.275(6)	$^5J_{H6,F3}$	-0.492(6)
$^4J_{NH,H6}$	-0.436(9)	$^5J_{NH,F3}$	0.12[c]
$^4J_{H6,H4}$	0.834(6)	$^6J_{NH,H4}$	0.10[d]

transitions calculated	80
transitions assigned	62
largest difference	0.049
rms error	0.016

[a] At 305 ± 1 K; ^1H chemical shifts in Hz, at 90.023 MHz, to low-field of TMS; ^{19}F chemical shift in Hz at 84.700 MHz, to low-field of C_6F_6;
analysis of ^1H and ^{19}F nmr spectra done with LAME while decoupling the methyl protons.

[b] Chemical shift only approximate.

[c] Estimated from a fit of two Lorenzian peaks to the F3 fluorine resonance.

[d] Estimated from linewidths.

7. 3-fluoro-2,4,6-tribromoaniline

The proton and fluorine nmr spectra of 3-fluoro-2,4,6-tribromoaniline are depicted in figures 16a and 16b respectively. Results of the analysis of this simple spin system are given in table 6.

Table 6. Spectral parameters[a] for a 6.3 mol % solution of 3-fluoro-2,4,6-tribromoaniline in C_6D_6.

ν_{NH_2}	300.00[b]
ν_{H5}	638.721(1)
ν_{F3}	983.477(1)[c]
$^4J_{H5,F3}$	6.867(1)
$^5J_{NH_2,H5}$	0.275(1)
$^5J_{NH_2,F3}$	1.170(1)

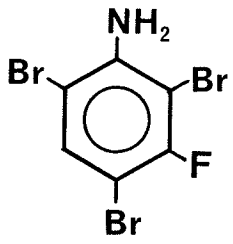

transitions calculated	24
transitions assigned	16
largest difference	0.004
observed peaks	12
rms error	0.002

[a] At 300 ± 1 K; ^1H chemical shifts in Hz, at 90.023 MHz to low-field of TMS, ^{19}F spectrum taken at 84.700 MHz, chemical shift of F3 is not referenced; analyses of both spectra done with LAME.

[b] Not iterated on in the LAME analysis. This value was estimated from the broad amino peak.

[c] Treated in the X approximation.

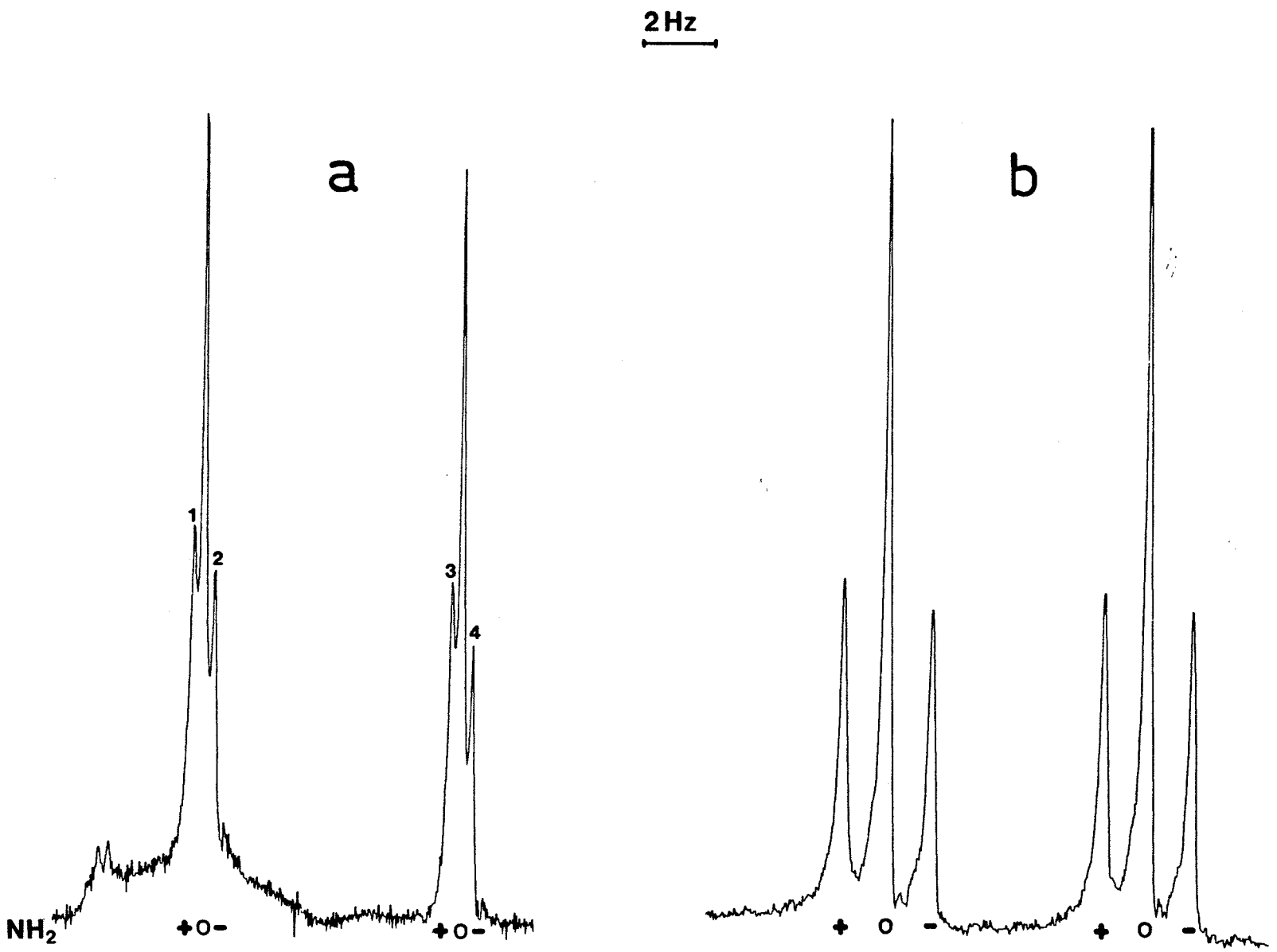
2Hz
a
b
1
2
3
4
NH2
+ o -
+ o -
+ o -
+ o -

Figure 16

a) The ring proton spectrum of 3-fluoro-2,4,6-tribromoaniline.

b) The ring fluorine spectrum of 3-fluoro-2,4,6-tribromoaniline.

a) determination of the relative sign of $^{5}J^{NH_2,F3}$ by weak irradiation experiments.

^{19}F spectra of the meta fluorine, while weakly irradiating peaks 1, 2, 3 and 4 of the meta proton resonance, are shown in figures 17a, 17b, 17c and 17d respectively. Here irradiation of the low-field and high-field peaks of each triplet of the meta proton causes splitting of the low-field and high-field peaks of both the meta fluorine respectively. This shows that $^{5}J^{NH_2,H5}$ and $^{5}J^{NH_2,F3}$ have the same sign. Since $^{5}J^{NH_2,H5}$ has been shown to be positive[41], $^{5}J^{NH_2,F3}$ is also positive.

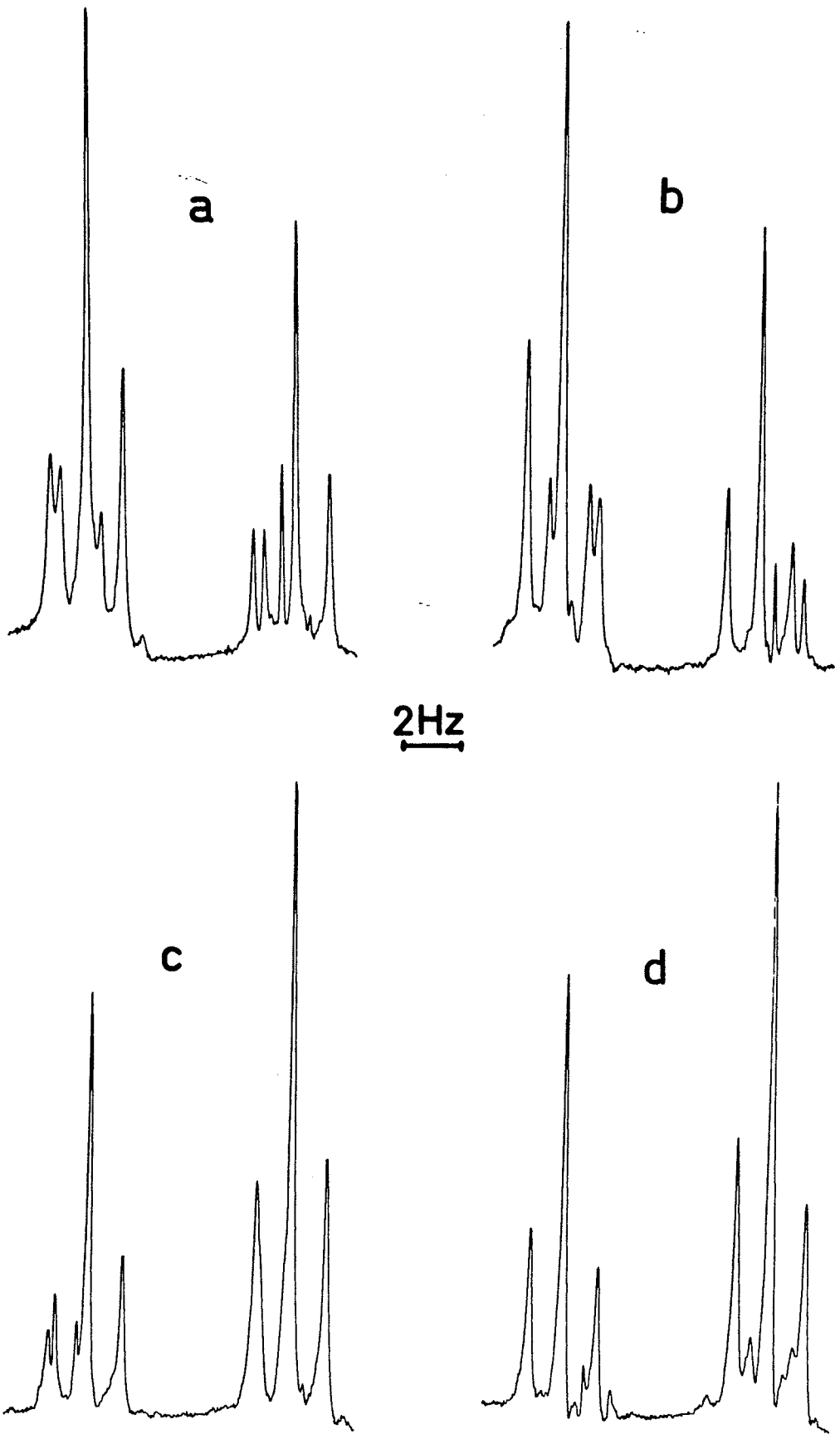
a
b
2Hz
c
d

Figure 17

a) The meta fluorine resonance while irradiating peak 1 (see figure 16a) of the meta proton resonance.

b) While irradiating peak 2 of the meta proton resonance.

c) While irradiating peak 3 of the meta proton resonance.

d) While irradiating peak 4 of the meta proton resonance.

8. 4-fluoroanaline

Results of the analysis of proton and fluorine nmr spectra of a 5.0 mol % solution of 4-fluoroaniline in C_6D_6 appear in table 7. Proton and fluorine nmr spectra, as well as computer simulations, appear in figures 18 and 19 respectively.

Table 7. Spectral parameters[a] for a 5.0 mol % solution of 4-fluoroaniline in C_6D_6.

ν_{NH_2}	300.00[b]		
ν_{H2}	546.569(1)		
ν_{H3}	603.656(1)	ν_{F4}	1400.000(1)[c]
$^3J_{H2,H3}$	8.743(2)	$^4J_{NH_2,H2}$	-0.209(2)
$^3J_{H3,F4}$	8.523(2)	$^5J_{H2,H5}$	0.357(1)
$^4J_{H2,F4}$	4.474(2)	$^5J_{NH_2,H3}$	0.300(2)
$^4J_{H2,H6}$	2.990(2)	$^6J_{NH_2,F4}$	0.262(2)
$^4J_{H3,H5}$	2.987(2)		

transitions calculated	256 (plus 64 amino)
transitions assigned	189
largest difference	0.028
rms deviation	0.010

[a] In Hertz. ^{19}F nmr spectrum at 84.700 MHz ^1H spectrum at 90.023, referenced to TMS. Analysis done by NUMARIT.

[b] Estimated chemical shift, no amino proton transitions assigned.

[c] F4 treated in the X approximation.

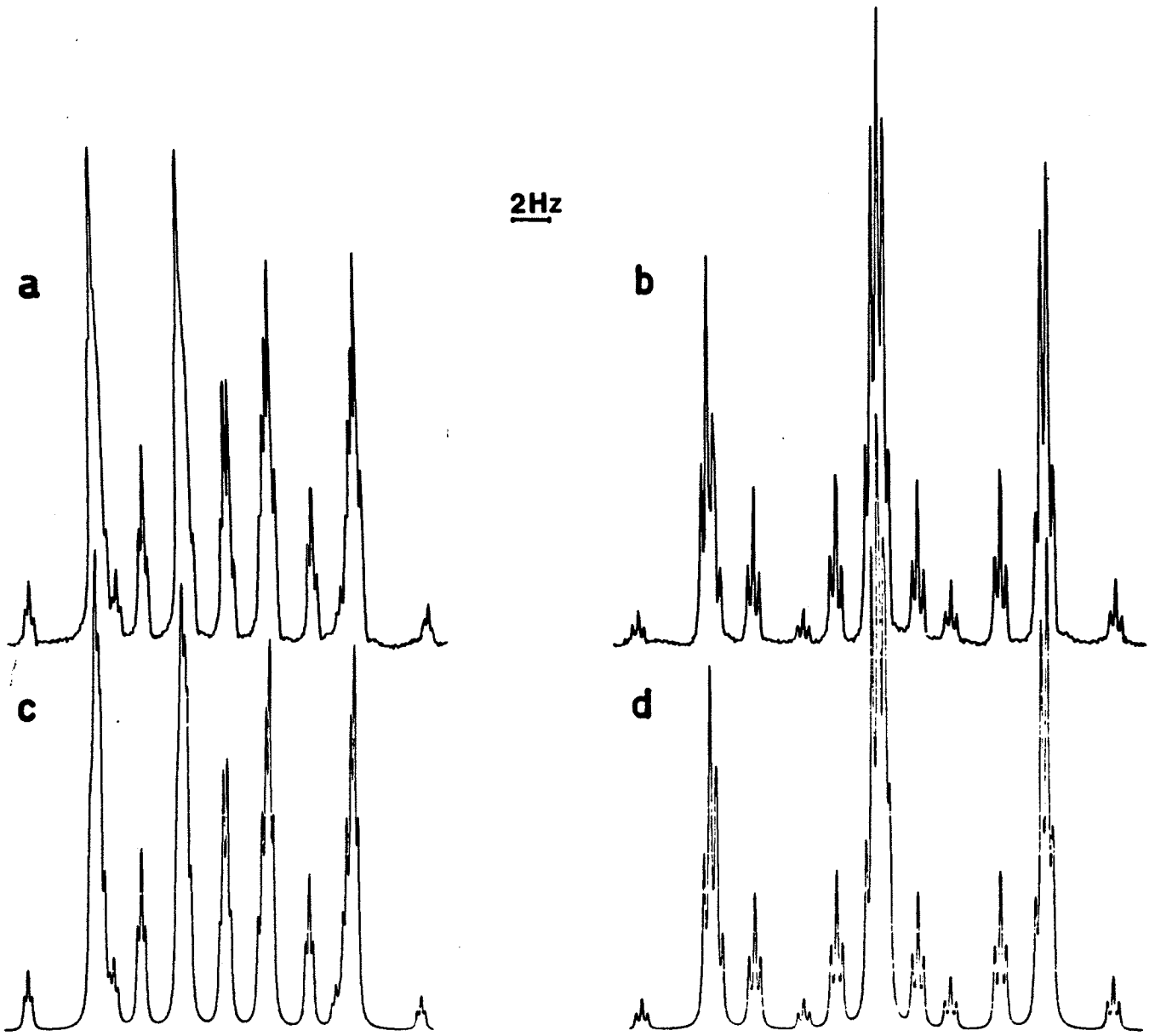
2Hz
a
b
c
d

Figure 18

a) The proton nmr spectrum of the ortho protons in 4-fluoroaniline.

b) The proton nmr spectrum of the meta protons.

c) Computer simulation of the ortho proton spectrum using the parameters from table 7.

d) Simulation of the meta proton spectrum.

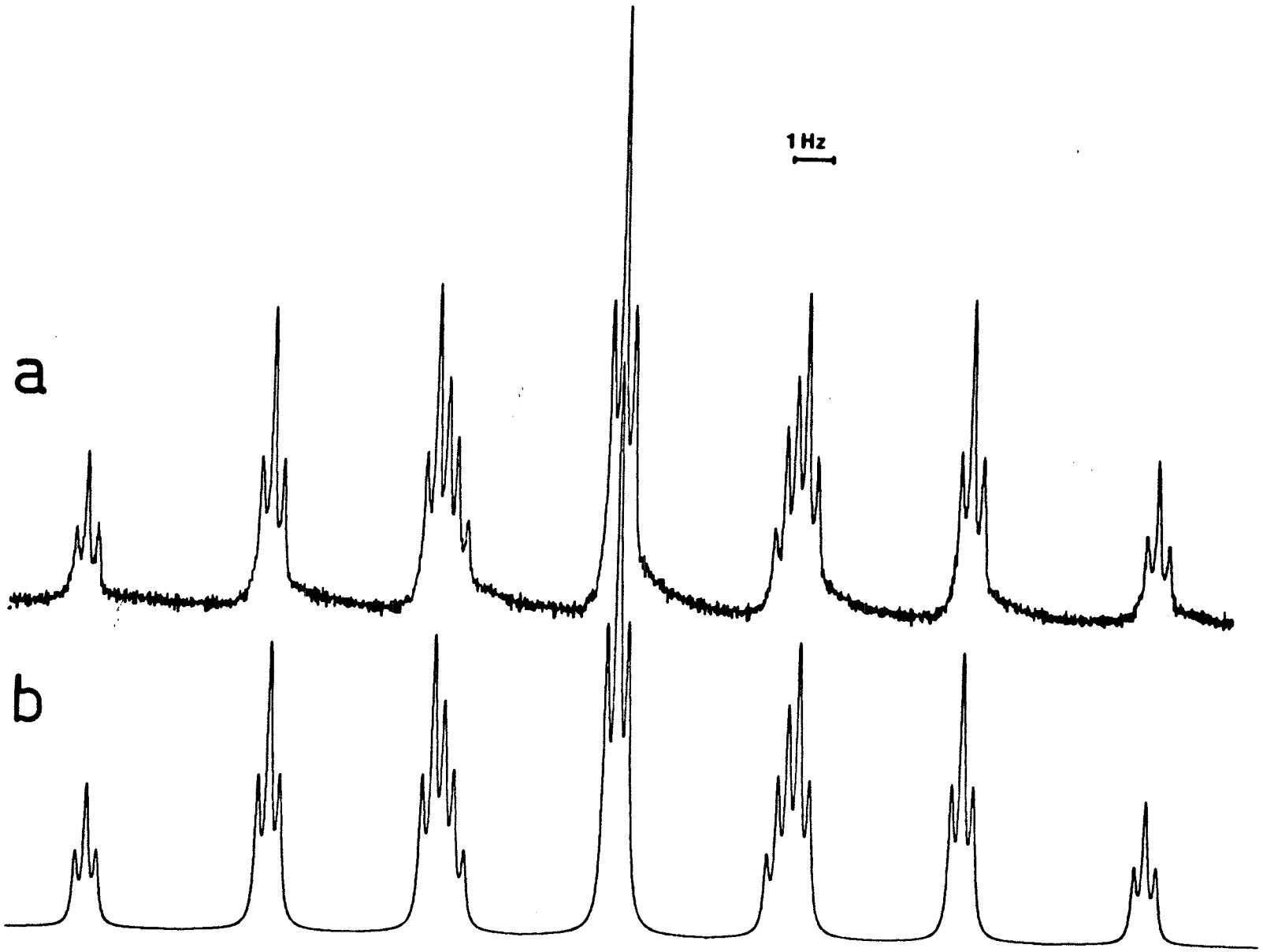
1 Hz
a
b

Figure 19

a) The fluorine spectrum of 4-fluoroaniline.

b) Computer simulation of the ^{19}F spectrum using the parameters from table 7.

a) determination of the relative sign of $^{6}J_{NH_2,F4}$ by double resonance experiments

Weak irradiation of meta proton peaks associated with the + spin state of the amino protons caused reduced intensity or splitting of the low-field peaks of the fluorine triplets. The same changes were seen on the high-field peaks of the fluorine triplets when the high-field peaks of the meta proton triplets were weakly irradiated. Therefore $^{6}J_{NH_2,F4}$ is positive, because $^{5}J_{NH_2,H5}$ is positive[42].

These experiments were simulated using the computer program DOR[44]. The results of a weak irradiation experiment, as well as spectra simulated with $^{6}J_{NH_2,F}$ positive and with $^{6}J_{NH_2,F}$ negative, are shown in figure 20.

In figure 20, the important comparisons are for the second band from the left. The experimental magnitude of the second field is not matched exactly in the double resonance Hamiltonian.

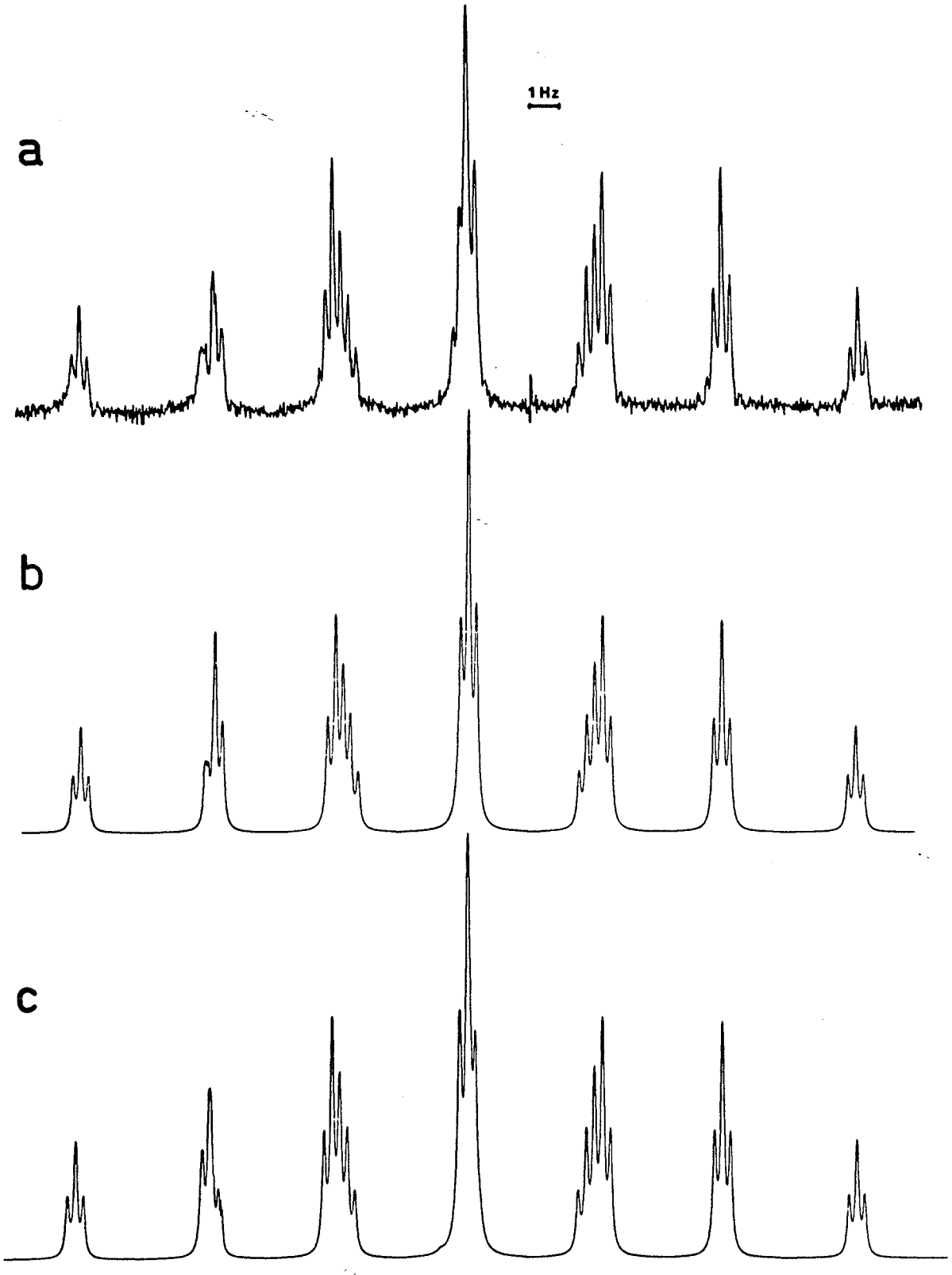
1 Hz
a
b
c

Figure 20.

a) The fluorine spectrum of 4-fluoroaniline while weakly irradiating a low-field peak of the triplets in the meta proton spectrum.

b) Computer simulation of the double resonance experiment with a positive $^{6}J_{NH_2,F4}$.

c) Computer simulation of the double resonance experiment with a negative $^{6}J_{NH_2,F4}$.

D. DISCUSSION

1. The Stereospecific $^4J^{NH,F}$

The INDO MO FPT values of $^4J^{NH,F}$ for different orientations of the N-H bond in 2-fluoro-N-methylaniline, 1, appear in table 8. A plot of $^4J^{NH,F}$ versus θ, the angle by which the N-H bond deviates from the benzene plane, is shown in figure 21. The solid curve in figure 21 represents a statistical fit of an A + B $\sin^2\theta$ function to the points from θ= 60° to θ = 180°. This $\sin^2\theta$ relationship strongly suggests a σ-π coupling mechanism. The calculated coupling deviates from the $\sin^2\theta$ curve for angles less than 60°. This negative deviation is likely due to a significant through-space coupling mechanism, which should dominate as the amino proton and the ortho fluorine nucleus become spacially proximate.

In 2-fluorotoluene[21], 2,2-fluorobenzaldehyde[45], 3, and 2-fluorophenol[46], 4, the angular dependence of $^4J^{XH,F}$, as calculated by the INDO MO FPT method, can be similarly decomposed into a positive δ-π mechanism and a negative through-space mechanism. The through-space component decreases in the series 4, 1, 3. This is understandable considering the strong dependence of the through-space coupling on the internuclear distance, which increases in the series.

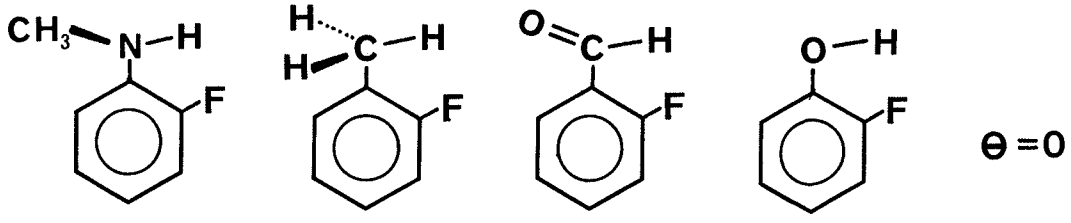

1 2 3 4

Table 8. INDO MO FPT calculated $^4J^{NH,F}$ for some conformations of 2-fluoro-N-methylaniline[a].

θ(deg)	$^4J^{NH,F}$(Hz)	θ(deg)	$^4J^{NH,FH}$(Hz)
0.0	-8.766	105.0	1.194
15.0	-7.200	120.0	0.567
30.0	-3.840	135.0	-0.228
45.0	-0.898	150.0	-1.046
60.0	-0.712	165.0	-1.777
75.0	1.446	180.0	-2.222
90.0	1.523		

[a] From the STO-3G optimized geometry. θ is the angle by which the N-H bond twists out of the benzene plane.

INDO CALC. 4J NH,F FOR DIFFERENT CONFORMATIONS OF
2-FLUORO-N-METHYLANILINE

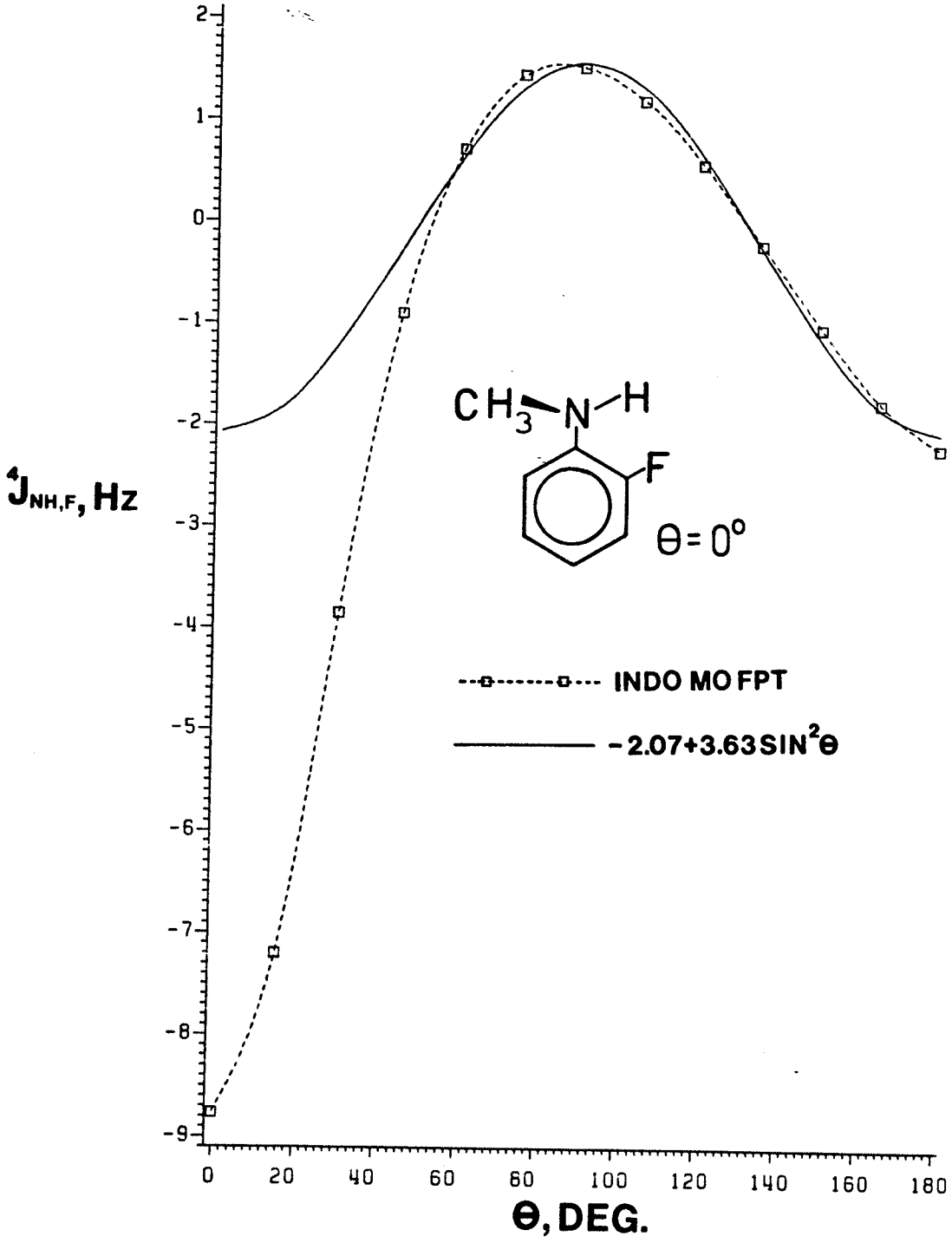

Figure 21

A plot of the angle dependence of $^{4}J^{NH,F}$ for 2-fluoro-N-methylaniline from INDO MO FPT calculations.

(θ is zero for the conformations 1 to 4).

In 2,4-dibromo-6-fluoro-N-methylaniline, the N-H bond lies nearly in the plane of the benzene ring, for two reasons. First, the steric repulsion between the ortho C-F bond and the methyl group is relieved by a decrease in θ. Second, a hydrogen bond between the ortho bromine substituent and the N-H group tends to hold the N-H and C-Br bonds coplanar. A conformation as in 5 may be envisioned, where θ is small.

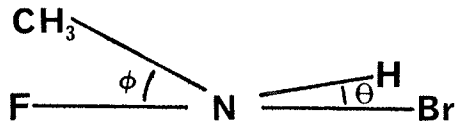

5

In benzene derivatives of type 6, both $^{5}J^{XH,H3}$ and $^{6}J^{XH,H4}$ can be good conformational indicators. $^{5}J^{XH,H3}$ is zero in the form 6a and has its maximum value in the trans conformation 6c. $^{6}J^{NH,H4}$ follows a $\sin^2\theta$ law to give a maximum value in the conformation 6b.

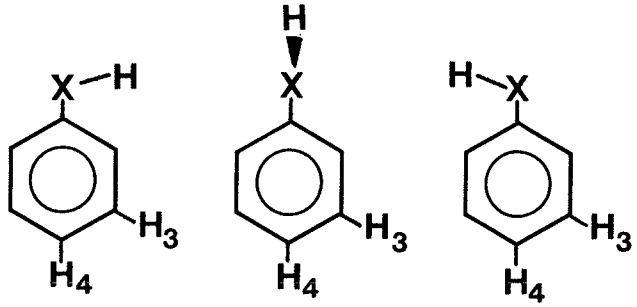

6a 6b 6c

In 2,4-dibromo-6-fluoro-N-methylaniline, $^{5}J^{NH,H3} < 0.05$ Hz and $^{5}J^{NH,H5} = 0.570(2)$ Hz. These magnitudes are consistent with a conformation 5. The rather large through-space coupling of 4.78 Hz between the ortho fluorine nucleus and the methyl protons indicates

that ϕ is not very large, since this coupling falls off rapidly as the methyl group moves away from the ortho C-F bond. In 2,3,5,6-tetrafluoroanisole, where the barrier to rotation about the C_1-O bond is effectively zero, $^5J_{CH_3,F}$ is only 1.30 Hz. If 2,4-dibromo-6-fluoro-N-methylaniline is in conformation 5, then the $^4J_{NH,F}$ of -2.549 Hz can be taken as the trans four-bond coupling.

In 2,5-difluoro-N-methylaniline a likely ground state conformation is 7, where both θ and ϕ are small.

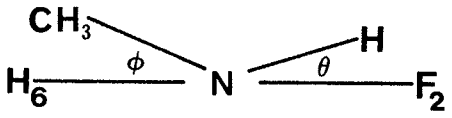

7

$^5J_{NH,H3}$ and $^5J_{NH,H4}$ could not be observed suggesting a small value for θ. A small ϕ value is implied by observation of a through-space coupling of about -0.40 Hz between the methyl protons and H6. In ortho substituted anisoles, where a conformation 8 is preferred, the through-space coupling, $^5J_{CH_3,H6}$, ranges from -0.23 to -0.38 Hz.

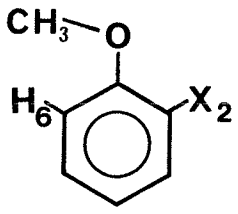

8

Hence, in 2,5-difluoro-N-methylaniline the $^4J_{NH,F2}$ of -2.847(19) can be taken as the cis four-bond coupling.

In the A + B $\sin^2\theta$ + C$\sin^2\theta/2$ curves calculated by the INDO method for $^nJ^{XH,H}$, $^nJ^{XH,F}$, $^nJ^{XC,H}$ and $^nJ^{XC,F}$ (where n = 4, 5 or 6), the value of A, the angle independent term, is often large, as with the calculated $^4J^{NH,F}$. Experimentally, the magnitude of A is found to be small or zero[22,46] in similar situations. It has been suggested that this term is therefore an artifact of the INDO calculation[47].

If $^4J^{NH,F}$ were to follow a $\sin^2\theta$ law, $^4J^{NH,F}_{cis}$ and $^4J^{NH,F}_{trans}$ would be equal. Although the experimental values differ by only 0.3 Hz, they are negative. A σ-π mechanism should result in positive numbers. The spacial proximity of the amino proton and the ortho fluorine nucleus in 2-fluoro-N-methylaniline suggested by ab initio calculations, and the probability of an N-H...F-C hydrogen bond, imply that the through-space mechanism will contribute to $^4J^{NH,F}$. In fact, INDO MO FPT suggests a large through-space contribution. Now, if the magnitude of $^4J^{NH,F}$ is due to a through-space coupling and the A term in the A + B $\sin^2\theta$ functional form of the σ-π mechanism is small another term must be included in order to account for the sizable $^4J^{NH,F}_{trans}$. A negative σ-mechanism, following a $\sin^2\theta/2$ law could account for this observation.

In a study of 2-fluorotoluene derivatives[21], Schaefer and coworkers rejected the angular dependence of $^4J^{CH,F}$ predicted by INDO and proposed an empirical curve. Both the INDO and empirical curves are sketched in figure 3. The empirical curve can be thought of as composed of a large σ-π mechanism, a negative σ mechanism and a small positive through-space mechanism. Derivatives of 2 differ from those of 1, 3 and 4 in that the through-space coupling in 2 is positive.

Positive through-space couplings between methyl protons and ring fluorine nuclei have been observed[48,49] and may be rather large.

In 2,3,5,6-tetrafluorophenol and in pentafluorobenzaldehyde, the barriers to internal rotation are so large that one need only consider the planar forms of the molecules as significantly populated at ambient temperatures. Then $^{4}J^{XH,F}$, as observed, is the average of $^{4}J^{XH,F}_{cis}$ and $^{4}J^{XH,F}_{trans}$. For 2-fluorophenols the average coupling is -2.44 Hz and the observed coupling in tetrafluorophenol is -2.49 Hz[22]. In 2-fluorobenzaldehydes the average coupling is -0.90 Hz[24] and the observed coupling in pentafluorobenzaldehyde is -1.07 Hz[51]. 2,6-difluoro-N-methylaniline also has a barrier sufficiently high (see part II of this thesis) to support a simple cis-trans equilibrium, as in 9 ⇌ 10. Then the observed $^{4}J^{NH,F}$ should be the average of $^{4}J^{NH,F}$ and $^{4}J^{NH,F}$.

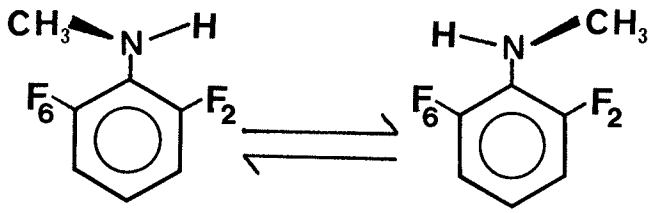

9 10

Evidence for this equilibrium comes from $^{5}J^{NCH_3,F}$ values. In 2,5-difluoro-N-methylaniline, where the methyl group lies trans to the ortho fluorine, $^{5}J^{NCH_3,F2}$ is 0.26 Hz. In 2,4-dibromo-6-fluoro-N-methylaniline, where the methyl group lies cis to the ortho fluorine, $^{5}J^{NCH_3,F6}$ is 4.78 Hz. The average of these two numbers, applicable to the equilibrium 9 ⇌ 10, is 2.52 Hz.

In 4-bromo-2,6-difluoro-N-methylaniline, $^{5}J^{CH_3,F}$ is 2.39 Hz. The difference between the predicted and observed values is only 0.13 Hz.

Unfortunately, the amino proton exchange in 2,6-difluoro-N-methylaniline or 2,6-difluoro-4-bromo-N-methylaniline could not be retarded sufficiently to observe $^{4}J^{NH,F}$.

The ^{1}H and ^{19}F spectra of some 2-fluoroaniline derivatives were analyzed in the hope that they might yield average $^{4}J^{NH,F}$ values. $^{4}J^{NH_2,F}$ is -0.348(4) Hz in 2-bromo-4,6-difluoroaniline, -0.552(4) Hz in 2,6-difluoro-4-bromoaniline and -0.495(2) Hz in 2,4,6-trifluoroaniline. These values are far from the average $^{4}J^{NH,F}$ of [(-2.847) + (-2.549)]/2 = -2.698 Hz, implied by data for the N-methylaniline derivatives.

In aniline, the amino protons do not lie in the plane of the benzene ring[52,53]. If this is also true for the 2-fluoroaniline derivatives, a large positive σ-π coupling mechanism will result in a positive shift in the observed $^{4}J^{NH_2,F}$ values. This does not seem likely, since hydrogen bonding to the ortho fluorines and bromines will pull the N-H bonds into the ring plane. $^{6}J^{NH_2,F}$ values which should follow a $\sin^2\theta$ law, are 0.08 Hz in 2,4,6-trifluoroaniline and <0.05 Hz in 2-bromo-4,6-difluoroaniline, suggesting that these molecules are nearly planar.

The difference of about 2 Hz between the $^{4}J^{NH_2,F}$ and the average $^{4}J^{NH,F}$ may be due to distortion of the amino geometry by the presence of a methyl group. Both the through-space and the σ coupling mechanisms are substituent dependent. A geometry distortion of the amino group could have a large effect on the internuclear distance between the amino proton and the ortho fluorines, hence a large effect on the through-space coupling.

INDO values for $^4J_{NH_2,F}$ were calculated for 2,6-difluoroaniline and delineate a curve similar to that in figure 21, with $^4J^{NH,F}_{cis}$ as -3.516 Hz and $^4J^{NH,F}_{trans}$ as -1.572 Hz. The calculated $^4J^{NH,F}$ is considerably smaller in the aniline. This is because the amino proton to ortho fluorine internuclear distance used in the INDO calculations is 2.32 Å whereas the internuclear distance is only 2.18 Å in 2-fluoro-N-methylaniline. When the methylamino group in 2-fluoro-N-methylaniline is twisted so that the internuclear distance becomes 2.32 Å, $^4J^{NH,F}$ drops to -3.2 Hz.

Now, considering only the 2-fluoroanilines, $^4J_{NH_2,F}$ in 2-bromo-4,6-difluoroaniline is about 0.15 Hz smaller than is $^4J_{NH_2,F}$ in the 2,4,6-trifluoro derivative. This difference is likely due to a perturbation of the σ mechanism by the presence of an ortho bromine. $^4J_{CH_3,F}$ in 2-fluorotoluenes has a marked substituent effect[21].

Clearly, $^4J^{NH,F}$ in 2-fluoro-N-methylaniline derivatives, although of the same sign as in the 2-fluoroaniline derivatives, cannot be used to predict $^4J_{NH_2,F}$ in the latter. The σ-π mechanism should yield positive four-bond couplings. The observed values are negative, so that σ and through-space components dominate these couplings, as expected from the conformation deduced from the other long-range couplings present in the molecules. It is concluded that $^4J^{NH,F}$ and $^4J_{NH_2,F}$ are not yet understood as conformational indicators.

2. The Stereospecific $^5J^{NH,F}$

Table 9 gives INDO MO FPT values for $^5J^{NH,F}$ for different angles, θ, in 3-fluoro-N-methylaniline. These data are plotted in figure 22. A curve of the type $A + B \sin^2\theta + C \sin^2\theta/2$, in which the coefficients have been adjusted to fit the data in table 9, also appears in figure 2. These calculations indicate that $^5J^{NH,F}$ has a positive σ contribution, with a $\sin^2\theta/2$ dependence, and a negative σ-π contribution with a $\sin^2\theta$ dependence. In 3-fluorophenol derivatives[22], $^5J^{OH,F}_{cis}$ and $^5J^{OH,F}_{trans}$ are -0.35 and 1.56 Hz, respectively. The average of these two values is 0.61 Hz. In 2,3,5,6-tetrafluorophenol, $^5J^{OH,F}$ is 0.59 Hz, in agreement with the average.

In 2-cyano-3-fluoro-N-methylaniline, where the N-H and C-F bonds are assumed to be in a <u>cis</u> arrangement, due to steric repulsion between the C≡N and the methyl group and to hydrogen bonding between the N-H group and the cyanide π bond, $^5J^{NH,F}_{cis}$ is 0.12(1) Hz. In 2,5-difluoro-N-methylaniline, where N-H...F-C hydrogen bonding and the steric repulsion between the <u>ortho</u> C-F bond and the methyl group should result in a θ value near 180°, $^5J^{NH,F}_{trans}$ is 1.78(1) Hz. The average is 0.95 Hz, assuming $^5J^{NH,F}_{cis}$ to be positive. In 3-fluoro-2,4,6-tribromoaniline, where the amino group is nearly planar due to hydrogen bonding to the <u>ortho</u> bromine substituents, $^5J^{NH_2,F}$ is 1.17 Hz. This is reasonably close to the average $^5J^{NH,F}$, considering the possible perturbation of the σ coupling mechanism by the bromine substituents and the change in the amino group geometry caused by methylation.

Table 9. INDO MO FPT calculated $^5J^{NH,F3}$ for some conformations of 3-fluoro-N-methylaniline[a].

θ (deg)	$^5J^{NH,F3}$	θ (deg)	$^5J^{NH,F3}$
0.0	0.429	103.8	-0.099
23.8	-0.041	113.8	0.459
33.8	-0.233	123.8	1.082
43.8	-0.514	133.8	1.706
53.8	-0.754	143.8	2.263
63.8	-0.910	153.8	2.699
73.8	-0.942	163.8	2.977
83.8	-0.822	173.8	3.076
93.8	-0.537		

[a] From STO-3G optimized geometry of N-methylaniline.

INDO CALC. 5J NH,F FOR DIFFERENT CONFORMATIONS OF
3-FLUORO-N-METHYLANILINE

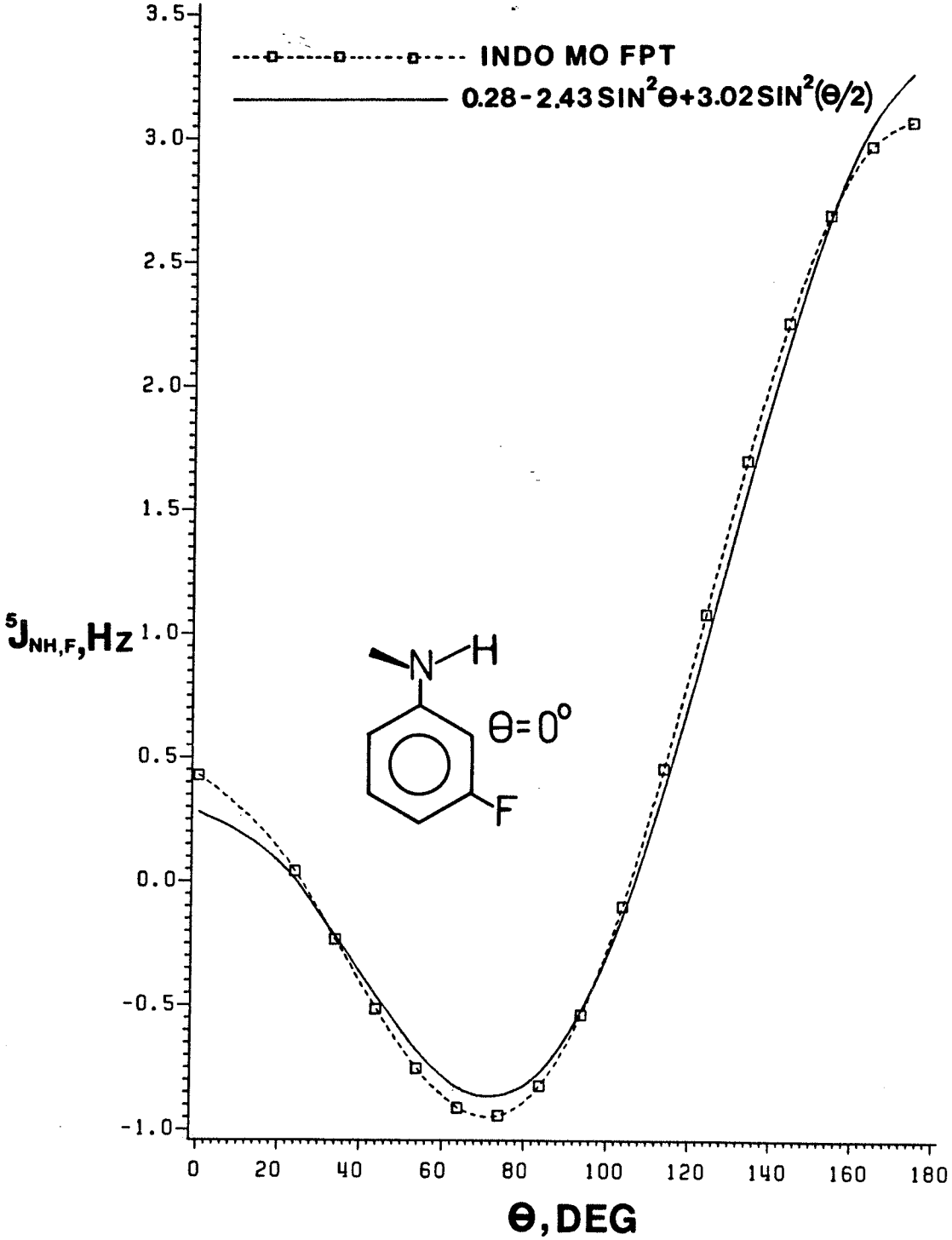

Figure 22

A plot of the angle dependence of $^{5}J^{NH,F}$ for 3-fluoro-N-methylaniline from INDO MO FPT calculations.

$^{5}J^{COH,F}$ couplings in 3-fluorobenzaldehydes give evidence of substituent perturbations on the σ-mechanism. In 3-fluoro-6-nitrobenzaldehyde[45], 3-fluoro-6-hydroxy-5-nitrobenzaldehyde[45] and 3-fluoro-2-hydroxybenzaldehyde[54], where $^{5}J^{COH,H}$ values (which show little substituent dependence [24,25]), indicate that the C-H,C-F trans form is preferred, the $^{5}J^{COH,F}$ values are 2.36, 2.5 and 1.87 Hz respectively. These couplings suggest that the average should lie between 0.94 and 1.25 Hz. In 3-fluorobenzaldehyde, where $^{5}J^{COH,H}$ indicates that the cis:trans ratio is about 45:55, $^{5}J^{COH,F}$ is 1.85 Hz[24].

The values of $^{5}J^{XH,F}$ are all in accordance with a positive component in the coupling mechanism. The existence of a negative σ-π component in $^{5}J^{XH,F}$ is demonstrated by $^{5}J^{CH_3,F}$ in 3-fluorotoluene, where the low barrier to methyl rotation averages the large positive σ component and the large negative σ-π component to give a coupling of only -0.23 Hz[20]. The theoretical prediction of a negative σ-π component (figure 22) could be tested by measuring $^{5}J^{NH,F}$ in 2,6-dibromo-3-fluoro-N-methylaniline. In this compound there might be a sufficient population of non-planar conformations such that the negative σ-π interaction would dominate. Unfortunately, attempts to stop the amino proton exchange in 2,6-dibromo-N-methylaniline were unsuccessful.

It appears that $^{5}J^{NH,F}$ is stereospecific and that it is not strongly perturbed relative to $^{5}J^{NH_2,F}$ by the presence of a methyl group on the nitrogen.

3. The Stereospecific $^6J^{NH,F}$

Values of $^6J^{NH,F}$ calculated by INDO MO FPT for different conformations of 4-fluoro-N-methylaniline and 4-fluoroaniline indicate that a σ-π mechanism dominates this coupling (see table 10). Indeed, the calculated values fit the expected A + B $\sin^2\theta$ function fairly well (see figure 23 for a plot of the angular dependence of $^6J^{NH,F}$ in 4-fluoro-N-methylaniline).

$^6J^{XH,F}$ in other para fluorobenzene derivatives also follows a positive σ-π mechanism. In 4-fluorobenzal chloride[30], where the barrier to internal rotation is 9.3 ± 1.3 kJ/mol, with an in plane C-H bond as the low energy conformation, $^6J^{CH,F}$ is only 0.22 Hz[29]. In 4-fluorotoluene, where there is almost free rotation and $^6J^{CH,F}$ is averaged over all angles, $^6J^{CH_3,F}$ is 1.12 Hz[29]. In 4-fluorothiophenol, $^6J^{SH,F}$ is 1.00 Hz[56]. In pentafluorothiophenol[45], a weak S-H...F-C hydrogen bond lowers the energy of the planar ground state and $^6J^{SH,F}$ drops to 0.26 Hz.

In 2,6-dibromo-4-fluorophenol and in 4-fluorobenzaldehyde, in which only the planar conformations need be considered, $^6J^{OH,F}$ is -0.27 Hz and $^6J^{COH,F}$ is -0.44 Hz[24]. These couplings, for presumably planar molecules, suggest that their relationship is A+B$\sin^2\theta$ rather than B$\sin^2\theta$. It is possible that an angle independent σ-mechanism is present in $^6J^{XH,F}$ in these molecules. The proton-proton couplings in saturated hydrocarbons, which are transmitted via a σ-mechanism, are known to alternate in sign with the number of intervening bonds. A negative contribution to $^6J^{XH,F}$ could follow such an alternation

Table 10. INDO MO FPT calculated $^{6}J^{NH,F}$ for some conformations of 4-fluoro-N-methylaniline[a] and 4-fluoroaniline[b].

θ(deg)	$^{6}J^{NH,F4}$ N-methylaniline	$^{6}J^{NH,F4}$ aniline
0.0	-0.216	-0.088
15.0	-0.048	0.133
30.0	0.305	0.498
45.0	0.743	0.918
60.0	1.168	1.295
70.0	1.470	1.534
90.0	1.555	1.560
105.0	1.389	-
120.0	1.025	1.212
135.0	0.578	0.819
150.0	0.177	0.405
165.0	-0.074	0.067
180.0	-0.120	-0.110

[a] From STO-3G optimized geometry of N-methylaniline.

[b] From STO-3G optimized geometry of 4-fluoroaniline.

INDO CALC. 6J NH,F FOR DIFFERENT CONFORMATIONS OF
4-FLUORO-N-METHYLANILINE

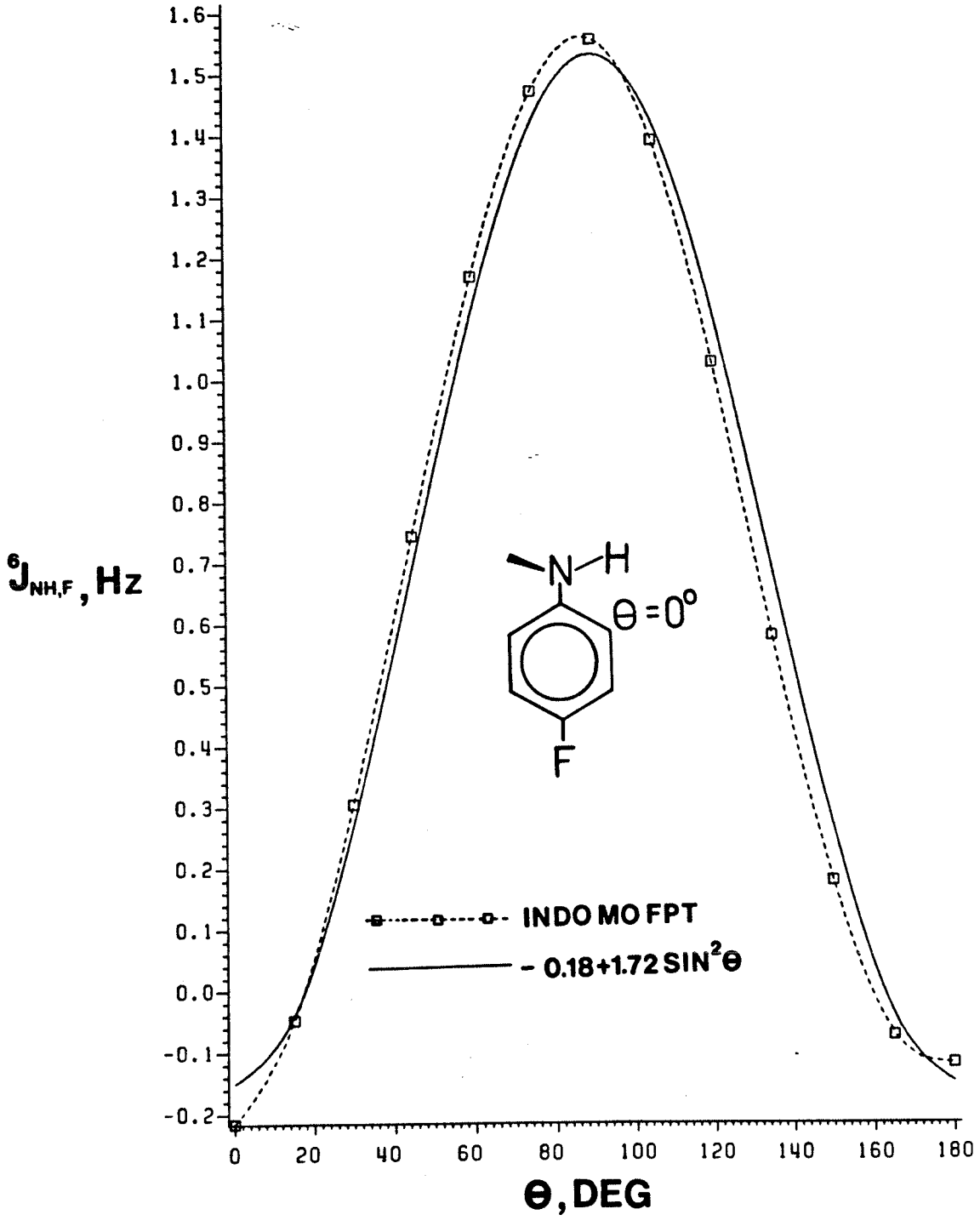

Figure 23

A plot of the angle dependence of $^{6}J^{NH,F}$ for 4-fluoro-N-methylaniline from INDO MO FPT calculations.

since it has been suggested in this thesis that the contributions to $^4J^{XH,F}$ and $^5J^{XH,F}$ are negative and positive respectively. That the σ mechanism is responsible for the constant term in a $^6J^{XH,F} = A + B \sin^2\theta$ relationship is difficult to confirm and the possibility can only be suggested here.

In 4-fluoroaniline, $^6J^{NH_2,F}$ is +0.264 Hz. This value suggests that the amino protons do not lie in the plane of the benzene ring. In aniline, $^6J^{NH_2,H}$ is -0.137 Hz. One can compare these values with the corresponding six-bond couplings in 4-fluorotoluenes and toluene. In toluene[28] and 4-fluorotoluene[57] the barriers to methyl rotation are nearly zero. Accordingly, the average value of $\sin^2\theta$ is 0.5 in both molecules. The ratios $^6J^{NH_2,F}/^6J^{CH_3,F}$ and $^6J^{NH_2,H}/^6J^{CH_3,H}$ are 0.236 and 0.221, respectively. Since the barrier to rotation about the C-N bond in aniline is large compared to kT (24 kJ/mol in the gas phase[58] and probably higher in solution), a molecular conformation as in 11 may be considered.

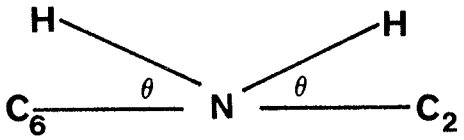

11

The inversion barrier is only 6.3 kJ/mol, and $\langle\sin^2\theta\rangle$ becomes the average of $\sin^2\theta$ over the populated inversion states.

Now, the fact that the ratios of ^6J are nearly equal implies

similar $\langle \sin^2\theta \rangle$ values for aniline and 4-fluoroaniline.

If one assumes the $^6J^{NH,H}$ value for aniline is equal to $^6J^{CH,H}$ for toluene and that $^6J^{NH,F} = {}^6J^{CH,F}$ for <u>para</u> fluoro derivatives, one can write

$$^6J^{NH_2,F} = 2.30 \langle \sin^2\theta \rangle \qquad (33)$$

$$^6J^{NH_2,H} = 1.24 \langle \sin^2\theta \rangle \qquad (34)$$

These equations yield $\langle \sin^2\theta \rangle$ values of 0.119 for 4-fluoroaniline and 0.110_5 for aniline. Although $\langle \sin^2\theta \rangle$ is the average value of $\sin^2\theta$, one might naively set $\langle \sin^2\theta \rangle$ equal to $\sin^2\theta$ and solve for the angle θ. This approach yields θ values of 20.2° and 19.4° for 4-fluoroaniline and aniline respectively. Because the inversion barrier is only 6.3 kJ/mol, these numbers represent minimum values.

A statistical fit of the data in table 10 to an $A + B \sin^2\theta$ function gave $^6J^{NH,F} = -0.21 + 1.68 \sin^2\theta$ for 4-fluoroaniline. For 4-fluorotoluene, INDO data can be fitted to yield $^6J^{CH,F} = -0.01 + 1.88 \sin^2\theta$. If the A term is ignored and $^6J_{90}$ is reduced by the ratio 1.68/1.88 for 4-fluoroaniline equation (33) becomes

$$^6J^{NH_2,F} = 2.06 \langle \sin^2\theta \rangle \qquad (35)$$

and θ can be estimated as 21.0°.

Structures for anilines, as determined by microwave spectroscopy, yield the angles ψ, between the H-N-H plane and the benzene ring, and

β, the H-N-H angle when projected onto the plane of the benzene ring. ψ and β are related to the dihedral angle θ by equation[59] (35).

$$\tan\theta = \cot(\beta/2)\sin\psi \qquad (35)$$

In aniline[52,53], ψ is 38° and is 115.05°, hence θ = 21°. In 4-fluoroaniline[60], ψ is 46.4° and β is 111.87° and equation (35) yields a value of 26°. STO-3G geometry optimizations[45] yielded a θ value of 31° for both molecules.

An increase in the angle θ on <u>para</u> substitution with fluorine is expected. The <u>para</u> fluorine reduces conjugation of the amino group.

The dihedral angle θ, deduced from the ^6J values, are rough approximations, yet they do not differ greatly from the microwave results.

In an <u>ab initio</u> MO study of the inversion barriers of <u>para</u> substituted anilines at the STO-3G level, Hehre and coworkers[61] calculated only small changes in the geometry at the nitrogen.

In 2,4,6-trifluoroaniline, $^6J_{NH_2,F}$ is 0.08 ± 0.01 Hz. An angle, θ, of 11 ± 1° is calculated by the crude procedure above. <u>Ortho</u> substitution by fluorine has lowered the approximate value of θ by 8°. Intramolecular N-H...F-C hydrogen bonding would result in such a decrease. In 2-bromo-4,6-difluoroaniline $^6J_{NH_2,F4}$ was not observed and is estimated as <0.05 Hz, suggesting further flattening at nitrogen.

E. SUMMARY AND CONCLUSIONS

The cis and trans values of $^{4}J^{NH,F}$ and $^{5}J^{NH,F}$ were determined for some ortho and meta fluorine substituted N-methylanilines. The results were compared with $^{4}J^{XH,F}$ and $^{5}J^{XH,F}$ in ortho and meta fluorine substituted toluenes, benzaldehydes, phenols and thiophenols. A comparison was also made with $^{4}J^{NH,F}$ and $^{5}J^{NH,F}$ calculated, as a function of θ, by the INDO MO FPT method.

The INDO technique was found to be inadequate in describing $^{4}J^{NH,F}$. A σ component had to be added to the coupling mechanism. Also a conformation independent, constant term had to be removed. The INDO technique also greatly overestimates the through-space contribution to $^{4}J^{NH,F}$.

The stereospecific $^{5}J^{NH,F}$ calculated by the INDO technique could be decomposed into σ and σ-π mechanisms. Both experiment and INDO calculations yield a positive $^{5}J^{NH,F}$ but INDO overestimates $^{5}J^{NH,F}_{trans}$.

Values of $^{6}J^{NH_2,F}$ were determined for 4-fluoroaniline and 2,4,6-trifluoroaniline and the dihedral angles between the N-H bonds and the plane of the benzene ring were estimated from the $^{6}J^{NH_2,F}$ values. A smaller θ for 2,4,6-trifluoroaniline suggests that N-H...F-C hydrogen bonding causes a flattening at the nitrogen.

It was suggested that the σ-π component of $^{6}J^{NH,F}$ is positive and INDO results for 4-fluoro-N-methylaniline and 4-fluoroaniline support this.

F. SUGGESTIONS FOR FUTURE RESEARCH

Carbon-13 enrichment of the methyl group in most N-methylanilines is relatively easy and would enable determination of stereospecific coupling between the methyl carbon and ring nuclei.

$^{6}J_{NH_2,F}$ seems to be a good indicator of the conformation of the amino substituent in 4-fluoroaniline derivatives. $^{6}J_{NH_2,F}$ in 2,6-diX-4-fluoroanilines might demonstrate the different hydrogen bonding characteristics of the X substituent.

The mechanism of some other sidechain proton to ring fluorine couplings have yet to be thoroughly examined. $^{5}J_{CH,F}$ in meta-fluorotoluenes could be investigated in pentafluorotoluene derivatives using the same method as Schaefer and coworkers[21] in their investigation of $^{4}J_{CH,F}$.

An investigation of the stereospecificity of long-range couplings between the sulfydryl proton and the ring fluorine nuclei in fluorinated thiophenols is possible and would be of interest.

REFERENCES FOR PART I

1. H. S. Gutowsky and D. W. McCall. Phys. Rev. 82, 748 (1951).
2. E. L. Hahn and D. E. Maxwell. Phys. Rev. 84, 1246 (1951).
3. N. F. Ramsey and E. M. Purcell. Phys. Rev. 85, 143 (1952).
4. N. F. Ramsey. Phys. Rev. 91, 303 (1953).
5. D. B. O'Reilly. J. Chem. Phys. 36, 274 (1962); 38, 2583 (1963).
6. J. A. Pople, J. W. McIver, Jr., and N. R. Ostund. J. Chem. Phys. 49, 2960 (1968).
7. J. A. Pople, J. W. McIver Jr., and N. S. Ostlund. J. Chem. Phys. 49, 2965 (1968).
8. J. A. Pople and G. A. Segal. J. Chem. Phys. 43. S136 (1965).
9. J. A. Pople, D. P. Santry and G. A. Segal. J. Chem. Phys. 43, S129 (1965).
10. J. A. Pople, D. L. Beveridge, and P. A. Dobosh. J. Chem. Phys. 47, 2026 (1967).
11. J. Kowalewski in: Progress in Nuclear Magnetic Resonance Spectroscopy Vol. 11. J. W. Emsley, J. Feeney and L. H. Sutcliffe (eds.) (Pergamon Press, Oxford, 1977).
12. J. Kowalewski in: Annual Reports in nmr Spectroscopy Vol. 12, E. F. Mooney (ed.) (Academic Press, New York, 1982).
13. M. Karplus. J. Chem. Phys. 30, 11 (1959).

14a. R. Wasylishen and T. Schaefer. Can. J. Chem. 50, 1852 (1972).

14b. T. Schaefer and R. Laatikainen. Can. J. Chem., 61, 2785 (1983).

15. T. Schaefer, T. A. Wildman and R. Sebastian. Can. J. Chem. 60, 1924 (1982).
16. H. M. McConnel. J. Mol. Spectrosc. 1, 11 (1957).

17. C. Heller and H. M. McConnell. J. Chem. Phys. 32, 1535 (1960).

18. T. Schaefer and R. Laatikainen. Can. J. Chem. 61, 224 (1983).

19. J. Hilton and L. H. Sutcliffe in: Progress in Nuclear Magnetic Resonance Spectroscopy, Vol. 10, J. W. Emsley, J. Feeney and L. H. Sutcliffe (eds.), (Pergamon Press, 1977, Oxford) p. 27.

20. T. Schaefer, W. Danchura and W. Niemczura. Can. J. Chem. 56, 2233 (1978).

21. T. Schaefer, R. Sebastian, R. P. Veregin, and R. Laatikainen. Can. J. Chem. 61, 29 (1983).

22. J. B. Rowbotham, M. Smith, and T. Schaefer. Can. J. Chem. 53, 986 (1975).

23. T. Schaefer and J. B. Rowbotham. Chem. Phys. Lett. 29, 633 (1974).

24. R. Wasylishen and T. Schaefer. Can. J. Chem. 49, 3216 (1971).

25. C. M. Moore and M. E. Hobbs. J. Amer. Chem. Soc. 71, 411 (1949).

26. T. Schaefer and T. A. Wildman. Can. J. Chem. 57, 450 (1979).

27. T. Schaefer, R. Sebastian and T. A. Wildman. Can. J. Chem. 57, 3005 (1979).

28. H. D. Rudolph and H. Seiler. Z. Naturforschung, 20, Teil A. 1682 (1965).

29. T. Schaefer, W. Danchura, W. Niemczura and J. Peeling. Can. J. Chem. 56, 2442 (1972).

30. W. J. E. Parr and T. Schaefer. Acc. Chem. Res. 13, 400 (1980).

31. R. A. W. Johnstone, D. W. Payling, and C. Thomas. J. Chem. Soc. (C) 2223 (1969).

32. C. F. Huebner, E. M. Donoghue, A. J. Plummer, and P. A. Furness. J. Med. Chem. 9, 830 (1966).

33. T. Schaefer and R. Sebastian. J. Magn. Res. 41, 395 (1980).

34. S. M. Castellano and A. A. Bothner-By. J. Chem. Phys. 41, 3863 (1964).

35. C. W. Haigh and J. W. Williams. J. Mol. Spectrosc. 32, 398 (1969).

36. A. R. Quirt and J. S. Martin. J. Magn. Res. 5, 318 (1971).

37. W. J. Hehre, R. F. Stewart, and J. A. Pople. J. Chem. Phys. 51, 2657 (1969).

38. W. J. Hehre, W. A. Lathan, R. Ditchfield, M. D. Newton and J. A. Pople, Program 236, Quantum Chemistry Program Exchange, Indiana University, Bloomington, Indiana.

39. SAS User's Guide: Statistics, A. A. Ray (ed.), (Statistical Analysis System Institute, 1982).

40. SAS/Graph User's Guide, K. A. Council and J. T. Helwig (ed.), (Statistical Analysis System Institute, 1981).

41. T. Schaefer and R. Wasylishen. Can. J. Chem. 48, 1343 (1970).

42. R. Wasylishen and T. Schaefer. Can. J. Chem. 49, 3627 (1971).

43. R. J. Abraham, D. B. Macdonald and E. S. Pepper. J. Chem. Soc. (B) 832 (1967).

44. G. Govil and D. H. Whiffen. Mol. Phys., 12, 449 (1967).

45. Unpublished data from this laboratory.

46. T. Schaefer, R. Laatikainen, T. A. Wildman, J. Peeling, G. H. Penner, J. Baleja, and K. Marat. Can. J. Chem. (1984).

47. T. Schaefer, J. Peeling, G. H. Penner, A. Lemire and R. Sebastian. Can. J. Chem., in press.

48. T. A. Wildman. Ph.D. Thesis, University of Manitoba, (1982).

49. M. Barfield, S. R. Walter, K. A. Clark, G. W. Gribble, K. W. Haden, W. J. Kelley, and C. S. LeHoullier. Org. Magn. Res. 20, 92 (1982).

50. R. E. Wasylishen and M. Barfield. J. Amer. Chem. Soc. 97, 4545 (1975).

51. T. Schaefer and K. Marat. Org. Mag. Res. 15, 294 (1981).

52. M. Quack and M. Stockburger. J. Mol. Spectrosc. 43, 87 (1972).

53. D. G. Lister, J. K. Tyler, J. H. Hog, and N. W. Larsen. J. Mol. Struct. 23, 253 (1974).

54. T. Schaefer, R. Sebastian, R. Laatikainen, and S. R. Salman. Can. J. Chem. 62, 326 (1984).

55. T. Schaefer, S. R. Salman and T. A. Wildman. Can. J. Chem. 58, 2364 (1980).

56. T. Schaefer and W. J. E. Parr. Can. J. Chem. 55, 552 (1977).

57. H. D. Rudolph, H. Driezler, A. Jaeschke and P. W. Wendling. Z. Naturforsch. 22A, 940 (1967).

58. N. W. Larsen, E. L. Hansen and F. M. Nicolaisen. Chem. Phys. Lett. 43, 584 (1976).

59. A. Wolf, U. Voets, and H-H. Schmidtke. Theoret. Chim. Acta, 54, 229 (1980).

60. A. Hastie, D. G. Lister, R. L. McNeil, and J. K. Tyler. J. Chem. Soc. Chem. Comm. 108 (1970).

61. W. J. Hehre, L. Radom, and J. A. Pople. J. Chem. Soc. Chem. Comm., 669 (1972).

PART II

The Barrier to Internal Rotation in 2,6-disubstituted N-methylanilines

A. INTRODUCTION

1. Conformational Analysis of N-methylaniline

What follows is a summary of experimental investigations of the methylamino group conformation, and its barrier to internal rotation, in N-methylaniline and some of its derivatives.

a) Infrared spectroscopy

Grindley, Katritzky and Topsom[1] have shown how the Hammett constant, σ_R^o, may be directly related to an energy scale, and have used infrared spectroscopic methods to suggest barriers to rotation for monosubstituted benzenes[2], where the substituent has a planar or nearly planar ground state because of conjugation between the sidechain and the benzene π system. The barriers are calculated from the equation

$$E_{(kcal)} = 33[|\sigma_R^o| - |(\sigma_R^o)tw|] - S \qquad (1)$$

where σ_R^o and $(\sigma_R^o)_{tw}$ are the Hammett resonance constants for the "in-plane" low-energy conformer and the orthogonal (90°) twisted conformer, respectively. S is the corresponding difference in strain energy (steric interaction with ortho C-H bonds) and, in the case of an amine, rehybridization energy.

Their calculations give a rotational barrier of 7.4 kcal/mol (31.0 kJ/mol) for N-methylaniline.

A vapor phase infrared investigation by Kydd and Dunham[3] yielded the following barriers: methyl torsion, 12.9 ± 2.0 kJ/mol, methylamino group torsion, 14.5 ± 0.5 kJ/mol and H-N-CH_3 inversion, 2.3 ± 0.5 kJ/mol. The large-amplitude vibrations associated with these three barriers were treated separately. The methyl torsion was given a potential of the form $V = \frac{1}{2} \sum_{n=1}^{6} V_n(1-\cos n\alpha)$, the potential function for methylamino torsion was assumed to have the

form $V = V_2/2\ (1-\cos 2\phi)$, and the inversion potential took the common form $V(x) = V_2X^2 + V_4X^4$.

The inversion barrier of the nitrogen in aniline is 6.3 kJ/mol[4]. Kydd and Dunham suggest that the lower barrier of inversion for N-methylaniline is a consequence of greater planarity at the nitrogen than in aniline. They consider this to be unusual since increased planarity implies greater conjugation of the nitrogen lone-pair with the benzene π system and hence a higher barrier in N-methylaniline. Experiment shows that aniline has a barrier to rotation about the C_1-N bond of 24.0 ± 0.5 kJ/mol. This is 9.5 kJ/mol higher than that for N-methylaniline. Kydd and Dunham suggest the possibility of partial nitrogen lone-pair delocalization into the N-C_α bond.

Butt and Topsom[5], in a study of the effect of <u>para</u> substitution on the frequencies and intensities of the N-H stretching vibrations, find that the frequency, ν_{NH}, increases with increasing π electron accepting ability of the substituent. This trend is consistent with an increase in the double bond character of the C_1-N bond and hence with an increase in the force constant for the N-H stretching vibration.

b) Microwave spectroscopy

A structure determination of the methylamino group in 4-fluoro-N-methylaniline, using low and high resolution microwave spectroscopy, has been carried out by Cervellati, Dal Borgo and Scappini[6]. A fit of sidechain structural parameters to the rotational constants gives a bond angle, H-N-C_α, of 115.6 ± 0.4°, and N-C_α bond length of 1.430 ± 0.005 Å and an angle ϕ of 18 ± 3°. The angle ϕ is shown in 1.

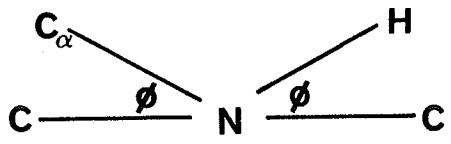

1

Flattening at the nitrogen from ϕ = 26° in 4-fluoroaniline[7] to 18° in 4-fluoro-N-methylaniline is attributed to steric effects arising from the bulky methyl and phenyl groups, in agreement with the trend towards nitrogen planarity in the series[8]: NH_3, NH_2CH_3, $NH(CH_3)_2$, $N(CH_3)_3$.

It is suggested that the shortening of the N-C bond, by about 0.04 Å relative to CH_3NH_2[9] and CH_3NHCl[10], is the result of reduced electron density at the nitrogen.

Cervellati, Dal Borgo and Lister[11] have criticized the structure determination of Cervellati, Dal Borgo and Scappini[6].

Because of the limited amount of experimental data, many of the structural parameters had to be assumed and held constant during the least-squares fit of the parameters to the rotational constants.

The inertial defect, Δ, is

$$\Delta = I_a + I_b - I_c = 2 \quad m_i c_i^2$$

where I_a, I_b and I_c are the principal moments of inertia, m_i is the mass and c_i the coordinate in the principal inertial axis system. The inertial defect has an angular dependence on the rotation of the sidechain in substituted benzenes and has been used to demonstrate the planarity of 4-fluoroanisole[12].

A similar treatment of 4-fluoro-N-methylaniline yields $\phi \simeq 19°$ for the normal isotopic species. The Δ value for the deuterated species is rather low and an interpretation of this result is not provided.

A microwave investigation of the normal amino-deuterated species of N-methylaniline in the ground and first excited torsional states was carried out by Cervellati, Corbelli, Dal Borgo and Lister[13]. The three large-amplitude vibrations, inversion of the N-H-CH_3 group, torsion of the H-N-CH_3 group about the N-C_1 bond and torsion of the methyl group, were treated as uncoupled one-dimensional problems, admittedly a rather poor approximation. The barriers were given as $8 < V_2 < 25$ kJ/mol for the internal rotation of the H-N-CH_3 group, 0.8 ± 0.3 kJ/mol or 1.8 ± 0.3 kJ/mol for inversion at nitrogen and $V_3 > 8$ kJ/mol for the barrier to

methyl rotation. The reduction of the inversion and H-N-CH_3 group rotation barriers with respect to aniline were again noted.

c) Photoelectron spectroscopy

Cowling and Johnstone[14] have applied two methods relating the photoelectron spectra of ring and amino methylated anilines to the twist angle, α, between the lone-pair on nitrogen and the π-orbitals on the benzene ring. The angle α is shown in 2.

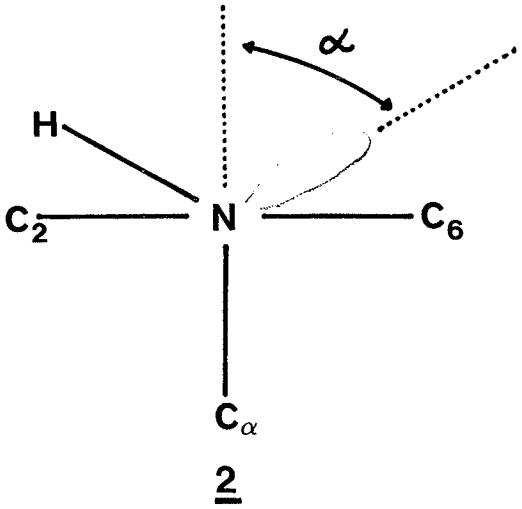

2

The first method assumes a linear relationship between the energy level of the lone-pair electrons on nitrogen and $\cos\alpha$ or $\cos^2\alpha$. For N-methylanilines α is taken as 0° for N-methylaniline and as 90° for N-methyl-cyclohexylamine. In the latter, conjugation between the nitrogen on the ring is absent.

In the second method, the difference in the energies of the π_2 and π_3 levels in anilines is taken as a measure of the resonance effect of the amino group on the orbital levels of benzene. This energy is assumed to have a linear relationship to $\cos\alpha$ or $\cos^2\alpha$. It is suggested that neither a simple $\cos\alpha$ nor a $\cos^2\alpha$ relationship

alone is satisfactory but that a complex relationship using powers of $\cos\alpha$ should be used.

The results of Cowling and Johnstone for ring-methylated N-methylanilines are reproduced in table 1.

Table 1

The conformations of some N-methylanilines as determined by Cowling and Johnstone (reference 14). The angle α is defined in the text.

	Method 1		Method 2	
aniline derivative	(from cosα)	(from $\cos^2\alpha$)	(from cosα)	(from $\cos^2\alpha$)
N-methyl	0	0	0	0
2-methyl-N-methyl	0	0	0	0
2,6-dimethyl-N-methyl	44	33	35	25
2,4,6-trimethyl-N-methyl	43	31	38	27

d) Nuclear magnetic resonance spectroscopy

i) long-range spin-spin couplings

Long-range amino proton to ring proton couplings have been reported by Schaefer and Wasylishen[15] for 2-nitro-4-chloro-N-ethylaniline. Amino proton exchange was retarded by strong hydrogen bonding to the ortho nitro group. The stereospecific five-bond $^5J^{NH,H}$ between the amino proton and the meta ring protons were $^5J^{NH,H3} < \pm 0.1$ Hz and $^5J^{NH,H5} = 0.67 \pm 0.03$ Hz. It was suggested that the molecule has the conformation shown in 3, firstly due to the strong hydrogen bond and secondly because of repulsive interaction between the ethyl and nitro groups.

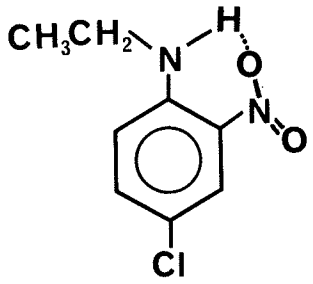

3

The observation of a through-space coupling of -0.39 ± 0.04 Hz between the methylene protons of the ethyl group and the ortho ring proton suggested the spacial proximity of these protons; consistent with the conformation in 3.

Gale and Wilshire[16] investigated the coupling between the NH proton and the H5 proton of the nitrophenyl ring in a series of

2-nitro and 2,4-dinitrodiphenylamines and noted that $^{5}J^{NH,H5}$ was absent in highly polar solvents, except when the unnitrated ring carried powerful electron-donating substituents in the 2' and 4' positions. The presence of $^{5}J^{NH,H5}$ was taken as evidence that intramolecular hydrogen bonding occurred between the amino proton and the ortho nitro group and that this hydrogen bond was only broken by highly polar solvents. The values of $^{5}J^{NH,H5}$ ranged from 0.55 Hz to 0.70 Hz.

Wilshire[17] has also investigated the hydrogen bond accepting abilities of the 2-substituents in N-methyl-, N-benzyl- and N-phenyl-ortho substituted-4-nitroanilines. Monitoring the presence of $^{5}J^{NH,H5}$ of these compounds in solvents of different polarity indicates that the strength of the hydrogen bond decreases in the following order

$$NH...COOCH_3 > NH...NO_2 \simeq NH...COCH_3 > NH...CHO > NH...CN$$

ii) dynamic nuclear magnetic resonance

Heidberg, Weil, Janusonis and Anderson[18] performed dynamic nmr experiments on 2,4,6-trinitro-N-methylaniline and observed the transformation of the A_2 spin system of the ring protons into an AB system with decreasing temperature. Lineshape analysis yielded an activation energy of 14.5 ± 0.3 kcal/mol (60.7 kJ/mol).

The stability of the "planar" molecule was attributed to strong hydrogen bonding between the amino proton and the ortho nitro groups

and to the increase in conjugation between the amino nitrogen lone-pair and the ring π system, induced by the nitro substituents.

Von Jouanne and Heidberg[19] later determined the activation parameters for hindered rotation of N-alkylamino groups in N-alkyl-2,4,5-trinitroanilines. The results are given in table 2. The trend here is a decrease in rotational barrier with an increase in size of the alkyl substituent.

By observing the temperature dependent, proton decoupled, ^{13}C nmr spectrum of N-methylaniline between -113°C and -133°C, Lunazzi, Magagnoli, Guerra and Macciantelli[20] determined the activation parameters for rotation about the Csp^2-N bond. Both the ortho and meta carbons were anisochronous at -133°C, yielding six lines in the aromatic region of the ^{13}C nmr spectrum compared to 4 lines found at higher temperatures. Line shape analysis yielded $\Delta G^{\ddagger}$ as 7.24 ± 0.02 kcal/mol (30.29 ± 0.08 kJ/mol), $\Delta H^{\ddagger}$ as 7.6 ± 0.2 kcal/mol (31.8 ± 0.8 kJ/mol) and $\Delta S^{\ddagger}$ as 2.0 ± 1.5 cal/mol K (8.4 ± 6.3 J/mol K). A barrier of 9.07 kcal/mol (37.95 kJ/mol) was computed by STO-3G MO calculations.

Lunazzi, Magagnoli and Macciantelli[21] next investigated the effect of para ring substitution and N-alkyl substitution on the barrier height. Free energies of activation at the coalescence temperature were determined and taken as temperature independent within experimental error since $\Delta S^{\ddagger}$ for N-methylaniline was small. The results of Lunazzi et al.[21] are reproduced in tables 3 and 4. Two definite trends are evident here. Electron release by the para substituent causes a reduction in the rotational barrier. This

follows because electron releasing *para* substituents reduce the conjugation that restricts rotation about the N-C_1 bond. The other trend is a reduction of the rotational barrier with increasing size of R, the alkyl group, in the H-N-R fragment. This is explained as a result of the twisting of the N-H-R plane and destabilization of the ground state due to reduced nitrogen-phenyl conjugation.

Anet and Ghiaci[22] used ^{13}C DNMR to determine the barrier to rotation about the N-C_1 bond in a $CHFCl_2$-CHF_2Cl solution of N-methylaniline. The barrier of 6.1 kcal/mol (25.5 kJ/mol) was lower than that found by Lunazzi *et al.* in a $(CH_3)_2O$ solution. A solvent dependence was also observed for the rotational barrier in 4-nitro-N-methylaniline. In acetone-d_6 the observed barrier was 10.9 kcal/mol (46.0 kJ/mol) by ^1H nmr. In CD_2Cl_2 the observed barrier was 10.2 kcal/mol (42.7 kJ/mol) by ^1H nmr. The solvent dependence of the rotational barrier in 4-nitro-N-methylaniline was explained as due to the large dipole moment of the molecule together with possible intermolecular hydrogen bonding by the NH group to the solvent molecules.

iii) ^{15}N coupling constants and chemical shifts

The hybridization of nitrogen can be related to the one-bond ^{15}N-^1H coupling constant and the one-bond ^{15}N-^{13}C coupling constant. The relationships proposed by Binsch[23] *et al.* are:

$$S_N = 0.43 \left| {}^1J^{15\text{-}N,H} \right| - 6 \qquad (3)$$

$$S_N \times S_C = 80 \left| {}^1J^{15\text{-}N,13\text{-}C} \right| \qquad (4)$$

Table 2

Activation energies for 2,4,6-trinitro-N-alkylanilines as determined by Von Jouanne and Heidberg[19].

R	E_A kcal/mol	E_A kJ/mol
CH_3	14.5 ± 0.2	60.7 ± 0.8
CH_2CH_3	14.53 ± 0.23	60.8 ± 1.0
$CH(CH_3)_2$	13.08 ± 0.14	54.7 ± 0.6
$C(CH_3)_3$	$\leq$ 10	$\leq$ 42

Table 3

Free energies to internal rotation about the Csp^2-N bond in 4-X-N-methylaniline as determined by Lunazzi, Magagnoli and Macciantelli[21].

X	$G^{\ddagger}$/kcal mol^{-1}	$G^{\ddagger}$/kJ mol^{-1}	Solvent
OCH_3	5.7 ± 0.2	23.8 ± 0.8	CHF_2Cl
F	6.90 ± 0.05	28.9 ± 0.2	$(CH_3)_2O$
H	7.24 ± 0.02	30.29 ± 0.08	$(CH_3)_2O$
Cl	7.70 ± 0.02	32.22 ± 0.08	$(CH_3)_2O$
$COCH_3$	9.45 ± 0.15	39.54 ± 0.63	$(CH_3)_2O$
NO_2	11.1 ± 0.1	46.4 ± 0.4	acetone-d_6

Table 4

Free energies to internal rotation about the Csp^2-N bond in N-alkylanilines as determined by Lunazzi, Magagnoli and Macciantelli[21].

R	$\Delta G^{\ddagger}$/kcal mol^{-1}	$\Delta G^{\ddagger}$/kJ mol^{-1}	Solvent
CH_3	7.24 ± 0.02	30.29 ± 0.08	$(CH_3)_2O$
CH_2CH_3	7.2 ± 0.1	30.3 ± 0.4	$(CH_3)_2O$
$CH(CH_3)_2$	6.8 ± 0.1	28.5 ± 0.4	$(CH_3)_2O$
$C(CH_3)_3$	6.3 ± 0.1	26.4 ± 0.4	CCl_2F_2-$CHFCl_2$

Schaefer and Wasylishen proposed the relation

$$S_N = -0.59\ {}^1J^{15\text{-}N,H} - 17.5 \qquad (5)$$

where S_N is the percent S character of the nitrogen.

Bothin-Strzalko, Pouet and Simonnin[25] found ${}^1J^{15\text{-}N,H}$ as 78 Hz, ${}^1J^{15\text{-}N,13\text{-}C}_{methyl}$ as 10.3 Hz and ${}^1J^{15\text{-}N,13\text{-}C}_{ring}$ as 13 Hz in N-methylaniline. The following values of S_N were deduced from ${}^1J^{15N,H}$: 27.5 using equation (3) and 28.5 from equation (5). Substitution of ${}^1J^{15\text{-}N,13\text{-}C}_{ring}$ into equation (4) gave S_N as 32.7 and substitution of ${}^1J^{15\text{-}N,13\text{-}C}_{methyl}$ into equation (4) gave S_N as 31.2 These results indicated that the nitrogen hybridization in N-methylaniline is intermediate between sp^3 and sp^2. Equation (5) gives S_N as 29 for aniline[15N] [24].

Dorie, Mechim and Martin[26] have related ${}^{15}N$ chemical shifts to barriers of rotation about the $N\text{-}C_1$ bond in <u>para</u> substituted anilines and N,N-dimethylanilines. According to Martin[27], the barrier to internal rotation in N-methylaniline can be taken as the average of the values for aniline and N,N-dimethylaniline. The barrier in N-methylaniline is calculated as (22.1 + 24.7)/2 = 23.4 kJ/mol in DMSO solution.

The use of ${}^{15}N$ chemical shifts is not reliable since barriers determined by this method disagree with accepted values[22].

2. Theoretical Considerations

A classical treatment[28] of the nmr phenomenon yields the Bloch equations for the rotating frame

$$\frac{du}{dt} = 2\pi v(\nu_o - \nu) - \frac{u}{T_2} \tag{6a}$$

$$\frac{dv}{dt} = -2\pi u(\nu_o - \nu) - \frac{v}{T_2} - \gamma B_1 M_z \tag{6b}$$

$$\frac{dM_z}{dt} = \frac{-(M_z - M_o)}{T_1} + \gamma B_1 v \tag{6c}$$

where v and u represent orthogonal magnetic moments which rotate in the x-y plane with the frequency ν of the observing field, B_1; ν_o is the precession frequency of the nuclear moment, T_1 is the longitudinal or spin-lattice relaxation time and T_2 is the transverse or spin-spin relaxation time. Under the steady state approximation ($\frac{du}{dt} = \frac{dv}{dt} = \frac{dM_z}{dt} = 0$) equations (6) can be solved for u, v and M_z.

$$u = \frac{2\pi\gamma B_1 M_o T_2^2(\nu_o - \nu)}{1 + 4\pi^2 T_2^2(\nu_o - \nu)^2 + \gamma^2 B_1^2 T_1 T_2} \tag{7a}$$

$$v = \frac{\gamma B_1 M_o T_2}{1 + 4\pi^2 T_2^2(\nu_o - \nu)^2 + \gamma^2 B_1^2 T_1 T_2} \tag{7b}$$

$$M_z = \frac{M_o[1 + 4\pi^2 T_2^2(\nu_o - \nu)^2]}{1 + 4\pi^2 T_2^2(\nu_o - \nu)^2 + \gamma^2 B_1^2 T_1 T_2} \tag{7c}$$

When B_1 is small, $M_z \approx M_o$ and $B_1^2 T_1 T_2 << 1$ and equations (7) can be simplified. The magnetic moment in the x-y plane can be represented by a complex number G, where

$$G = u + iv \tag{8}$$

Then (6b) gives

$$\frac{dG}{dt} = -G[\frac{1}{T_2} - 2\pi i(\nu_o - \nu)] - i\gamma B_1 M_o \tag{9}$$

Under steady state conditions the complex quantity G, takes the form

$$G = [\frac{2\pi C T_2^2 (\nu_o - \nu)}{1 + 4\pi^2 T_2^2 (\nu_o - \nu)^2}] - i[\frac{C T_2}{1 + 4\pi^2 T_2^2 (\nu_o - \nu)^2}] \tag{10}$$

where $C = \gamma B_1 M_o$. The imaginary part, v, gives the lineshape of the absorption signal.

Modification of the Bloch equations to take into account exchange between two sites A and B, where there is no nuclear spin-spin coupling J_{AB}, can be done classically. Both Gutowsky *et al.*[29] and McConnell[30] have treated the two-site case.

The rate equations for this exchange are given by

$$A \underset{k_B}{\overset{k_A}{\rightleftharpoons}} B \tag{11a}$$

$$\frac{d[A]}{dt} = -k_a [A] \tag{11b}$$

$$\frac{d[B]}{dt} = -k_B[B] \tag{11c}$$

Under equilibrium conditions the time dependence of magnetization in site A is

$$\frac{dG_A}{dt} = -k_A G_A + k_B G_B \tag{12}$$

Simplification of (9) yields

$$\frac{dG_A}{dt} = -\alpha_A G_A - iC_A \tag{13a}$$

where

$$\alpha_A = \frac{1}{T_{2A}} - 2\pi i(\nu_A - \nu)$$

Similarly

$$\frac{dG_B}{dt} = \alpha_B G_B - iC_B \tag{13b}$$

Summation of exchange and relaxation effect on the change in magnetization yields modified Bloch equations

$$\frac{dG_A}{dt} = -\alpha_A G_A - iC_A - k_A G_A + k_B G_B \tag{14a}$$

$$\frac{dG_B}{dt} = -\alpha_B G_B - iC_B - k_B G_B + k_A G_A \tag{14b}$$

Solving for G_A and G_B under slow passage (steady state) conditions and taking the imaginary part of their sum, G, gives the bandshape of the exchanging system. If P_A and P_B are taken as the fractional populations in sites A and B, then C_A can be represented by $P_A C_o$ and C_B by $P_B C_o$ and the magnetization G is given as,

$$G = \frac{-iC_o(k_A + k_B + \alpha_A P_B - \alpha_B P_B)}{\alpha_A k_B + \alpha_B k_A + \alpha_A \alpha_B}$$

where P_A and P_B are related by equation (16).

$$P_A + P_B = 1 \tag{16a}$$

$$P_A k_A = P_B k_B \tag{16b}$$

Separation of the x-y magnetization, G, into its real and imaginary components yields the bandshape of the nmr signal

$$v = \frac{-C_o\{ P[1 + \tau(\frac{P_B}{T_{2A}} + \frac{P_A}{T_{2B}})] + QR\}}{P^2 + R^2}$$

where

$$P = \tau \left[\frac{1}{T_{2A}T_{2B}} - 4\pi^2\Delta\nu^2 + \pi^2(\delta\nu)^2\right] + \frac{P_A}{T_{2A}} + \frac{P_B}{T_{2B}}$$

$$Q = \tau \left[2\pi\Delta\nu - \pi\delta\nu \ (P_A - P_B)\right]$$

$$R = 2\pi\Delta\nu \left[1 + \tau\left(\frac{1}{T_{2A}} + \frac{1}{T_{2B}}\right)\right] + \pi\delta\nu\tau\left(\frac{1}{T_{2B}} - \frac{1}{T_{2A}}\right)$$

$$+ \pi\delta\nu(P_A - P_B)$$

$$\delta\nu = \nu_A - \nu_B$$

$$\Delta\nu = \frac{\nu_A + \nu_B}{2} - \nu$$

and

$$\tau = \frac{P_A}{k_B} = \frac{P_B}{k_A}$$

If $\delta\nu$ and k are much larger than the linewidth in the absence of exchange, $1/\pi T_2$, (17) simplifies to

$$v = \frac{Kk\delta\nu^2}{k^2(\Delta\nu)^2 + 4\pi^2(\nu_A - \nu)^2(\nu_B - \nu)^2} \qquad (18)$$

Upon differentiation of (18) with respect to ν, a simple relationship can be found between the rate constant and the separation between maxima, $\delta\nu_e$,

$$k = \frac{\pi}{\sqrt{2}}\sqrt{\delta\nu^2 - \delta\nu_e^2} \qquad (19)$$

At the coalescence temperature $\delta\nu$ equals the half-height linewidth and (19) reduces to the well known expression

$$k = \frac{\pi\delta\nu}{\sqrt{2}} \qquad (20)$$

Equation (20) holds under the condition that $\delta\nu >> 1/\pi T_2$.

The Eyring equation (21) relates the rate constant of a process such as the two-site exchange to the activation parameters for such a process

$$k = \frac{\kappa k_B}{h} T \exp\left(\frac{-\Delta G^{\ddagger}}{RT}\right) \qquad (21)$$

where k_B is the Boltzmann constant, h is Planck's constant, R is the gas constant and κ is the transmission coefficient, often assumed to be equal to unity.

If (20) is substituted for k in (21), then an expression for the free energy of activation can be obtained at the temperature of coalescence,

$$\Delta G_c^{\ddagger} = RT[\ 22.962 + \ln(T/\delta\nu)\ ] \qquad (22)$$

The Eyring equation (21) can also take the form,

$$k = \frac{k_B T}{h} \exp\left(\frac{\Delta H^{\ddagger} - T\Delta S^{\ddagger}}{kT}\right) \qquad (23)$$

The logarithmic form of the equations is

$$\ln\left(\frac{k}{T}\right) = \frac{-\Delta H^{\ddagger}}{R}\frac{1}{T} + \frac{\Delta S^{\ddagger}}{R} + \ln\left(\frac{k_B}{h}\right) \qquad (24)$$

A plot of ln (k/T) versus 1/T yields a straight line and the activation parameters $\Delta H^{\ddagger}$ and $\Delta S^{\ddagger}$ can be obtained from the slope and intercept of the plot.

Whereas evaluation of $\Delta G^{\ddagger}$ only involves measurement of $\delta\nu$ (and hence k) at the coalescence temperature and application of equation (22), evaluation of $\Delta H^{\ddagger}$ and $\Delta S^{\ddagger}$ involves determination of the rate constant at temperatures below and above coalescence and a least-squares analysis of the plot of ln (k/T) versus 1/T.

Multi-site exchange involving exchange between n sites requries the steady state solution of n modified Bloch equations. The total magnetization, G, is the sum of the magnetization of the n nuclei

$$G = \sum_{i=1}^{n} G_i \qquad (25)$$

Separation of the real and imaginary parts of G can be lengthy and usually must be done by computer.

It is also possible to calculate the activation parameters for weakly coupled systems undergoing exchange by using the modified

Bloch equations, but strongly coupled systems require a full density matrix treatment. The density matrix method, which is applicable to line-shape calculations for all kinds of exchanging systems, will not be discussed here but several articles on the subject are available. The topic is also covered by Sandström[34].

3. Introduction to the Problem

Experimental studies of N-methylanilines suggest that the methylamino group lies nearly in the plane of the benzene ring; an angle ϕ of less than 20° is indicated in all cases.

Estimated barriers to rotation of the methylamino group are in the range $8 < V_2 < 25$ kJ/mol in the gas phase and $23 < V_2 < 32$ kJ/mol in solution. The barrier to rotation about the $N-C_1$ bond decreases with substitution of the methyl group by larger alkyl (R) groups, both for the unsubstituted molecule and the 2,4,6-trinitro derivative. This decrease in barrier has been explained as a result of destabilization of the ground state.

The intent of this study was to investigate the destabilization of the "nearly planar" ground state in N-methylaniline by ortho substitution, firstly by DNMR techniques and secondly by ab initio molecular orbital energy calculations.

B. EXPERIMENTAL METHOD

1. Compounds

4-Bromo-2,6-difluoro-N-methylaniline was made by bromination of 2,6-difluoroaniline (Aldrich) in the usual way, followed by N-methylation by the method of Johnston, Payling and Thomas[35].

2,6-dimethyl-N-methylaniline was purchased from the Aldrich chemical company.

2. Sample preparation

A solution in dimethylether, containing 0.11 g of 4-bromo-2,6-difluoro-N-methylaniline, 0.11 g of acetone-d_6, 1.5 ml of dimethylether and 1 drop C_6F_6 was transferred on a vacuum line to a 5 mm od nmr sample tube. The latter was flame-sealed and stored in a refrigerator while not in use. The acetone-d_6 was used for internal locking purposes and C_6F_6 served as a linewidth standard.

A solution containing about 1 gram of 2,6-dimethyl-N-methyl-aniline, 3 ml of dimethylether, and about 0.5 g of acetone-d_6 was prepared in a 10 mm od nmr tube by the same method.

3. Spectroscopic method

The ^{19}F spectra were recorded in the FT mode on a WH90 nmr spectrometer at 84.7 MHz (centerband), under conditions of ^{1}H noise decoupling. The amplitude of the decoupling field was kept low enough to prevent significant sample heating. The pulse width was 5 μs, the digitized response was accumulated for 1.02s into 4 K and the sweep width was 2000 Hz. These conditions applied at temperatures where the peak widths were rather large. As many as 64 scans were performed. At the lowest temperatures, shimming was performed on the FID of C_6F_6 and the sample was not spun. A very high flow rate of cooling gas was necessary in order to reach 114 K and the temperature was checked by means of a copper-constantan thermocouple. Spectra were accumulated at a given temperature, approached from lower as well as from higher temperatures, so that a check on lineshapes obtained near and at the coalescence temperature was possible.

The ^{13}C spectra for the 2,6-dimethyl-N-methylaniline sample were also recorded in the FT mode on a WH90 nmr spectrometer at 22.63 MHz (centerband), under conditions of ^{1}H noise decoupling. The pulse width was 12 μs, the digitized response was accumulated for 2.64 sec into 32 K and the sweep width was 6000 Hz. The compound began to precipitate at temperatures below 130 K.

4. Computations

Ab initio molecular orbital calculations were performed at the STO-3G level with the programs GAUSSIAN 70 [36] and MONSTERGAUSS [37].

All curves were statistically fitted to functions of the form $V(\phi) = V_2 \sin^2 (\phi - A)$ using th SAS nonlinear regression program NLIN[38].

Computations were performed on an Amdahl 470/V8 or an Amdahl 580/5850 system.

C. EXPERIMENTAL RESULTS

1. Dynamic nmr results

a) 4-bromo-2,6-difluoro-N-methylaniline

Figure 1 shows some typical fluorine nmr spectra for the temperature range 114 K to 124 K. The temperature range, 114 K to 135 K, in which the substrate peak displayed greater linewidths than the reference peak, is too small for a reliable decomposition of $\Delta G^{\ddagger}$ into $\Delta H^{\ddagger}$ and $\Delta S^{\ddagger}$. Complete separation into two peaks could not be achieved even at 114 K, the lowest temperature attainable. Repeated experiments in which coalescence was reached from both lower and higher temperatures, together with thermocouple measurement of temperatures indicated by the dial settings of the Bruker B-VT-1000 variable temperature controller, yield a coalescence temperature, T_c, of 120 ± 2 K. The total peak width at half height at coalescence was 100 ± 2 Hz. The half height peak width of the reference peak was 4 ± 1 Hz. If the peak separation at zero exchange rate, $\delta\nu$, is taken as the sum of the static splitting and the natural width[34] a reasonable estimate would be 96 ± 5 Hz. Now, using equation (22) yields $\Delta G^{\ddagger}_{120}$ = 23.1 ± 0.5 kJ/mol. As in previous studies[21,22], a transmission coefficient of unity was assumed.

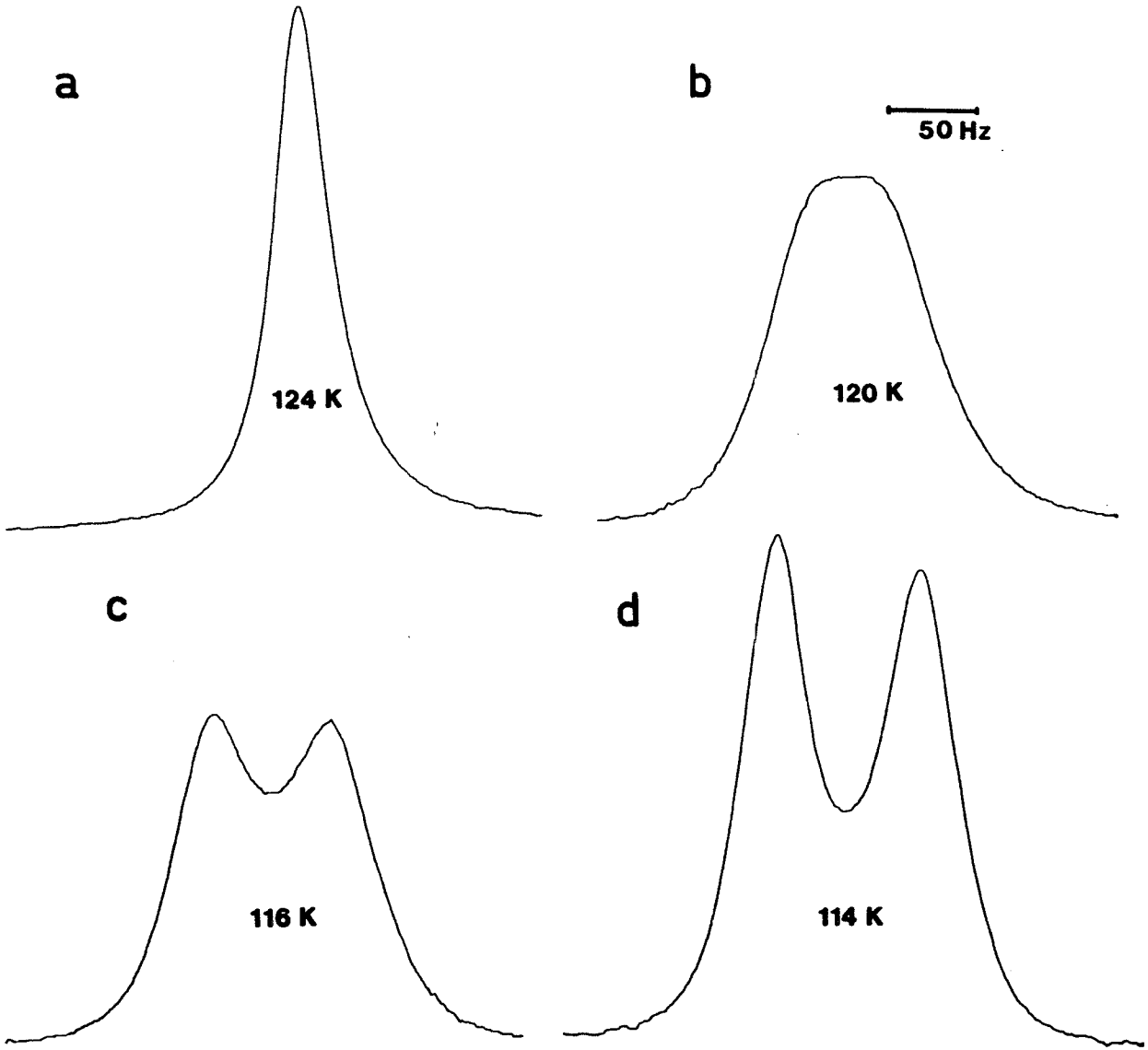
a
124 K
b
50 Hz
120 K
c
116 K
d
114 K

Figure 1

The ^{19}F nmr spectra of 2,6-difluoro-4-bromo-N-methylaniline at temperatures between 114 K and 124 K.

b) 2,6-dimethyl-N-methylaniline

The ^{13}C chemical shifts for the ring carbons in 2,6-dimethyl-N-methylaniline in dimethyl ether at various temperatures are given in table 5. Like the ortho and meta ring carbons, the ortho methyl carbons showed no relative broadening at 130 K. The compound precipitated at temperatures below 130 K.

Table 5

Ring carbon chemical shifts for 2,6-dimethyl-N-methylaniline at various temperatures[a].

	C_1	C_2	C_3	C_4
287 K	148.5	129.3	128.9	121.6
250 K	148.5	129.1	128.9	121.4
200 K	148.6	128.8	128.9	121.2
160 K	148.6	128.6	129.0	121.1
130 K	148.7	128.5	129.1	-

[a]Chemical shifts in ppm with respect to TMS, internal reference is CH_3OCH_3.

2. Geometry Optimizations

Figures 2, 3, 4 and 5 depict the results of geometry optimizations at the STO-3G level for N-methylaniline, 2,6-difluoro-N-methylaniline, 2,6-dichloro-N-methylaniline and 2-fluoro-N-methylaniline respectively. Throughout the optimization procedure the benzene ring was held as a hexagon while the carbon-carbon bond lengths were varied simultaneously. Ring protons and fluorines were kept coplanar with the benzene ring. C_{3v} symmetry of the methyl group about the nitrogen-methyl carbon bond axis was also retained.

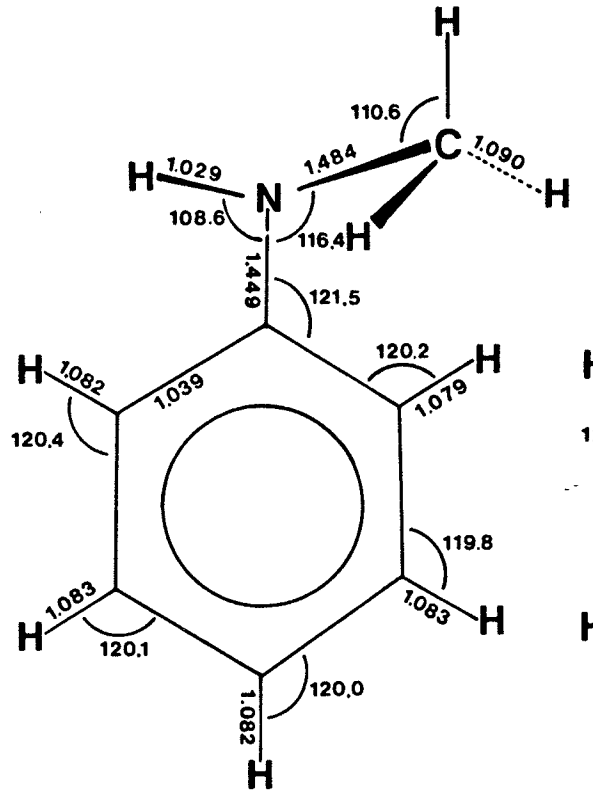

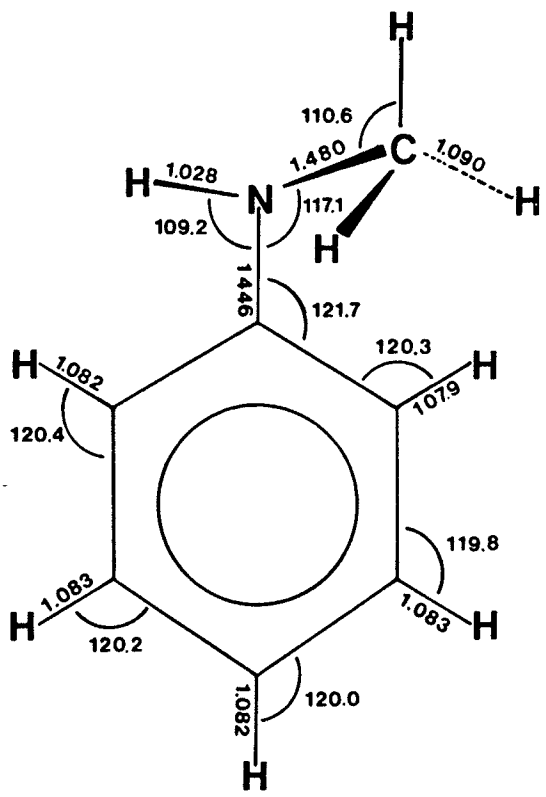

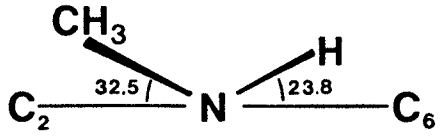

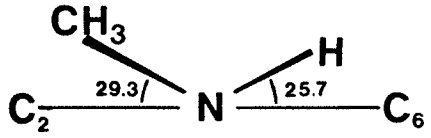

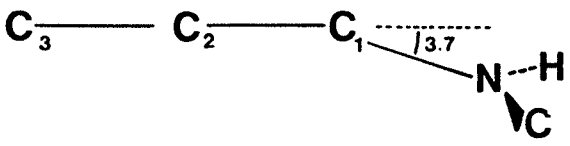

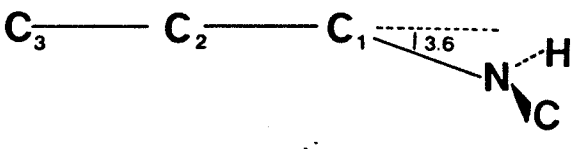

GAUSSIAN 70 **MONSTERGAUSS**

Figure 2

The STO-3G MO computed ground state structures of N-methylaniline using the programs GAUSSIAN 70 and MONSTERGAUSS.

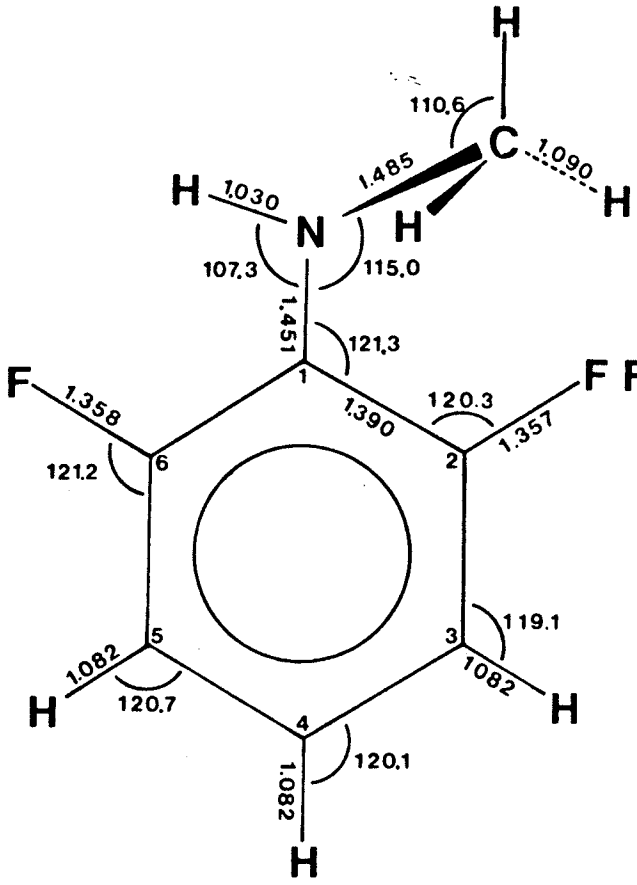

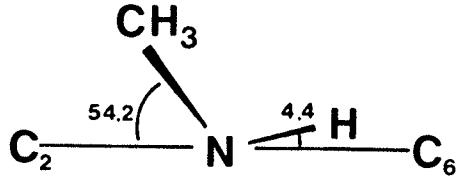

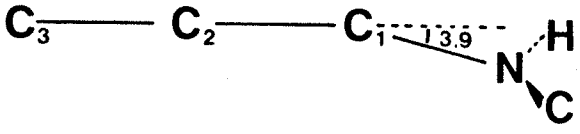

GAUSSIAN 70

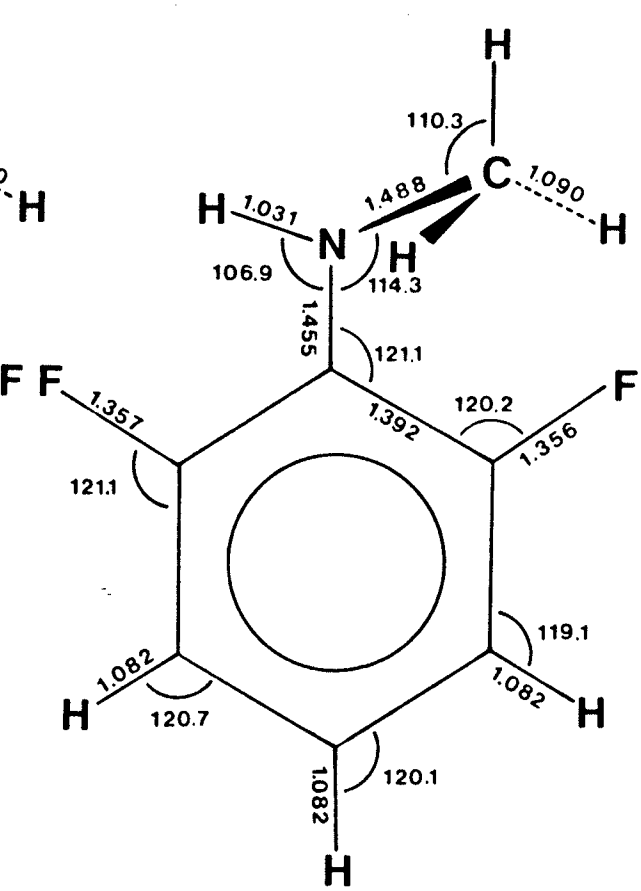

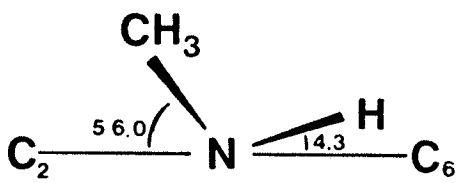

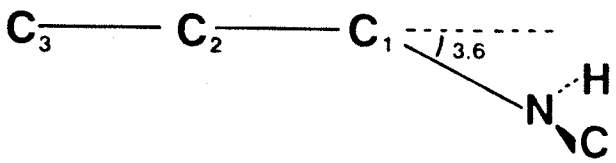

MONSTERGAUSS

Figure 3

The STO-3G computed ground state structures of 2,6-difluoro-N-methylaniline using the programs GAUSSIAN 70 and MONSTERGAUSS.

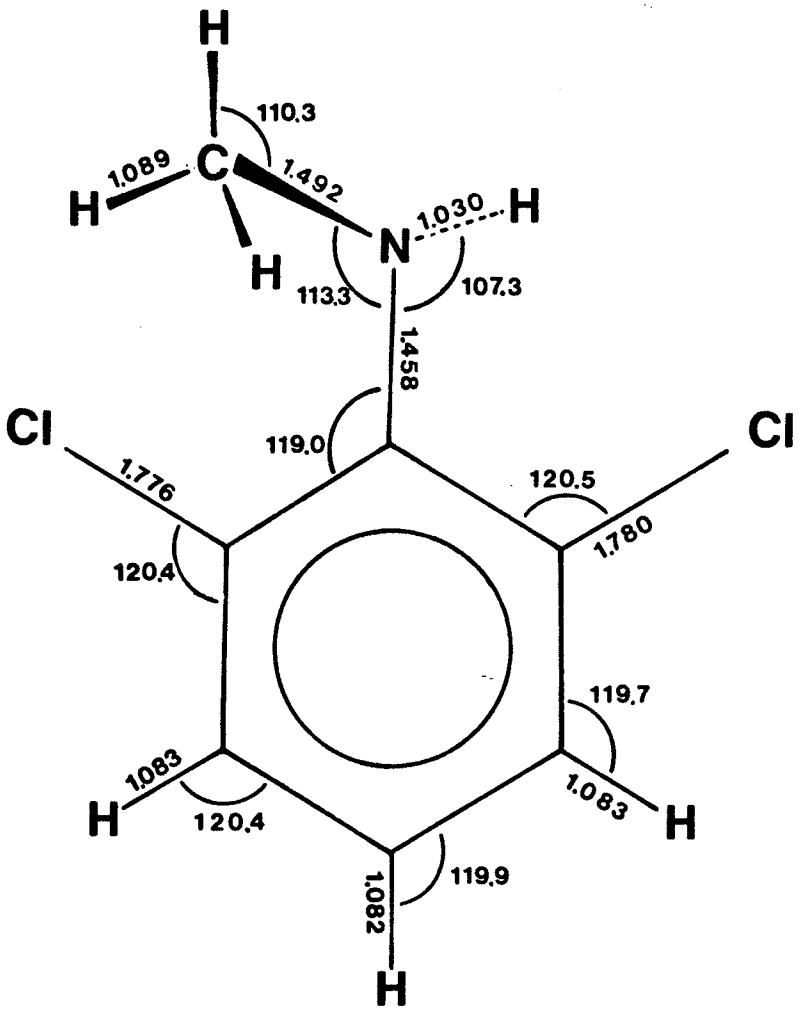
H
110.3
1.089
C
1.492
H
1.030
H
N
H
113.3
107.3
1.458
Cl
119.0
Cl
1.776
120.5
1.780
120.4
119.7
1.083
H
120.4
1.083
H
119.9
1.082
H

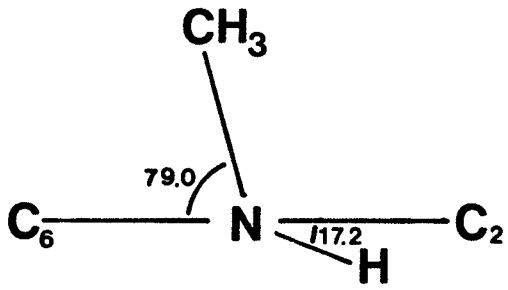
CH3
79.0
C6
N
C2
117.2
H

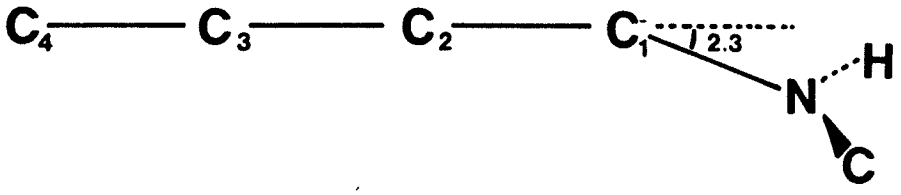
C4
C3
C2
C1
123
H
N
C

Figure 4

The STO-3G MO computed ground state structure of 2,6-dichloro-N-methylaniline using the program MONSTERGAUSS.

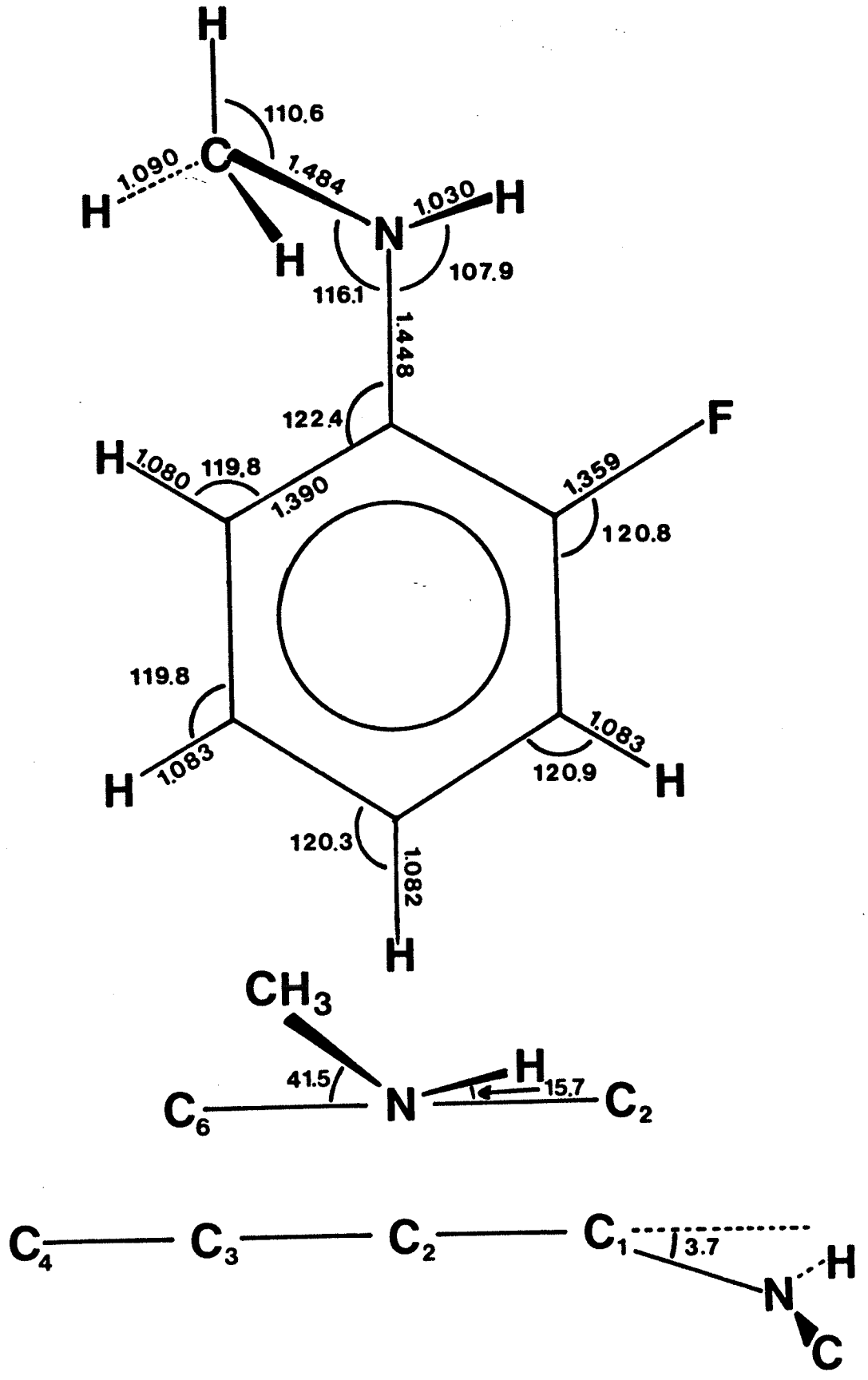
H
110.6
C
1.090
H
1.484
H
1.030
H
N
H
116.1
107.9
1.448
122.4
F
H
1.080
119.8
1.390
1.359
120.8
119.8
1.083
H
120.9
1.083
H
120.3
1.082
H
CH3
41.5
H
15.7
N
C6
C2
C4
C3
C2
C1
3.7
H
N
C

Figure 5

The STO-3G MO computed ground state structure of 2-fluoro-N-methylaniline using the program GAUSSIAN 70.

3. Computed barriers

a) Rotation about the Csp^2-N bond

Some results of the partial geometry optimizations for N-methylaniline, 2,6-difluoro-N-methylaniline and 2,6-dichloro-N-methylaniline appear in tables 6, 7 and 8, respectively, with reference to the numbering system shown in figure 6. The geometry parameters were optimized in the same order as they appear in the first column of tables 6 and 7.

In figures 7 and 8 the STO-3G MO energies, relative to their respective ground states, are plotted for N-methylaniline and its 2,6-difluoro derivative. The curves represent least squares fits to the computed points for twofold potential barriers of the form

$$V(kJ/mol) = (19.1 \pm 0.9) \sin^2 (\phi - 141.5 \pm 0.7°) \qquad (26)$$

for N-methylaniline and

$$V(kJ/mol) = (22.0\ 1\ 0.8) \sin^2 (\phi - 120.9 \pm 0.8) \qquad (27)$$

for 2,6-difluoro-N-methylaniline. Errors are given at the 95% confidence level.

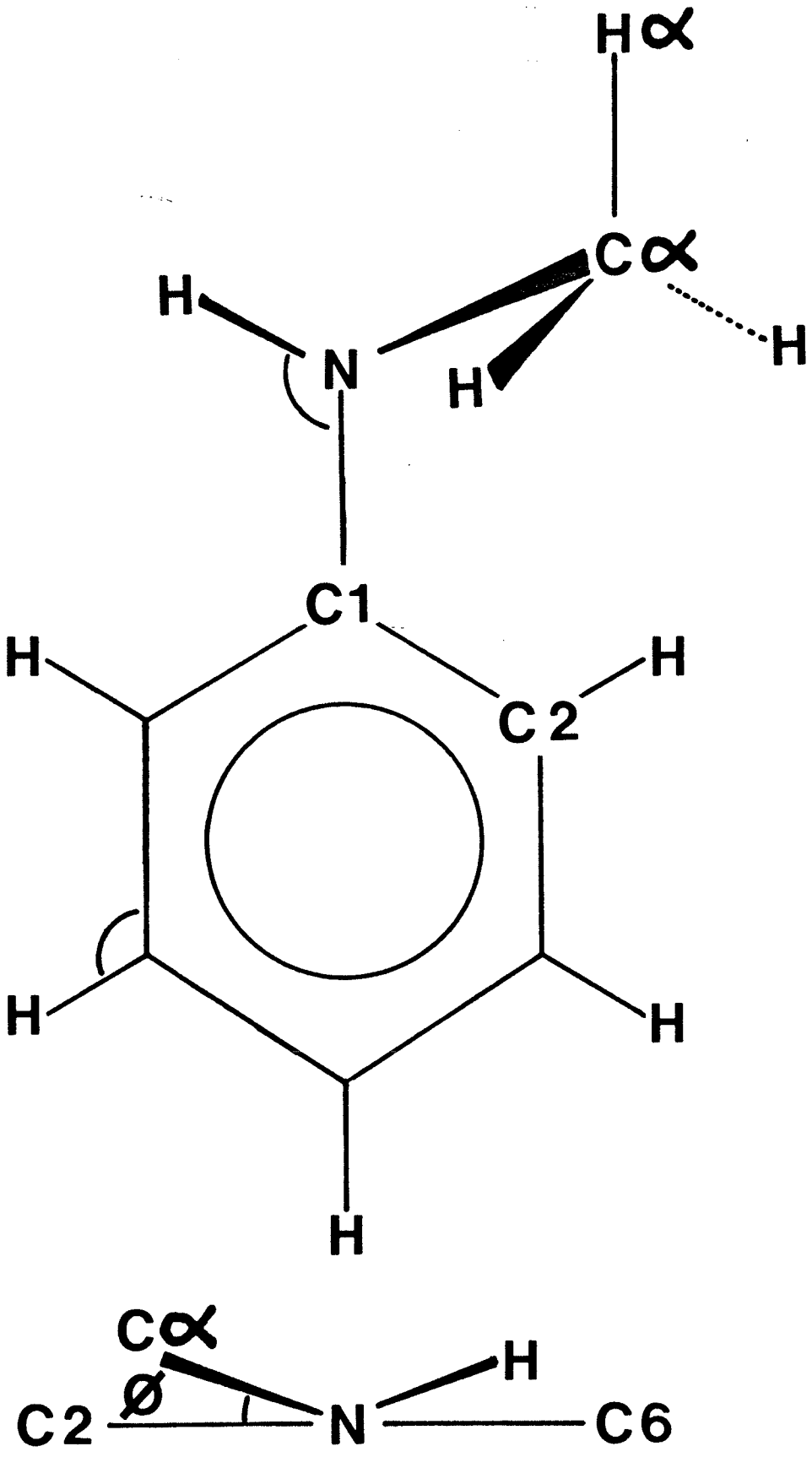
Hα
Cα
H
H
N
H
C1
H
H
C2
H
H
H
H
Cα
Ø
H
C2
N
C6

Figure 6

N-methylaniline in a conformation with $\phi = C_2C_1NC_\alpha$. Some atoms used in the description of the geometries are identified.

Table 6

Some Results of Partial Geometry Optimization in STO-3G Calculations for N-methylaniline[a].

$C_2C_1NC_\alpha$	0	15	30
$C_1NC_\alpha H$	182.3	173.5	169.2
C_2C_1NH	235.0	250.2	266.2
C_2C_1N	116.4	116.3	116.6
C_1NH	109.4	109.8	109.6
C_1N	1.455	1.459	1.464
$C_3C_2C_1N$	179.5	180.4	180.9
Dipole Moment (D)	1.262	1.198	1.156
Total Energy (Hartrees)	-320.785,337	-320.783,327	-320.781,425
Relative Energy (kJ/mol)	7.1	12.4	17.4

...Table 6 continued...

...Table 6 continued...

$C_2C_1NC_\alpha$	45	60	75
$C_1NC_\alpha H$	172.9	179.3	181.5
C_2C_1NH	282.2	299.3	315.0
C_2C_1N	117.0	117.6	118.2
C_1NH	109.0	108.2	107.8
C_1N	1.468	1.469	1.466
$C_3C_2C_1N$	180.7	180.2	179.8
Dipole Moment (D)	1.149	1.158	1.176
Total Energy (Hartrees)	-320.780,428	-320.780,789	-320.782,395
Relative Energy (kJ/mol)	20.0	19.0	11.2

...Table 6 continued...

...Table 6 continued...

$C_2C_1NC_\alpha$	105	120	135
$C_1NC_\alpha H$	178.9	179.6	186.2
C_2C_1NH	344.6	358.8	12.9
C_2C_1N	118.9	119.7	120.8
C_1NH	107.9	108.2	108.1
C_1N	1.457	1.453	1.456
$C_3C_2C_1N$	180.8	182.5	183.4
Dipole Moment (D)	1.229	1.268	1.316
Total Energy (Hartrees)	-320.785,611	-320.787,047	-320.787,782
Relative Energy (kJ/mol)	6.4	2.6	0.7

...Table 6 continued...

...Table 6 continued...

C_2C_1NC	150	165	180
$C_1NC_\alpha H$	192.4	189.8	181.2
$C_2C_1NH_\alpha$	26.7	40.1	54.8
C_2C_1N	121.7	122.9	123.6
C_1NH	108.5	109.4	109.8
C_1N	1.448	1.450	1.454
$C_3C_2C_1N$	183.7	184.0	183.7
Dipole Moment (D)	1.348	1.333	1.278
Total Energy (Hartrees)	-320.788,013	-320.787,347	-320.785,715
Relative Energy (kJ/mol)	0.1	1.8	6.1

[a]Using the program GAUSSIAN 70, angles in degrees, bondlengths in Ångstroms.

Table 7

Some Results of Partial Geometry Optimization in STO-3G Calculations for 2,6-difluoro-N-methylaniline[a].

$C_2C_1NC_\alpha$	0	7	15	30
$C_1NC_\alpha H$	179.3	175.6	172.8	161.4
C_6C_1NH	234.3	240.3	248.4	268.2
C_2C_1N	113.3	114.0	114.2	114.4
C_1NH	109.3	109.3	109.5	109.6
C_1NC_α	119.1	119.4	119.2	116.7
$C_3C_2C_1N$	179.0	179.2	179.4	179.1
C_1N	1.455	1.456	1.458	1.465
Dipole moment (D)	1.305	1.300	1.323	1.486
Total energy (Hartree)	-515.697,039	-515.696,531	-515.695,939	-515.695,166
Relative energy (kJ/mol)	17.7	19.0	20.6	22.6

...Table 7 continued...

...Table 7 continued...

$C_2C_1NC_\alpha$	35	45	60	75
$C_1NC_\alpha H$	169.6	158.0	180.0	181.1
C_6C_1NH	271.5	283.5	299.8	316.8
C_2C_1N	115.0	116.7	117.3	118.3
C_1NH	109.2	109.0	108.4	107.8
C_1NC_α	116.6	115.8	113.6	112.5
$C_3C_2C_1N$	179.0	179.1	178.9	179.4
C_1N	1.466	1.486	1.468	1.467
Dipole moment (D)	1.486	1.582	1.642	1.672
Total energy (Hartree)	-515.695,578	-515.695,549	-515.697,885	-515.699,513
Relative energy (kJ/mol)	21.5	21.6	15.5	11.2

...Table 7 continued...

...Table 7 continued...

$C_2C_1NC_\alpha$	90	105	125.8	150
$C_1NC_\alpha H$	180.9	181.4	182.1	203.7
C_6C_1N	331.7	347.2	4.4	22.2
C_2C_1N	118.4	119.5	121.3	122.2
C_1NH	107.5	106.8	107.3	108.4
C_1NC_α	112.6	112.6	115.0	118.8
$C_3C_2C_1N$	180.0	181.3	183.9	185.3
C_1N	1.463	1.461	1.451	1.445
Dipole moment (D)	1.639	1.559	1.455	1.259
Total energy (Hartree)	-515.699,513	-515.702,711	-515.703,774	-515.701,333
Relative energy (kJ/mol)	7.1	2.8	0.0	6.4

...Table 7 continued...

...Table 7 continued...

$C_2C_1NC_\alpha$	165	173	180
$C_1NC_\alpha H$	193.5	184.7	180.88
C_6C_1NH	36.6	44.2	50.9
C_2C_1N	122.8	125.3	125.2
C_1NH	109.1	109.5	109.5
C_1NC_α	120.2	119.7	119.9
$C_3C_2C_1N$	185.9	184.7	184.3
C_1N	1.447	1.449	1.451
Dipole moment(D)	1.190	1.186	1.179
Total energy (Hartree)	-515.699,592	-515.698,968	-515.698,080
Relative enregy (kJ/mol)	11.0	12.6	14.9

[a]Angles in degrees, bondlengths in Ångstroms.

Table 8

Some Results of Geometry Optimization in STO-3G Calculations for 2,6-dichloro-N-methylaniline[a].

$C_2C_1NC_\alpha$	0	15[b]	30
$C_1NC_\alpha H$	180.6	169.7	160.4
C_6C_1NH	179.9	-	167.1
C_2C_1N	115.5	115.1	115.8
C_1NH	113.7	110.9	110.1
C_1NC_α	130.2	126.4	124.5
$C_3C_2C_1N$	180.1	-	181.7
C_1N	1.409	1.427	1.430
Diple moment	0.704	1.301	1.562
Total Energy (Hartree)	-1228.779,246	-1228.780,641	-1228.782,200
Relative energy (kJ/mol)	24.2	20.5	16.4

...Table 8 continued...

...Table 8 continued...

$C_2C_1NC_\alpha$	45	60	79
$C_1NC_\alpha H$	149.1	179.5	180.0
C_6C_1NH	175.0	183.8	197.2
C_2C_1N	117.3	118.5	121.0
C_1NH	109.0	108.2	107.3
C_1NC_α	121.1	117.9	113.3
$C_3C_2C_1N$	181.9	181.0	182.3
C_1N	1.438	1.449	1.458
Dipole moment	1.885	2.197	2.471
Total energy (Hartree)	-1228.784,267	-1228.786,145	-1228.788,455
Relative energy (kJ/mol)	11.0	6.1	0.0

...Table 8 continued...

$C_2C_1NC_\alpha$	105	120	135
$C_1NC_\alpha H$	176.5	180.3	206.9
C_6C_1NH	220.8	238.0	260.9
C_2C_1N	122.4	124.0	125.2
C_1NH	106.5	106.8	109.0
C_1NC_α	112.1	114.6	118.4
$C_3C_2C_1N$	183.9	184.7	181.2
C_1N	1.468	1.472	1.464
Dipole moment	2.616	2.539	2.303
Total Energy (Hartree)	-1228.785,253	-1228.780,517	-1228.776,754
Relative energy (kJ/mol)	8.4	20.8	30.7

[a]Using the program MONSTERGAUSS, angles in degrees, bondlengths in Ångstroms.

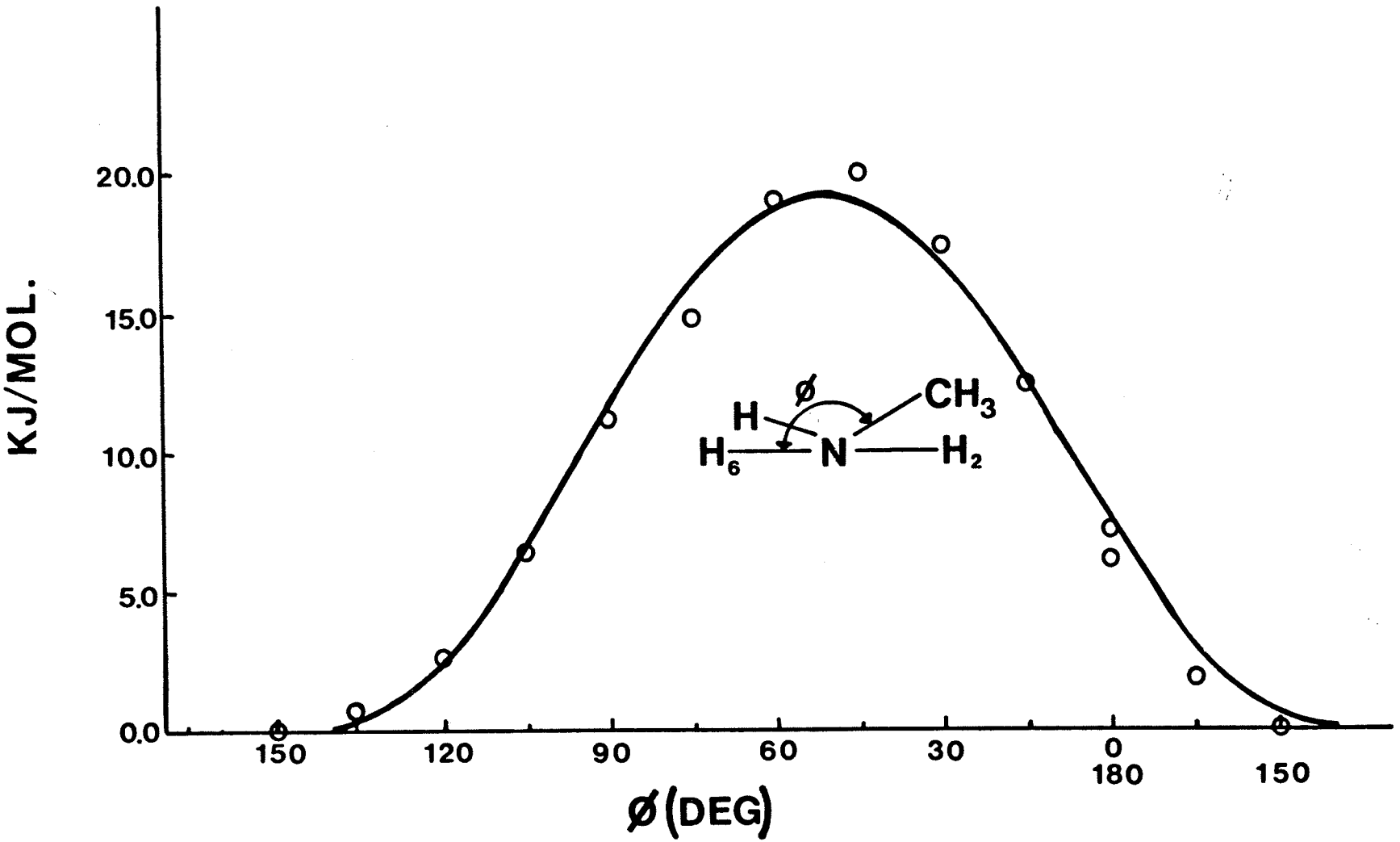
KJ/MOL.
20.0
15.0
10.0
5.0
0.0
150
120
90
60
30
0
180
150
Ø (DEG)
Ø
H
CH3
H6
N
H2

Figure 7

STO-3G MO computed energies for N-methylaniline as a function of dihedral angle ϕ. The solid curve is that for equation (26).

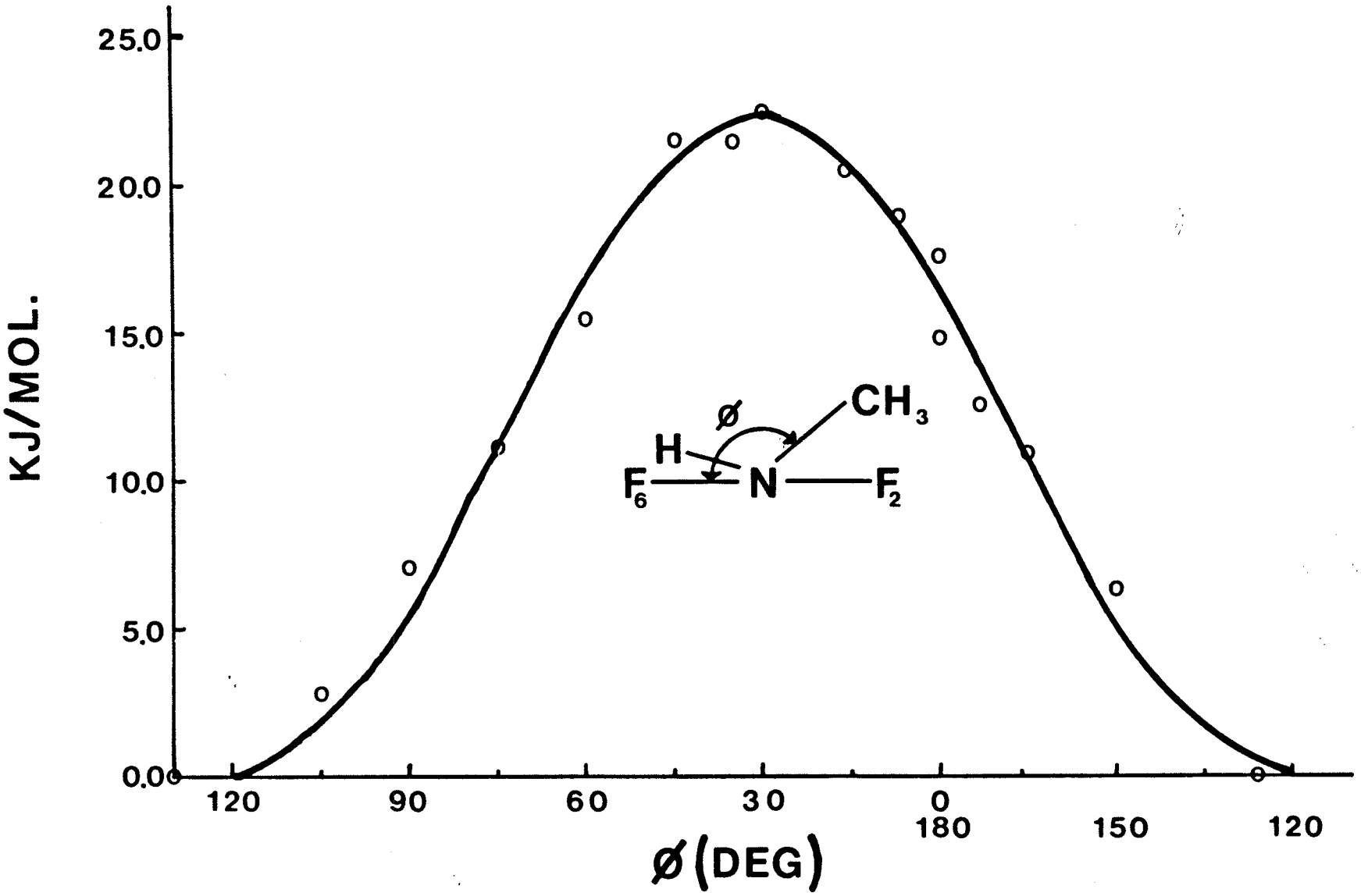
25.0
20.0
15.0
10.0
5.0
0.0
KJ/MOL.
120
90
60
30
0
180
150
120
Ø (DEG)
Ø
H
CH3
F6
N
F2

Figure 8

The STO-3G MO computed energies for 2,6-difluoro-N-methyl-aniline as a function of the dihedral angle ϕ. The solid curve is that for equation (27).

b) Methyl rotation

The energies for rotation of the methyl group are presented in table 9. The barrier to rotation of the methyl group in the ground state of N-methylaniline is 11.7 kJ/mol and is approximately a threefold barrier.

Table 9

STO-3G calculated energies for methyl rotation in N-methylaniline[a].

$C_1NC_\alpha H_\alpha$	Total Energy (H)	Relative Energy (kJ/mol)
192.8	-320.788, 049	0.0
202.8	-320.787, 434	0.8
212.8	-320.786, 959	2.8
222.8	-320.786, 915	5.6
232.8	-320.784, 843	8.4
242.8	-320.783, 990	10.6
252.8	-320.783, 584	11.7
262.8	-320.783, 785	11.2
272.8	-320.784, 578	9.1
282.8	-320.785, 744	6.0
292.8	-320.786, 924	2.9
302.8	-320.787, 764	0.7

[a]The optimized geometry of figure 2 was used for all other parameters during the methyl rotation.

c) Barrier to Nitrogen inversion

Inversion barriers for N-methylaniline were calculated in two ways: inversion of the ground state conformer shown in figure 2 and inversion of the high energy conformer with $\phi = 45°$. The energy difference between these conformations and the conformations in which the N-H bond is forced to be coplanar with the Csp^2-N and $N-CH_3$ bonds were taken as the inversion barriers. The barriers to nitrogen inversion for the ground state was 17.4 kJ/mol. Inversion of the high energy conformer cost 16.5 kJ/mol.

C. DISCUSSION

1. N-methylaniline

a) The ground state geometry

The STO-3G MO calculated ground state conformation of N-methylaniline is depicted in figure 2. An ab initio optimized geometry has not been previously reported.

Experimental data in the gas phase[3,6,13] suggest that the geometry about nitrogen in aniline becomes more planar upon methylation. A geometry optimization of aniline at the STO-3G level of molecular orbital theory yields an angle of 31° between the N-H bond and the C_1-C_2 bond of the benzene ring. A flattening at nitrogen is more easily seen if one projects the N-H and N-C bonds of the sidechain onto a plane perpendicular to the $C_6C_1C_2$ plane as in 4 and 5

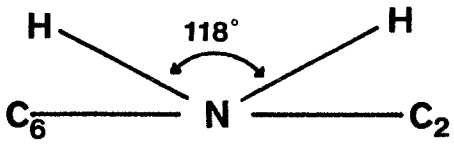

4

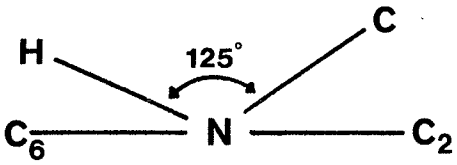

5

It has been assumed that N-methylaniline is planar in solution[2,14]. Six-bond coupling constants between the para proton and the nucleus of the sidechain in benzene derivatives have been shown to

follow the relationship $^{6}J^{X,H-4} = {}^{6}J^{90}\langle\sin^2\phi\rangle$ [40] where $^{6}J^{90}$ is the coupling when the angle the β nucleus makes with the benzene ring, ϕ, is 90° and where $\langle\sin^2\phi\rangle$ is the expectation value of $\sin^2\phi$, $^{6}J^{90}$ for the β-carbon in ethylbenzene is 0.618 ± 0.016[41] and is 0.625 ± 0.007[42] for anisole. In a benzene solution of ^{15}N-methylaniline-^{13}C, $^{5}J^{13N-C,H4}$ is less than 0.05 Hz[39]. If a value of 0.62 Hz is taken for $^{6}J^{90}$, then $\langle\sin^2\phi\rangle$ is less than 0.08. This low value implies a very small <u>average</u> value of ϕ.

b) The barrier to rotation about the Csp^2-N bond

The STO-3G MO energies in figure 7 can be fit reasonably to the twofold potential in equation (26), although the energies calculated for each value of ϕ are subject to some error in that the calculated energies for $\phi = 180°$ and $\phi = 0°$ are not equal, even though they represent the same conformation. This is a result of performing only partial optimizations for each conformation and because the starting parameters for optimizations at each conformation were not always close to the final optimized geometry. Despite any uncertainty in the individual data points the energies at 180° and 0° are still within the standard deviation quoted in equation (26). The twofold nature of the calculated barrier supports the assumption of such a barrier in the analysis of microwave[13] and infrared[3] data.

In aniline the STO-3G MO barrier takes the form

$$(20.5 \pm 0.7) \sin^2 (\phi - 32.8 \pm 1.5°) \qquad (28)$$

This is only 1.4 kJ/mol higher than that calculated for N-methylaniline. Torsion data [13,43] imply that the barrier in aniline is 9.8 ± 2.5 kJ/mol higher than that in N-methylaniline. The reduction of the barrier on methylation likely results from destabilization of the ground state by steric interaction between the methyl group and the ortho C-H bonds. Such a decrease in barrier height can be seen on methylation of benzaldehyde to give acetophenone; DNMR[44] and gas phase data[45] agree that acetophenone has a lower barrier than benzaldehyde. In the gas phase[46,47]

methylation of phenol to give anisole increases the barrier. Similarly, in solution thioanisole[48] has a higher barrier than thiophenol[40]. The barrier increase in anisole and thioanisole might be attributed to electron donation by the methyl group to the C_1-O or C_1-S bonds resulting in an increased bond order. If this were so, a similar increase should occur with aniline and N-methylaniline.

In ethylbenzene[49], where steric interaction dominates in the rotation of the sidechian, the barrier is 5.0 kJ/mol with the methyl group preferring a plane perpendicular to the benzene ring.

In both aniline and N-methylaniline the high energy conformer is that in which the benzene ring bisects the H-N-H or H-N-CH_3 bonds, i.e. when the nitrogen lone-pair is presumably in the plane of the benzene ring. This conformation is the one in which the least 2p-π conjugation exists.

The shielding of the C4 nucleus in N-methylaniline is very nearly that of C4 in aniline[50], implying very similar 2p-π conjugation in the two compounds. Atomic charges on C4, as calculated by <u>ab initio</u> MO theory have been related to the ^{13}C chemical shift[51]. At the STO-3G level, MO theory calculates the net atomic charges at C4 as 6.07658 electrons for aniline and 6.07758 electrons for N-methylaniline. If the NH_2 group in aniline is rotated by 90° from its ground state the net atomic charge on C-4 becomes 6.06523. Hence methylation of aniline appears to increase the charge density at C4 by less than one-tenth of the decrease calculated as the NH_2 group is rotated by 90° about the C_1-N bond.

c) Barrier to Methyl Rotation

The STO-3G calculations in table 9 yield a roughly threefold barrier to rotation of the methyl group in N-methylaniline. The barrier height is 11.7 kJ/mol. Methyl torsion data[3] yielded a barrier of 12.9 ± 0.2 kJ/mol, with the assumption of a threefold potential.

d) The Nitrogen Inversion Barrier

The inversion barrier for N-methylaniline in its ground state was calculated as 16.5 kJ/mol. Infrared torsion results gave 2.3 ± 0.5 kJ/mol. A similar overestimate in the calculated barrier was found for aniline[52].

For ammonia, STO-3G MO calculations overestimate the inversion barrier while 4-31G give too small a barrier. The best results have been obtained with at least a double-zeta basis together with inclusion of d-orbitals on nitrogen[54]. Such orbitals have been shown to be almost entirely responsible for the magnitude of the calculated barrier in ammonia[55] and may well be responsible for the barrier magnitudes in its derivatives.

2. 2,6-difluoro-N-methylaniline

The doublet in figure 1d displays an asymmetry at 114K. It is possible that a stereospecific quadrupolar coupling, $^{3}J^{14}\text{-N,F}$, exists and causes a broadening of one of the ^{19}F peaks. As the temperature increases the quadrupolar relaxation rate of the ^{14}N would increase, reducing the asymmetry. A small amount of impurity was present at higher temperatures, possibly due to the unmethylated aniline. This impurity peak was not seen at lower temperatures and may have broadened and moved under one of the peaks of the doublet, increasing its intensity. In any case, this asymmetry will have a negligible contribution to the error quoted for $\Delta G^{\ddagger}$ since equation (22) is rather insensitive to $\delta\nu$, the peak width at coalescence.

The barrier to rotation in 4-bromo-2,6-difluoro-N-methylaniline is 23.1 ± 0.4 kJ/mol in dimethyl ether solution. It would be of interest to estimate the barrier in 2,6-difluoro-N-methylaniline. The effect of the para bromine on the barrier can be estimated by using a correlation between V_2 in thiophenols[56] in CCl_4 solution and $\Delta G^{\ddagger}$ in N-methylanilines[21] in dimethyl ether solutions for five common para substituents (H, OCH_3, F, Cl, NO_2). The correlation in this case is reasonably good, having a correlation coefficient of 0.965, significant at the 95% confidence level. Since V_2 is known for 4-bromothiophenol[56], the increase in $\Delta G^{\ddagger}$ caused by a para bromine substituent can be estimated as 2.1 ± 0.3 kJ/mol. This value suggests a barrier of 21.0 ± 0.7 kJ/mol for 2,6-difluoro-N-methylaniline in dimethylether solution, about 9

kJ/mol lower than that for N-methylaniline[21]. STO-3G calculations, on the other hand, give the 2,6-difluoro-N-methylaniline barrier as 3.1 kJ/mol higher than in N-methylaniline.

In benzoyl-X compounds (X = H, F, CH_3) and in phenol STO-3G calculations overestimate the experimental gas phase barriers by 3 to 4 kJ/mol. In the gas phase, V_2 is 14.5 ± 2.0 kJ/mol for N-methylaniline, hence the STO-3G barrier is 4.6 ± 2.9 kJ/mol too high. If this difference can be applied to 2,6-difluoro-N-methylaniline, then a gas phase barrier of 16.8 ± 2.8 kJ/mol might be suggested.

A comparison of the estimated gas phase and ether solution barriers for 2,6-difluoro-N-methylaniline yields an increase of only 3.4 ± 3.3 kJ/mol (the increase in N-methylaniline is 15.8 ± 2.1 kJ/mol). This might be expected if the polar ortho C-F bonds restrict hydrogen bonding between the N-H bond and the lone-pairs on the oxygen of the solvent molecules.

A comparison of the barriers to rotation about the Csp^2-N bond for N-methylaniline and for 2,4,6-trinitro-N-methylaniline in different solvents demonstrates the medium effect on the barriers. In both molecules the barrier increases in solvent that are good hydrogen bond acceptors. In N-methylaniline, the barrier increases from 25.5 kJ/mol in a freon mixture to 30.3 kJ/mol in dimethylether solution. In 2,4,6-trinitro-N-methylaniline, the barrier increases from 42.7 kJ/mol in CD_2Cl_2 to 46.0 kJ/mol in acetone-d_6. It would be of interest to determine the barrier for 2,4,6-trinitro-N-

methylaniline in dimethylether solution. This barrier should be close to that in CD_2Cl_2 if the ortho nitro groups restrict hydrogen bonding to the solvent oxygen..

The effect of nitrogen hybridization on $^1J^{15}N,H$ is well established and relationships such as equations (3) and (5) have been proposed[23,24]. Wasylishen et al. have suggested that this relationship can be used to show a flattening of the nitrogen in ortho substituted anilines, where the ortho substituents are hydrogen bond acceptors. Their data are reproduced in table 10 together with $^1J^{15}N,H$ values for 2,4,6-trifluoroaniline and 4-fluoroaniline. The trend demonstrated by the molecules in table 10 suggests that there is N-H...F-C hydrogen bonding in 2,4,6-trifluoroaniline. No doubt this hydrogen bonding is also present in 2,6-difluoro-N-methylanilnes.

STO-3G MO calculations provide evidence for an attractive interaction between the N-H bond and the ortho fluorine in 2-fluoro-N-methylaniline. The geometry optimized structure shown in figure 5 indicates that the H-N-CH_3 sidechain twists by about 9° from its position in N-methylaniline, decreasing the amino proton to ortho fluorine internuclear distance. If the hydrogen bond in 2,6-difluoro-N-methylaniline is as strong as that in the 2-fluoro derivative, then a similar twist of the H-N-CH_3 should occur. The methylamino group actually twists by about 20°. This larger twist is likely a result of steric repulsion between the methyl group and the other ortho C-F bond.

Destabilization of the planar conformation by ortho fluorines is demonstrated by STO-3G MO calculations on ethylbenzene, anisole, thioanisole and their 2,6-difluoro derivatives. Application of the J method[40], with the assumption of a twofold barrier for the molecules in solution, also demonstrates destabilization of the planar state in the 2,6-difluoro derivatives. Results of ab initio calculations and the J method are given in table 11. Strong conjugation between the nitrogen lone-pair and the π system of the benzene ring is likely the major component in the barrier in 2,6-difluoro-N-methylaniline and as a result the contribution from steric interaction between the methyl group and the ortho fluorines is not as pronounced as for those in table 11.

Another effect to consider is the reduction of 2p-π conjugation by the presence of two electron donating ortho fluorines. Unfortunately it is difficult to separate the electronic and steric effects of ortho substituents on rotational barriers.

An interaction not often considered to contribute to the rotational barrier in aniline derivatives is that between the nitrogen long-pair and the ortho C-X bond. This interaction may be steric if overlap of orbitals is involved, as with a bulky ortho group, or it may take the form of a dipole-dipole interaction between $N^{+}\!\!-\!\!\div^{-}$ and $C^{+} - X^{-}$. It is difficult to judge just how important this contribution is in the barrier to rotation in 2,6-difluoro-N-methylaniline.

A more complete decomposition of the barrier in 2,6-difluoro-N-

methylaniline into its many components would be a formidable, if not impossible, task and will not be attempted in this work.

Table 10

$^{1}J^{15}N,H$ for some ortho substituted anilines.

compound	$^{1}J^{15}N,H$
aniline[a]	-78.9
4-fluoroaniline[b]	-77.8
2,4,6-trifluoroaniline[b]	-81.1
2-chloroaniline[a]	-82.3
2,4-dibromoaniline[a]	-83.1
2,4,6-tribromoaniline[a]	-85.5
2-acetyl aniline[a]	-88.6

[a] reference 61

[b] unpublished results from this laboratory

Table 11

Barriers to internal rotation for some benzene derivatives as determined by STO-3G MO theory and the J method.

	STO-3G MO	J method
ethylbenzene	$7.6 \pm 0.5 \sin^2(\phi + 90)$ [a]	$5.0 \sin^2(\phi + 90)$ [b]
2,6-difluoroethyl-benzene	$14.3 \pm 0.8 \sin^2(\phi + 90)$ [a]	$25 \sin^2(\phi + 90)$ [c]
anisole	$5.7 \pm 0.5 \sin^2\phi + 2.6 \pm 0.4 \sin^2 2\phi$ [d]	$> 25 \sin^2\phi$ [a]
2,3,5,6-tetrafluoro-anisole	$4.6 \pm 0.4 \sin^2(\phi + 90)$ [f]	0.0 [e]
thioanisole	$6.2 \pm 0.2 \sin^2\phi$ [f]	$5.4 \sin^2\phi$ [f]
2,6-difluorothio-anisole	$9.7 \pm 0.6 \sin^2(\phi + 90)$ [f]	$6.7 \sin^2(\phi + 90)$ [f]

[a] unpublished results from this lab

[b] reference 49

[c] reference 58

[d] reference 59

[e] reference 42

[f] reference 48

3. 2,6-dichloro-N-methylaniline

The geometry optimization of 2,6-dichloro-N-methylaniline yields a geometry (shown in figure 4) in which the N-CH_3 and N-H bonds lie at angles of 79° and -17.2° respectively. Evidently chlorine substitution at the ortho positions results in a substantial destabilization of the more planar ground state. Energies and other molecular parameters have been calculated for different conformations of the methylamino group and are given in table 8. Unfortunately, no geometries with ϕ between 0° and 135° could be optimized. These data suggest that the barrier in 2,6-dichloro-N-methylaniline is large, the relative energies at 0° and 135° being 24.2 kJ/mol and 30.7 kJ/mol respectively. An attempt to fit the available energy values to a function of the form A $\sin^2$ (ϕ-B) was unsuccessful.

Although steric interaction between the methyl group and the ortho chlorines is the predominant component in the rotational barrier, the fact that the energy of the molecule is not a maximum at ϕ = 0° suggests that other forces are working in the opposite direction. Also, if steric repulsion were solely responsible for the barrier then the minimum energy should occur at ϕ = 90°, where the methyl group to ortho chlorine distance is greatest. No doubt the 2p-π conjugation is trying to stabilize a more planar conformation.

4. 2,6-dimethyl-N-methylaniline

At 130 K, the lowest temperature at which the compound remained in solution, no relative broadening of the C2 and C6 peaks was observable. In N-methylaniline the shift difference between C2 and C6 is 6.0 ppm at 140 K. If this is also the shift difference for the dimethyl derivative, then the upper limit to $\Delta G^{\ddagger}$ would be 24.6 kJ/mol. In N-t-butylaniline the C2,C6 shift difference is 3.6 ppm, likely a result of an increase in ϕ in the ground state conformation. If the C2,C6 shift difference is taken as 3.6 ppm in 2,6-dimethyl-N-methylaniline, then the upper limit to $\Delta G^{\ddagger}$ for rotation is 25.2 kJ/mol. On the other hand, if an ortho methyl group is taken as creating steric hindrance comparable to an ortho chlorine, this value is much too low. Indeed, STO-3G MO calculations in which the methylamino group was rotated without geometry optimization gave an energy minimum at $\phi = 75°$ with a barrier of about 100 kJ/mol. All attempts to optimize bond angles or bond lengths in the methylamino group resulted in a failure of the calculations to converge, hence the energy quoted is very likely an overestimate. Nevertheless, the rough calculations indicate that there is a strong destabilization of the ground state in 2,6-dimethyl-N-methylaniline.

Destabilization of the planar ground state in N-methylaniline should result in loss of 2p-π conjugation, hence loss of electron density at C4 resulting in a shift of the C4 resonance to higher frequency. In N-methylaniline at 200K, δ_4 is 115.8 ppm . In the

2,6-dimethyl derivative, after correction for the ortho methyl groups, δ_4 is 122 ppm, a shift to higher frequency, as predicted.

If the N-C bond is orthogonal to the benzene ring, inversion at nitrogen as in 6 ⇌ 7, would render the C2 and C6 chemical shifts equivalent since the inversion is a low-energy process that cannot be stopped at typical DNMR temperatures. Even if the N-C bond is not perpendicular to the benzene ring inversion can cause the C2 and C6 resonances to coalesce so long as the N-C and N-H bonds are on opposite sides of the benzene ring. If the N-C and N-H bonds are on the same side of the ring, an inversion of the type 8 ⇌ 9 will occur, yielding non equivalent C2 and C6 signals.

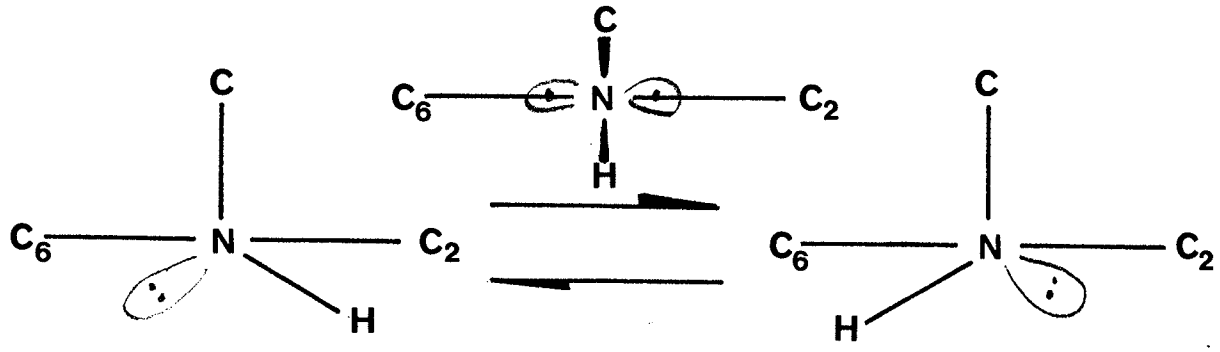

6 ⇌ 7

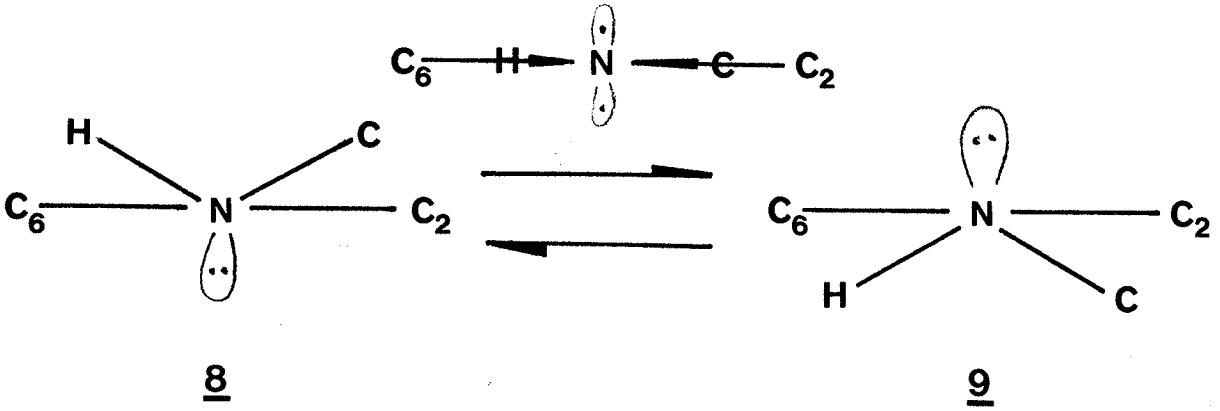

8 ⇌ 9

This argument suggests that the barrier to rotation about the Csp^2-N bond in N-methylaniline can only be determined by the DNMR method if the ground state has the N-Cα and N-H bonds on the same side of the benzene ring. If this is true and one assumes structures of the type 2, where α and ϕ differ by 120°, ability to determine the barriers for 2,6-difluoro-N-methylaniline and N-t-butylaniline implies that these molecules have a ground state where the angle ϕ is less than about 60°.

E. SUMMARY AND CONCLUSIONS

In this work ^{13}C and ^{19}F nuclear magnetic resonance spectroscopy, together with ab initio molecular orbital calculations, have been used to investigate the effect of ortho di-substitution on the ground state conformation and the barrier to methylamino group rotation in N-methylanilines.

The evidence gathered here suggests that the rotational barrier has contributions from 2p-π conjugation, steric interaction between the methyl group and the ortho substituents, hydrogen bonding between the N-H and the ortho C-X bond, hydrogen bonding between the N-H and polar solvents in solution, and perhaps interaction between the nitrogen lone-pair and the ortho C-X bonds.

Barriers to rotation about the Csp^2-N bond for some 2,6-disubstituted-N-methylanilines are summarized in table 12.

Experimental data and molecular orbital calculations suggest that the nearly planar ground state, stabilized by strong 2p-π conjugation, is destabilized by the presence of bulky ortho substituents. Only in the 2,4,6-trinitro compound can the enhanced conjugation and strong N-H...O-N hydrogen bond overcome the steric component in the barriers.

Despite the high STO-3G MO barrier in 2,6-dimethyl-N-methyl-aniline, the exchange could not be stopped at temperatures as low as 130 K. It was suggested that rapid inversion, as in 6 $\rightleftharpoons$ 7, rendered C2 and C6 equivalent; hence the rotational barrier could not be determined by the DNMR method.

In N-methylaniline and its 2,6-difluoro derivative inversion of the type $\underline{8} \rightleftharpoons \underline{9}$ is believed to occur, resulting in non equivalent C2(F2) and C6(F6) nuclei.

Table 12

Calculated and experimental barriers to rotation about the Csp^2-N bond in some 2,6-diX-N-methylanilines.

X	method	Barrier kJ/mol	reference
H	STO-3G	19.1 ± 0.9	a
H	gas phase	14.5 ± 2.2	3
H	$CHFCl_2$-CHF_2Cl	25.5	22
H	CH_3OCH_3	30.3 ± 0.1	20,21
F	STO-3G	22.0 ± 0.8	a
F	CH_3OCH_3	21.0 ± 0.7	a
Cl	STO-3G	>30.7	a
CH_3	STO-3G	~100	a
2,4,6-trinitro	CD_2Cl_2	42.7	18
2,4,6-trinitro	acetone-d_6	46.0	18

[a] this work

F. SUGGESTIONS FOR FUTURE RESEARCH

STO-3G MO calculations suggest that, in the gas phase, 2,6-difluoro-N-methylaniline should have a larger barrier to Csp^2-N rotation than N-methylaniline. It would be of interest to have a gas phase barrier for 2,6-difluoro-N-methylaniline to compare with the estimated barrier.

Solvent effects seem to be important for those barriers determined by DNMR. A further investigation of solvent effects seems warranted.

A DNMR study of 2,6-dicyano-N-methylaniline would be interesting. The cyano group is a good N-H hydrogen bond acceptor and is not very bulky. This should result in a fairly stable planar form. Unfortunately, 2,6-dicyano-N-methylaniline is probably not very soluble, especially at lower temperatures.

The stereospecific six-bond coupling between the amino proton or carbon nucleus and para fluorine nucleus or proton might be useful in predicting the ground state conformations in 2,6-disubstituted-N-methylanilines. It is also possible that the five-bond coupling to the para carbon nucleus obeys the same stereospecific mechanism. Unfortunately, the rapid exchange of the amino proton often prevents the observation of coupling to that nucleus. Quadrupolar relaxation of the ^{14}N nucleus causes broadening of the methylamino proton or carbon signals and disallows the measurement of small couplings. ^{13}C Enrichment of the methyl carbon together with observation of the ring nuclei could overcome this problem.

Stereospecific coupling to the ^{15}N nucleus has been observed and is dependent on the orientation of the nitrogen lone-pair[56]. It would be of interest to investigate the possibility of a stereospecific coupling from the ^{15}N nucleus to the para carbon, fluorine or hydrogen nuclei.

REFERENCES FOR PART II

1. T. B. Grindley, A. R. Katritzky and R. D. Topsom. Tetrah. Lett., 26, 2643 (1972).
2. T. B. Grindley, A. R. Katritzky and R. D. Topsom. Perkin Trans., III 289 (1974).
3. R. A. Kydd and A. R. C. Dunham. J. Mol. Struct. 98, 39 (1983).
4. N. W. Larsen, E. L. Hansen and F. M. Nicolaisen. Chem. Phys. Lett., 43, 584 (1976).
5. G. L. Butt and R. D. Topsom, Spectrochim. Acta., Part A, 34, 975 (1978).
6. R. Cervellati, A. Dal Borgo, and F. Scappini. J. Mol. Struct. 56, 69 (1979).
7. A. Hastie, D. G. Lister, R. L. McNeil and J. K. Tyler. Chem. Comm. 108 (1970).
8. a) P. Helminger and W. Gordy. Phys. Rev., 188, 100 (1969);
   b) K. Takagi and Kojima. J. Phys. Soc. Jpn., 30, 1145 (1971);
   c) J. E. Wollrab and V. W. Laurie. J. Chem. Phys., 48, 5058 (1968);
   d) J. E. Wollrab and V. W. Laurie. J. Chem. Phys., 51, 1580 (1969).
9. A. M. Mirri and W. Caminati. J. Mol. Spectrosc., 47, 204 (1973).
10. W. E. Steinmetz. J. Am. Chem. Soc., 96, 685 (1974).
11. R. Cervellati, A. Dal Borgo and D. G. Lister. J. Mol. Struct., 65, 293 (1980).

12. D. G. Lister and N. L. Owen. J. Chem. Soc. Faraday Trans. 2, 69, 1304 (1973).

13. R. Cervellati, G. Corbelli, A. Dal Borgo and D. G. Lister. J. Mol. Struct., 73, 31 (1981).

14. S. A. Cowling and R. A. W. Johnstone. J. Electr. Spectr., 2, 161 (1973).

15. T. Schaefer and R. Wasylishen. Can. J. Chem., 48, 1343 (1969).

16. D. J. Gale and J. F. K. Wilshire. Aust. J. Chem., 25, 2145 (1972).

17. J. F. K. Wilshire. Aust. J. Chem., 35, 2497 (1982).

18. J. Heidberg, J. A. Weil, G. A. Janusonis, and J. K. Anderson. J. Chem. Phys. 41, 1033 (1964).

19. J. von Jouanne and J. Heidberg. J. Am. Chem. Soc., 95, 487 (1973).

20. L. Lunazzi, C. Magagnoli, M. Guerra, and D. Macciantelli. Tetr. Lett., 32, 3031 (1979).

21. L. Lunazzi, C. Magagnoli, and D. Macciantelli. J. Chem. Soc. Perkin Trans. II 1704 (1980).

22. F. A. L. Anet and M. Ghiaci. J. Am. Chem. Soc., 101, 6857 (1979).

23. G. Binsch, J. B. Lambert, B. W. Roberts, and J. D. Roberts. J. Am. Chem. Soc., 86, 5564 (1964).

24. R. Wasylishen and T. Schaefer. Can. J. Chem., 49, 3627 (1971).

25. T. Bottin-Strzalko, M. J. Pouet, and M. P. Simonnin. Org. Magn. Res., 8, 120 (1976).

26. J. Dorie, B. Mechin, and G. Martin. Org. Magn. Res., 12, 229 (1979).

27. Reference 2b of 22, (private communicaton from G. Martin to F. Anet).

28. F. Bloch. Phys. Rev., 70, 460 (1946).

29. H. S. Gutowsky, D. W. McCall, and C. P. Slichter. J. Chem. Phys., 21, 279 (1953).

30. H. M. McConnell. J. Chem. Phys., 28, 430 (1958).

31. P. D. Buckley, K. W. Jolley, and D. N. Pinder. Progress in N.M.R. Spectrosc., 10, 1 (1975).

32. G. J. Binsch. J. Am. Chem. Soc., 91, 1304 (1969).

33. B. W. Goodwin. M.Sc. Thesis, University of Manitoba (1969).

34. J. Sandström. "Dynmaic NMR Spectroscopy", Academic Press, London (1982).

35. R. A. W. Johnstone, D. W. Payling, and C. Thomas. J. Chem. Soc., (C) 2223 (1969).

36. W. J. Hehre, W. A. Lathan, R. Ditchfield, M. D. Newton, and J. A. Pople. Program 23b, Quantum Chemistry Program Exchange, Indiana University, Bloomington, Indiana.

37. Program MONSTERGAUSS, M. R. Peterson and R. A. Poirier. University of Toronto, Ontario, Canada, 1981.

38. SAS User's Guide: Statistics, A. A. Ray (ed.), (Statistical Analysis System Institute, 1982).

39. Unpublished data from this Laboratory.

40. W. J. E. Parr and T. Schaefer, Acc. Chem. Res., 13, 400 (1980).

41. T. Schaefer, J. Peeling, and G. H. Penner. Can. J. Chem., 61, 2773 (1983).

42. T. Schaefer, R. Laatikainen, T. A. Wildman, J. Peeling, G. H. Penner, J. Baleja, and K. Marat. Can. J. Chem., 62 (1984).

43. N. W. Larsen, G. L. Hansen, and F. M. Nicoliasen. Chem. Phys. Lett. 43, 584 (1976).

44. T. Drakenberg, R. Jost, and J. Sommer. J. C. S. Chem. Comm., 1011 (1974).

45. F. A. Miller, W. G. Tateley, and R. E. Witowski. Spectrochim. Acta 23A, 891 (1967).

46. W. G. Tately, F. A. Miller, and R. E. Witowski. Technical Report AFML-TR-66-408.

47. S. Fewster. Ph.D. Thesis, University of Manchester (1970).

48. J. Baleja. M.Sc. Thesis, University of Manitoba, (1984).

49. T. Schaefer, L. Kruczynski, and W. Niemczura. Chem. Phys. Lett. 38, 498 (1976).

50. A. K. Bose and D. R. Srinivason. Tetrah. 31, 3025 (1975).

51. W. J. Hehre, R. W. Taft, and R. Topsom, in: Progress in Physical Organic Chemistry, Vol. 12, R. W. Taft (ed.), (Wiley-Interscience, New York, 1976) 159.

52. A. Wolf, U. Voets, and H. H. Schmidtke. Theor. Chim. Acta (Berl.) 54, 175 (1979).

53. A. Veillard in: Quantum Mechanics of Molecular Conformations, B. Pullman (ed.), (Wiley and Sons, London, 1976) Chapter 1.

54. P. W. Payne and L. C. Allen in: Applications of Electronic

Structure Theory, H. F. Schaefer (ed.), (Plenum, London, 1976), Chapter 2.

55. A. Rauk, L. C. Allen, and E. Clementi. J. Chem. Phys., 52, 4133 (1970).

56. T. Schaefer and T. A. Wildman. Chem. Phys. Lett., 80, 280 (1981).

57. D. Gust and M. W. Fagan. J. Org. Chem., 45, 2511 (1970).

58. T. Schaefer, R. P. Veregin, R. Laatikainen, R. Sebastian, K. Marat, and J. L. Charlton. Can. J. Chem., 60, 2611 (1982).

59. T. A. Wildman, Ph.D. Thesis, University of Manitoba (1982).

60. G. C. Levy and R. L. Lichter. "Nitrogen-15 Nuclear Magnetic Resonance Spectroscopy". Wiley-Interscience, New York (1979).

61. R. Wasylishen, J. B. Rowbowtham, L. Ernst and T. Schaefer. Can. J. Chem., 50, 2575 (1972).